Titre: Title:	Modeling, Simulation and Real-time Control of Active Filters
Auteur: Author:	Alireza Javadi
Date:	2009
Type:	Mémoire ou thèse / Dissertation or Thesis
Référence: Citation:	Javadi, A. (2009). Modeling, Simulation and Real-time Control of Active Filters [Mémoire de maîtrise, École Polytechnique de Montréal]. PolyPublie. https://publications.polymtl.ca/221/

UNIVERSITÉ DE MONTRÉAL

MODELING, SIMULATION AND REAL-TIME CONTROL OF ACTIVE FILTERS

ALIREZA JAVADI

DÉPARTEMENT DE GÉNIE ÉLECTRIQUE

ÉCOLE POLYTECHNIQUE DE MONTRÉAL

MÉMOIRE PRÉSENTÉ EN VUE DE L'OBTENTION

DU DIPLÔME DE MAÎTRISE ÈS SCIENCES APPLIQUÉES

(GÉNIE ÉLECTRIQUE)

Decembre 2009

UNIVERSITÉ DE MONTRÉAL

ÉCOLE POLYTECHNIQUE DE MONTRÉAL

Ce mémoire intitulé:

MODELING, SIMULATION AND REAL-TIME CONTROL OF ACTIVE FILTERS

Présenté par : JAVADI Alireza

En vue de l'obtention du diplôme de: Maîtrise ès sciences appliquées

a été dûment accepté par le jury d'examen constitué de :

M. HURTEAU Richard, D.Ing., président

M. OLIVIER Guy, Ph. D., membre et directeur de recherche

M. SIROIS Frédéric, Ph. D., membre et codirecteur de recherche

M. APRIL Georges-Émile, M. Sc., membre

DÉDICACE

To My Wife

My Parents and All Family Members and Friends

ACKNOWLEDGMENT

I would like to say special thanks and offer special gratitude to my dear professor Guy Olivier for his excellent technical, moral support, and pedagogical guidance as my supervisor throughout the time that this research project has being carried out.

I would like to say special thanks to my dear co-supervisor, Mr. Frederic Sirois for his assistance and helpful advises during the laboratory tests.

I would like to also pay my gratitude and appreciations to my wife, my parents, and all family members and friends that have been of enormous help for the duration of this research work. My success in carrying out and completion of this project would certainly not have been possible without their generous supports.

RÉSUMÉ

Depuis toujours, la production et la distribution de l'énergie électrique à été réalisée en considérant que les ondes de tension et de courant étaient parfaitement sinusoïdales et que leur fréquence était fixe (50 ou 60 Hz). De fait, jusqu'au début des années quatre-vingt ces hypothèses étaient très largement vérifiées. Seuls quelques équipements produisaient des courants déformés non-sinusoïdaux : courants de magnétisation des transformateurs et de moteurs, ballasts de fluorescents et redresseurs ca/cc. Ces charges ne constituaient qu'une très faible partie des charges raccordées aux réseaux et n'avaient généralement aucune conséquence néfaste. Les progrès fantastiques de l'électronique ont complètement modifié la situation. Les téléviseurs couleur, les gradateurs pour l'éclairage, les équipements audio, les fours micro-onde et les ordinateurs personnels nécessitent tous l'emploi de convertisseurs électroniques pour fonctionner.

En plus de ces appareils, l'industrie fait appel de plus en plus à des variateurs de vitesse pour les moteurs électriques eux aussi électroniques. Tous ces appareils constituent autant de sources de pollution harmonique. Même si, individuellement, leur puissance est faible, ensemble ils constituent une formidable source de pollution harmonique qui entraîne des conséquences sérieuses sur les réseaux électriques de basse et moyenne tension. En quelques années seulement, les problèmes associés à cette pollution harmonique sur la qualité de l'énergie électrique sont devenus l'un des problèmes les plus importants auxquels les ingénieurs doivent faire face.

Le rôle des filtres actifs est de compenser, sans consommé aucune puissance active, les harmoniques sur le système de transport d'énergie et d'améliorer l'efficacité du système électrique. La compensation de la puissance non-actif va considérablement augmenter le facteur de puissance et va réduire le coefficient de distorsion (THD) et aussi réduire les pertes. Cela signifie que le système peut laisser circuler plus de puissance active. Bien sûr, l'effet des harmoniques sur les appareils comme les transformateurs et les machines disparaîtra.

Le présent mémoire de maîtrise est consacré à la simulation et la commande en temps réel d'un filtre actif pour compenser et annuler les harmoniques de courant. On y propose tout d'abord un modèle de contrôle approprié pour le filtrage actif tiré de la littérature, pour ensuite simuler le modèle de contrôle du filtre à l'aide du logiciel Simulink de MATLAB et en faisant des

modification a l'aide du logiciel Opal-RT qui permet de réaliser l'interface avec le matériel physique, pour la commande en temps réel.

Finalement, le modèle sera implanté en laboratoire à l'aide des simulateurs en temps-réel de RT-Lab. sur le réseau triphasé de 120/240 V avec une charge non-linéaire constituée d'un redresseur triphasé. Les résultats expérimentaux obtenus en laboratoire démontrent une concordance avec les résultats obtenus par simulation. L'efficacité des différentes méthodes de commande et leur réponse transitoire font l'objet de comparaisons.

Enfin, ce mémoire propose trois recommandations pour la poursuite des travaux futurs dans ce domaine.

ABSTRACT

Historically, production and distribution of electricity were carried out taking into account that the voltage and current were perfectly sinusoidal and their frequency was fixed (50 or 60 Hz). In fact, prior to the early eighties, these assumptions were quite verified. Only few types of equipment generate deformed and non-sinusoidal currents: the magnetization current of transformers and motors, fluorescent ballasts and AC/ DC rectifiers. Actually, these equipments constituted a negligible portion of charges connected to the networks and generally did not introduce significant distortion. Fantastic progress in electronics has changed the situation. Color televisions, dimmers for lighting, audio equipments, microwave ovens and personal computers, all require the use of electronic converters to operate.

In addition to these devices, variable speed drives for industrial electric motors, which are made of electronic devices, are also other sources of harmonic pollution. Although, individually, their power is low, together they constitute a considerable source of harmonic pollutions which have serious consequences in the low or medium voltage power networks. In just a few years, issues of the harmonic pollution regarding the quality of electric power had become one of the most important problems that engineers should have confronted.

The role of active filters is to compensate harmonics in the power system and improve the efficiency of the electrical power system without any active power consumption. Compensation of non-active power substantially improves the power factor and reduces the total harmonic distortion index (THD) and also the total losses. This means that the system can transfer more active power with the same capacity. Another effect of harmonic compensation is the elimination of associated problems on electrical equipment such as transformers and electrical machines.

This master dissertation is dedicated to simulation and real-time control of an active filter to compensate current harmonics in a typical electric system. First, a control model appropriate for the active filter based on a literature review is proposed. Then, the control model is simulated using the Simulink toolbox of MATLAB. The model is then interfaced with the real world by using Opal-RT software to achieve an interconnection with the physical hardware for a real-time control. The final system constitutes a Hardware in the loop (HIL) application.

Finally, the model is implanted in laboratory with RT-Lab real-time Simulators to interact with a three phase 120/240 V system and a three phase rectifier as a non-linear load. Experimental results are also compared with simulation results. Moreover, the provided real-time structure makes it feasible to apply and compare different control designs and their transient state responses.

This report proposes two recommendations for future works in this area.

CONDENSÉ EN FRANÇAIS

0.1 Introduction

Les normes récentes imposent des limites sur les harmoniques qu'une installation peut injecter sur le réseau électrique qui l'alimente. Quelques solutions existent pour rencontrer ces exigences : filtres passifs, annulation magnétique sélective d'harmoniques au moyen de transformateurs déphaseurs, filtres actifs. Une autre approche est d'éviter à la source la génération d'harmoniques en concevant des redresseurs dits propres qui imposent une allure sinusoïdale aux courants qu'ils appellent du réseau. Ces solutions innovatrices, mais très chères ont été utilisées avec succès pour les ballasts de fluorescences et les blocs d'alimentation d'ordinateurs de dernière technologie. Malheureusement, ces technologies ne sont pas encore matures.

Une autre solution consiste à rendre les courants déformés sinusoïdaux en injectant un autre courant déformé de sorte que la somme des deux courants est une sinusoïde; ce sont les filtres actifs. Cette solution conceptuellement des plus attrayantes est complexe et très coûteuse à mettre en œuvre. La complexité de cette solution réside à la fois dans le calcul en temps réel du courant à injecter qui doit continuellement être recalculé en fonction du courant instantané de la charge à compenser et aussi dans la réalisation de l'onduleur qui doit littéralement fabriquer le courant compensatoire. La solution simultanée de ces deux problèmes exige des capacités très importantes de calcul en temps réel. Les premières solutions commerciales ont fait leur apparition. Mais beaucoup de travail reste à faire pour améliorer les performances et en réduire les coûts.

La compensation des harmoniques liez à la puissance non active est un moyen efficace pour résoudre le problème, résultant une amélioration dans la qualité de l'alimentation [34]. Les harmoniques de courant peuvent distraire la forme d'onde de la tension d'alimentation et produisent des résonances dans le réseau [5]. Il reste encore de nombreux problèmes, causés par les harmoniques, cruciales à régler. Le filtre actif est le principal enjeu technique pour faire face à ces problèmes [25]. De nombreuses approches ont été développées pour réaliser un compensateur variable instantané [1]. Cependant, leur efficacité n'a pas encore été testée dans la réalité afin d'assurer une compensation adéquate de la puissance non active.

0.2 Les définitions de puissance électrique

Il a été approuvé que les définitions classiques de la puissance électrique; active, réactive et apparente ne remplissent pas les conditions engendrées par les harmoniques et les déséquilibres. Par conséquent, des différentes définitions de puissance et des méthodes de calcul ont été proposées dans le domaine fréquentiel, ainsi que dans le domaine du temps. Trois définitions principales seront étudiées brièvement dans le deuxième chapitre pour donner une meilleure compréhension de la définition de puissance du réseau électrique dans les différentes conditions. La définition générale de puissance électrique définie par Budeanu, la définition de Depenbrock et Emanuel, ainsi que celle introduite par Czarnecki sera étudiée.

La définition couramment utilisée de la puissance établie par Budeanu peut être appliquée pour une analyse fréquentielle du système pour des situations sans distorsion. Cela signifie que pour une étude de puissance pour en cas de déséquilibré, les tensions et les courants peuvent être décomposée en série de Fourier pour calculer les harmoniques et les paramètres du système, comme le facteur de puissance. Il doit être prise en note que les méthodes utilisent dans le domaine fréquentiel ne peuvent être instantanée dans le temps, c'est pourquoi il convient de préciser que chaque méthode est applicable dans quel domaine.

Budeanu définit globalement quatre types de puissance pour un système monophasé; puissance apparente (S), puissance active (P), puissance réactive (Q), et la puissance de distorsion (D). Cette définition ne couvre pas tous les aspects des phénomènes tels que la distorsion et le déséquilibre, même le facteur de puissance dans certaines situations ne couvre pas toutes les parties de la puissance non active du système.

Depenbrock et Emanuel ont défini la puissance selon les concepts physiques de la puissance apparente, donc ces deux auteurs ont défini la puissance efficace (Se) étant la puissance active maximale transmissible pour une valeur rms déterminée de la tension et du courant. Cette définition a était développé après une étude plus complexe sur les définitions de Budeanu, afin de couvrir les contraints de l’ancienne approche. Leur définition est pratique et simple et peut être utilisée par les instruments de mesure. Chaque légère différence d'interprétation de la puissance conduit à une nouvelle définition.

Czarnecki a introduit un concept de décomposition orthogonale du courant pour la première fois en mars 1988. Czarnecki a proposé une définition plus attrayante dans laquelle le courant peut être décomposé en cinq composantes orthogonales qui contribuent à des phénomènes physiques différents. Mais il y a encore de l'incompétence dans cette définition.

0.3 La définition des puissances instantanées

Pour les systèmes monophasés, les notions telles que la puissance active et réactive, ainsi que le facteur de puissance sont bien définies. Diverses tentatives ont été proposées pour généraliser ces concepts à un système triphasé avec des courants et des tensions déséquilibrées et déformées. La plus récente théorie qui a était décrit par Akagi en 1984, introduit la notion de puissance réactive instantanée. Ce concept est très intéressant pour des raisons pratiques, en particulier pour analyser la compensation instantanée de la puissance réactive sans consommation d'énergie.

Après cette définition, des auteurs ont défini la théorie généralisée de la puissance, qui est une théorie plus complexe basée sur des calculs vectoriels applicables aux systèmes multiphasés. Par la suit Willems à proposer est un moyen simple et efficace pour réduire le processus de calcul. La théorie de Willems est basée sur la théorie du p-q et la décomposition orthogonale des courants.

Trois principales définitions de puissance instantanée sont présentées. La théorie de p-q instantanée d'Akagi est la première et principale théorie pour le calcul instantané des puissances sera présentée. Malheureusement, cette approche est limitée à un système triphasé. Bien que les calculs présentés par cette théorie sont simples, mais elles ne donnent pas un sens physique clair pour les différentes puissances. L'imprécision de cette méthode dépend de la probabilité d'obtenir une valeur infinie dans les différentes étapes de l'algorithme de contrôle. Les méthodes de contrôle dominant utilisé dans les filtres actifs industriels semblent être basées sur cette théorie en raison de sa rapidité.

La théorie généralisée de la puissance instantanée essaie d'étendre la théorie d'Akagi aux systèmes multiphasés. En utilisant les calculs vectoriels, il utilise l'idée d'Akagi, et donne une sensation plus physique aux concepts des puissances instantanées. En outre, de nombreux éléments indésirables apparaissent dans la compensation avec cette méthode qui fait en sorte que cette théorie soit moins pratique que la théorie de p-q instantanée.

Pour les systèmes de plus que trois phases, la théorie Willems pourrait être utile. Si l'objectif est d'obtenir un courant sinusoïdal de puissance ou de compenser toutes les puissances non actives, nous n'avons pas d'autre choix que la théorie généralisée. La théorie Willems est le meilleur choix si l'objectif est seulement de compenser la partie imaginaire (réactive) de la puissance instantanée. La méthode de Willem assure un facteur de puissance unitaire et compense la majorité des harmoniques présents dans le courant.

0.4 Résultats des essais de l'implantation du filtre actif en temps réel

Basé sur les théories étudiées et les simulations un contrôleur temps réel a été réalisé pour être mis en œuvre sur un simulateur en temps réel d'Opal-RT. Le contrôleur temps réel a été ensuite utilisé pour éliminer les harmoniques d'une charge non-linéaire. Les équipements utilisés en laboratoire pour ces essais seront présentés. Enfin, les résultats expérimentaux seront présentés et analysés.

En ce qui concerne la transformation de Clark sur un système en trois phases, la théorie p-q introduites par Akagi semble un bon départ pour réaliser un compensateur instantanée de la puissance réactive, mais dans le cas d'une compensation de la puissance non-active, d'autres méthodes devraient être utilisées. Bien entendu, l'hypothèse sera réfutée si les résultats des tests en temps réel montrent une compensation non instantanée ou une onde non-sinusoïdale du courant fourni par la source. La méthode proposée pour un test en temps réel est de simuler le filtre actif sur un simulateur d'Opal-RT pour le connecter à un système physique. Vue que la théorie d'Akagi pour la puissance instantanée (p-q instantanée) semble être le meilleure approche à nos jours. Donc, cette théorie a été utilisée pour la mise en œuvre dans le contrôleur en temps réel.

Enfin, le modèle a été mis en œuvre dans le laboratoire sur simulateur triphasé (120/240 V) et un redresseur triphasé entent que charge non-linéaire. Les résultats expérimentaux sont aussi comparés avec les résultats de simulation. Les instruments de test en temps réel, la procédure de l'essai, les résultats temps-réel seront présentés. Ce chapitre se concentre sur les tests et la méthodologie et la réalisation en temps réel d'un tel contrôleur.

Les équipements utilisés dans les tests vont être étudiées en détail. Le simulateur en temps-réel ainsi qu'un onduleur de puissance et une la charge non linéaire sont indispensables pour réaliser

ces tests. Certains instruments sont nécessaires pour réaliser un test en temps réel à cet effet la charge non linéaire qui est composée de deux redresseurs en parallèle et une charge résistive. Le simulateur en temps réel étant pas capable de produire des tensions et des courants suffisamment élevées, un onduleur de puissance a été utilisé pour produire le courant de compensation. Le simulateur en temps réel après avoir calculé le courant de compensation va générer les impulsions nécessaires qui vont être envoyé à l'onduleur pour produire le courant désiré.

Les résultats obtenus pour les différents essais sont figurées dans le quatrième chapitre de ce mémoire. Les résultats confirment que le projet a été réalisé avec succès. Par de tels résultats, il est possible de conclure que chaque partie du projet individuellement a été effectué correctement; la théorie du contrôle a était bien choisi, le modèle était un modèle approprié basé sur la théorie et le simulateur en temps réel a fonctionné correctement. Bien sûr, les autres éléments telle que l'onduleur et la charge non linéaire sont ajustés et ont fonctionné correctement pour ces essais.

L'objectif défini dans le projet était fondé sur un simple module de MLI (PWM) qui, en raison des résultats obtenus, l'auteur a été encouragé à aller plus loin pour développer un modulateur d'hystérésis (Hystérésis PWM). La modulation par hystérésis élimine les inconvénients du simple PWM. Même avec le block de PWM, le courant produit par l'onduleur a exactement la même forme que le courant de compensation. Un point faible dans cette méthode est que l'utilisation d'un filtre passif pour réduire l'amplitude des harmoniques autour de la fréquence de commutation est indispensable. L'autre point faible est l'absence d'un contrôle sur le courant produit par l'onduleur pendant le fonctionnement du filtre. Le deuxième problème disparait complètement en changeant le bloc PWM par un PWM avec hystérésis. La mise en œuvre du bloc PWM avec hystérésis a prolongé le projet avec une nécessité de faire une étude théorique, des simulations, la modélisation et l'intégration du bloc dans le contrôleur. Bien sûr de nombreuses configurations aurait dû être fait pour mettre la nouvelle méthode en marche.

L'utilisation du PWM avec hystérésis démontre la capacité de ces filtres. Ainsi grâce aux différents essais en temps réel, la capacité du filtre et la théorie utilisée pour les calculs a été illustré. Finalement, avec les essais durant un changement de charge, la réponse dynamique du filtre actif a été étudiée.

0.5 Conclusion

La production et la distribution d'énergie électrique ont été élaborées en considérant que la tension et le courant ont des formes d'onde parfaitement sinusoïdale. Avec les progrès de l'électronique, les questions de la qualité d'onde et la pollution causée par les harmoniques sont devenues l'un des problèmes les plus importants. Interférences de communication, les pertes par chauffage électrique, et les erreurs dans les coordinations des réseaux ont était les effets typiques indésirables des harmoniques.

Après une étude approfondie, quatre méthodes tirées de la littérature sont en mesure d'éliminer complètement ou partiellement le problème des distorsions dans les réseaux électriques; une inductance série dans la ligne, le filtre passif qui est une méthode relativement peu coûteuse, le transformateur Zigzag qui est appliqué pour les installations commerciales pour contrôler les composantes homopolaires des harmoniques, et finalement les filtres actifs qui sont relativement de nouveaux types de dispositifs destinés à éliminer les harmoniques. Ces types de filtres sont basés sur des appareils électroniques de puissance en les rendant plus fiables et plus flexibles que les autres méthodes mentionnées.

Dans ce mémoire de maîtrise un filtre actif a été modélisé et simulé pour assures un contrôle adéquat en temps réel des harmoniques de courant dans un système triphasé en laboratoire. L'objectif de ce projet a été accompli par une revue des théorèmes et les concepts de puissance électrique dans des conditions non sinusoïdales. Par la suite les algorithmes de contrôle ont été comparés. À cette fin, nous avons fait appel à la théorie de puissance instantanée d'Akagi (théorie p-q) qui est l'une des meilleures approches à nos jours. Finalement, un modèle de contrôle approprié pour le filtre actif basé sur les revues de littérature a été proposé. Le modèle de contrôle a été simulé pour assurer le bon fonctionnement du modèle.

Enfin, le modèle a été mis en œuvre en laboratoire sur un simulator en temps réel avec un redresseur triphasé comme charge non linéaire. Les résultats expérimentaux ont été comparés avec les résultats de simulation. En outre, grâce au circuit réalisé en laboratoire, il est possible de développer et de comparer les différentes conceptions de commande et leurs réponses en régime transitoire.

Les résultats expérimentaux illustrent un travail innovateur réalisé dans ce projet. Le modèle du filtre actif a pu compenser les harmoniques dans le réseau électrique et d'améliorer l'efficacité du système d'alimentation sans aucune consommation d'énergie active. La compensation de la non-puissance active améliore considérablement le facteur de puissance et réduit l'indice total de distorsion harmonique (THD), ainsi que les pertes totales dans le système. Cela signifie une évolution dans le domaine du réseau électrique, car le système aurait la capacité de transférer plus de puissance active avec la même capacité des installations. Les contributions de ce projet étaient: la réalisation d'un système en temps réel dans le laboratoire et la mise en œuvre en temps réel d'un filtre actif sur un système triphasé pour compenser les harmoniques d'une charge non linéaire.

En conclusion, les résultats obtenus en temps réel, démontrent que en utilisant les théories instantanées, il est possible de compenser les harmoniques et les autres problèmes de qualité d'énergie comme le du facteur de puissance pour un système triphasé avec ou sans le fil de neutre. Ces résultats démontrent que le simulateur en temps réel est en mesure de réaliser tout type de contrôleurs pour l'asservissement d'un réseau électrique en laboratoires.

TABLE OF CONTENTS

DÉDICACE III

ACKNOWLEDGMENT IV

RÉSUMÉ V

ABSTRACT VII

CONDENSÉ EN FRANÇAIS IX

TABLE OF CONTENTS XVI

LISTE OF TABLES XIX

LISTE OF FIGURES XX

LISTE OF ABREVIATIONS XXIV

LISTE OF APPENDIX XXVII

CHAPITRE 1 INTRODUCTION 1

1.1 Harmonic in Power Systems 1

1.2 Harmonic Current and Voltage Sources 2

1.3 Harmonic Compensation Methods 2

1.4 Master dissertation Objectives 5

1.5 Methodology 6

CHAPITRE 2 ELECTRIC POWER DEFINITIONS 7

2.1 Introduction 7

2.2 General powers definition 7

2.2.1 Budeanu's definition 7

2.2.2 Instantaneous power (W) 9

2.2.3 Active power (W) 10

2.2.4 Reactive power (var) 11

2.2.5 Apparent power (VA) 11
2.2.5.1 Arithmetic apparent power S_A 11
2.2.5.2 Vector apparent power S_V 12
2.2.6 Author's contribution 13
2.3 Depenbrock and Emanuel definition 15
2.4 Czarnecki definition 18
2.5 Summary 21
CHAPITRE 3 INSTANTANEOUS POWER THEORIES AND SIMULATIONS 23
3.1 Introduction 23
3.2 Instantaneous p-q Theory 24
3.3 Generalized instantaneous reactive power 39
3.4 Willems approach on reactive power compensation 43
3.5 Comparison of approaches 44
3.6 Summary 52
CHAPITRE 4 LABORATORY REAL TIME CONTROL OF THE ACTIVE FILTER 53
4.1 Introduction 53
4.2 Equipments and ambitions 54
4.3 Laboratory tests 60
4.4 Real-time Results 68
4.4.1 Control using pulse width modulation (PWM) 68
4.4.2 Control using Hysteresis PWM generation 72
4.4.3 Compensation during load changes 87
4.5 Summary 92
CHAPITRE 5 CONCLUSION AND FUTURE WORKS 94

5.1 Conclusion....94

BIBLIOGRAPHY....96

APPENDIX....99

LISTE OF TABLES

Table 3.1 Instantaneous reactive compensation 31

Table 3.2 Instantaneous powers 35

Table 4.1 Magnitude of each harmonic before and after compensation 86

LISTE OF FIGURES

Fig. 1.1 Low-pass broadband filter....3

Fig. 1.2 Power system with a shunt compensator on the load side 5

Fig. 2.1 Arithmetic S_A, and Vector S_V , apparent powers: Unbalanced nonsinusoidal conditions [6]....13

Fig. 3.1 Schema to better understand the physical meaning of the instantaneous powers....31

Fig. 3.2 Load voltage and current, source current, Instantaneous powers 32

Fig. 3.3 Instantaneous reactive compensation (q) 33

Fig. 3.4 Phase "a" voltage and current of load and source, source currents, instantaneous active and reactive power, load and source zero sequence current ($i0$)....36

Fig. 3.5 a) load voltages and currents b) source currents c) instantaneous active and reactive power d) active filter zero-sequence current ($i0$), e) compensation currents $(iC\alpha, iC\beta)$ 37

Fig. 3.6 Load, source, and active filter instantaneous active and reactive power 38

Fig. 3.7 Decomposition of current in a 3D space 41

Fig. 3.8 a) source voltages b) load currents c) instantaneous powers d) zero-sequence current of the load, for the case with zero phase degree....46

Fig. 3.9 Source currents a) without zero-sequence compensation b) with zero-sequence compensation for the case with zero phase degree 47

Fig. 3.10 Compensating current injected by the active filter, source currents for the case with zero phase degree 48

Fig. 3.11 a) Source voltages, b) load currents, c) instantaneous powers, d) zero-sequence current of the load for the case with 30 phase degree 49

Fig. 3.12 Source currents a) without zero-sequence compensation b) with zero-sequence compensation for the case with 30 phase degree 50

Fig. 3.13 Compensating current injected by the active filter, source currents for the case with 30 phase degree 51

Fig. 4.1 Power System laboratory at École Polytechnique de Montréal 54

Fig. 4.2 Two diode bridges connected in parallel.....55

Fig. 4.3 The three phase source panel, the resistive load and the autotransformer 56

Fig. 4.4 The Probes and the patch panel, the probes and connection cables (front view).....57

Fig. 4.5 The real time simulator (MX-station), the analog card (left), the digital cards (right) 58

Fig. 4.6 The Probes and the patch panel, the probes and connections cables (front view) 58

Fig. 4.7 The three phase inverter, source for the electronic boards.....59

Fig. 4.8 Schematic of the control of the active filter controller.....61

Fig. 4.9 Under mask of the active filter controller block 62

Fig. 4.10 Hysteresis Block parameters 63

Fig. 4.11 Current-regulated voltage source inverter [36] 63

Fig. 4.12 Pulse width modulation (PWM) block, block parameters 64

Fig. 4.13 Oscilloscopes view during the execution of the test 65

Fig. 4.14 Laboratory circuit block diagram.....66

Fig. 4.15 Industrial active filter implementation block diagram with an energy storage component 67

Fig. 4.16 Instantaneous active, reactive and zero-sequence power of the non-linear load 69

Fig. 4.17 Instantaneous calculated compensating currents, carrier signal.....70

Fig. 4.18 Instantaneous load, source, compensating and calculated currents 70

Fig. 4.19 The first phase (“a”) source voltage and current.....71

Fig. 4.20 The three phase voltages and currents, the dc voltage of the non-linear load.....73

Fig. 4.21 Instantaneous active, reactive and zero-sequence powers, calculated compensation currents 73

Fig. 4.22 Hysteresis PWM impulsions 74

Fig. 4.23 Instantaneous load, source, compensating and calculated currents for the second case 75

Fig. 4.24 The phase “a” source voltage and current for the second case 76

Fig. 4.25 The three phase voltages and currents, the dc voltage of the non-linear load..... 77

Fig. 4.26 Instantaneous active, reactive and zero-sequence powers, calculated compensation currents for the third case 77

Fig. 4.27 Instantaneous load, source, compensating and calculated currents for the third case 78

Fig. 4.28 The first phase “a” source voltage and current for the third case 78

Fig. 4.29 The minimum margin calculation 80

Fig. 4.30 The three phase voltages and currents, the dc voltage of the non-linear load..... 81

Fig. 4.31 Instantaneous active, reactive and zero-sequence powers 81

Fig. 4.32 Instantaneous load, source, compensating and calculated currents for the case four 82

Fig. 4.33 The phase “a” source voltage and current for the case four 82

Fig. 4.34 Instantaneous load, source, compensating and calculated currents for the case five. 83

Fig. 4.35 The first phase “a” source voltage and current for the case five 84

Fig. 4.36 The frequency spectrum before and after harmonic compensation 85

Fig. 4.37 The fundamental, fifth, seventh, eleventh and thirteenth harmonic orders 85

Fig. 4.38 High order harmonics spectrum 86

Fig. 4.39 The three phase source voltages, the dc voltage of the non-linear load during transient current tests 87

Fig. 4.40 The three phase load currents, the instantaneous active, reactive and zero-sequence powers of the non-linear load for the decreasing load 88

Fig. 4.41 The calculated compensation currents, the phase “a” source voltage and current for the decreasing load 88

Fig. 4.42 Instantaneous load, source, compensating and calculated currents during the change in the load current for the decreasing load 89

Fig. 4.43 The three phase load currents.....90

Fig. 4.44 The three phase load currents, the instantaneous active, reactive and zero-sequence powers of the non-linear load for the increasing load.....90

Fig. 4.45 The calculated compensation currents, the phase “a” source voltage and current for the increasing load.....91

Fig. 4.46 Instantaneous load, source, compensating and calculated currents during the increase of the load current for the increasing load.....91

LISTE OF ABREVIATIONS

B	Susceptance
C	Capacitance
CSC	Current source converter
D	Distorted power
eff	Effective value
f	Frequency
FFT	Fast Fourier transformation
G	Conductance
h	Harmonic order
H	Henry
HIL	Hardware in the loop
Hz	Hertz
IGBT	Insulated gate bipolar transistor
L	Inductance
N	Non-active power
ω	Angular frequency
P	Active power
PF	Power factor
PLL	Phase-locked loop
PWM	Pulse width modulation
Q	Reactive power
R	Resistance

rms	Root mean square
s	Second
S	Apparent power
THD	Total harmonic distortion
VA	Volt-ampere
vai	Volt-ampere imaginary
var	Volt-ampere reactive
VSC	Voltage source converter
W	Watt
Z	Impedance

Multiple and sub-multiple of SI unities

M:	$10^6 = 1\,000\,000$	mega
k:	$10^3 = 1\,000$	kilo
m:	0.001	mili
μ:	$10^{-6} = 0.000\,001$	micro

Mathematical symbols

Bold (***V*** or ***v***)	Matrix
Asterisk (*V**)	Complex conjugate
V	rms value
v	Instantaneous value
$\vec{V}$	Vector in frequency domain
$\vec{v}$	Instantaneous vector

$\lvert V \rvert$	Absolute value
$\lvert \vec{V} \rvert$ or $\lvert \vec{v} \rvert$	Generalized rms value of the vector $\vec{V}$ or $\vec{v}$

LISTE OF APPENDIX

APPENDIX I – Comparison for three phase- three wires system 99

APPENDIX II – Comparison for three phase- four wires system 100

APPENDIX III – Comparison of Generalized theory and Willems 102

APPENDIX IV – Published Papers 103

CHAPITRE 1 INTRODUCTION

1.1 Harmonic in Power Systems

In normal conditions, generated and distributed electric energy must be sinusoidal with predetermined frequency and magnitudes. Since the beginning of the power systems, there has been harmonic distortions due to nonlinear equipments such as generators, transformers, motors, etc. furthermore, harmonic pollution in power systems has significantly increased owing to large proliferation of power electronic devices. Consequently, the reactive power compensation in non-sinusoidal conditions became one of the most important problems in power systems.

Here some effects of harmonics on electric systems are counted:

- Communication interference; magnetic (or electrostatic) coupling between electrical power circuits and communication circuits can cause what is known as communication interference, induced line noise, interference with power line carrier systems and relay malfunctions.
- Losses as heating; it is common to refer to heating as $R.I^2$ losses. By using superposition, the total losses can be expressed as sum of individual harmonic losses, excessive losses and overheating of transformers, motors, capacitors, and blown capacitor fuses.
- Solid-state device malfunctions; harmonics can cause solid-state devices to malfunction if the equipment is sensitive to zero crossings. A resonance condition can cause a current waveform to have zero crossings occur more than once every half-cycle, nuisance tripping of relays and breakers, errors in measurement equipment, unstable operation of zero voltage crossing firing circuits and interference with motor controllers.
- Neutral currents; which flow into the system and causes additional losses and other associated problems.

1.2 Harmonic Current and Voltage Sources

The Power quality problems caused by single phase rectifier loads are well known. Electronic equipments used for data processing such as laptops, typically features a simple diode bridge rectifier at the front end of the power circuit. The rectifier, in conjunction with its capacitive filter is a nonlinear load and draws current with high crest factor and rich in harmonics, resulting in power quality problems. They also contribute adversely by degrading the supply voltage waveform. Moreover they cause overheating of transformers and neutral conductors, create equipment malfunction and inefficient use of electric energy.

With the modern technology, it is possible to rectify the three phase ac power to dc power using static rectifiers for dc drives as well as static inversion for ac drives. Though more versatile than past methods, these newer technologies may have detrimental effects on the quality of the ac system, especially when they comprise a significant portion of the system. Rectification generates harmonic voltages and currents that can cause problems; middle of the harmonic distortion range can lead to insulation failures due to overheating and over voltages, malfunction of solid-state equipments, communication interference, overheating of motors, transformers and generators and also can excite system resonances, etc. The common addition of power factor correction capacitors to such a system generally increases the likelihood occurrence of such problems. Lower frequencies such as inter-harmonics may cause torque problems for shafts of motors and generators.

All the devices with nonlinear characteristics that derive their input power from a sinusoidal electrical system may be responsible for injecting harmonic currents and voltages into the electrical system. The principal sources of undesirable harmonics are rectifiers and electric arc furnaces. The common applications of rectifiers are solid-state drives and uninterruptible power supplies (UPS). Nowadays with the increment of nonlinear loads in the electric grids, these problems are not only isolated but much more common than in the past.

1.3 Harmonic Compensation Methods

A simple mitigation action such as adding a shunt capacitor bank can effectively modify an unfavorable system frequency response, and so reduce the harmonics to an acceptable level.

i. In-line reactor

In-line reactor or choke is a simple solution to control harmonic distortion generated by adjustable speed drives. The solution is come up with inserting a relatively small reactor, or choke, at the input of the drive. The inductance prevents the capacitor to be charged in a short time and forces the drive to draw current over a longer time and reduces the magnitude of the current with much less harmonic content while still delivering the same energy.

ii. Passive filters

Passive filter, which is relatively inexpensive in comparison with the other harmonic reduction methods, is the most used method. Inductance, capacitor and the load as a resistance are tuned in a way to control the harmonics. However, they suffer from interfering with the power systems. Actually, passive filters are designed to shunt harmonics from the lines or block their flow through some parts of the systems by tuning the elements to create a resonance at the selected frequency.

These filters are tuned and fixed according to the impedance of the point at which they will be connected and hence cannot be adjusted instantaneously in accordance to the load. As a result their cutoff frequency changes unexpectedly after any change in the load impedance resulting in producing a resonance with other elements installed in the system. The most common type of shunt passive filter is the single tuned (notch) filter which is a combination of an inductance and a capacitor. The other one is the low-pass broadband filter which is an inductor in series and a capacitor bank in parallel with the power system as shown in the figure 1.1.

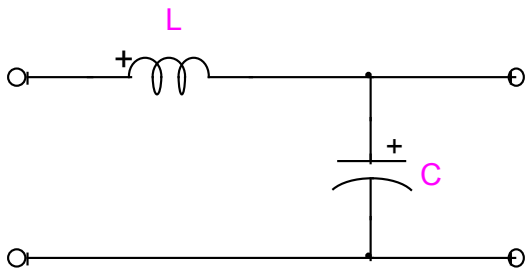

Fig. 1.1 Low-pass broadband filter

iii. Zigzag transformers

Zigzag transformers are applied for commercial facilities to control zero-sequence harmonic components. The Zigzag transformers are not being used only as ordinary transformers; they additionally act as filters for zero-sequence currents by offering low impedance paths to neutral. This reduces the amount of current that flows in the neutral back toward the supply by providing a shorter path for the current.

iv. Active filters

Active filters are relatively new types of devices for eliminating harmonics. This kind of filter is based on power electronic devices and is much more expensive than passive filters. They have the distinct advantage that they do not resonate with the power system and they work independently with respect to the system impedance characteristics. They are used in difficult circumstances where passive filters don't operate successfully because of resonance problems and they don't have any interference with other elements installed anywhere in the power system. They can also address more than one harmonic at the same time and solve other power quality problems like flicker, etc.

They are particularly useful for large distorting loads fed from relatively weak points on the system. The most important advantage of theses filters is their ability to be adjusted instantly with the load changes without any energy storage components, so they can compensate harmonics completely without consuming any active power and there is no need to be frequently adapted to the load changes. In addition, they can provide compensating current from zero to their maximum capacity according to the load currents; so if the load does not need any compensating current, the compensators will not inject any current and even if the frequency of harmonics of the load changes, the filters can easily adapt to compensate the new harmonics without any need for tuning in the hardware.

Active filters inject a current to the junction point in a way that the sum of the compensating and the load current become a sinusoidal wave form seen from the source as illustrated in figure 1.2. The substantial issue of active filters is how to calculate the suitable compensating current which will be clarified in the next chapter. Active filters are also being programmed to do power factor correction as well as harmonic suppression.

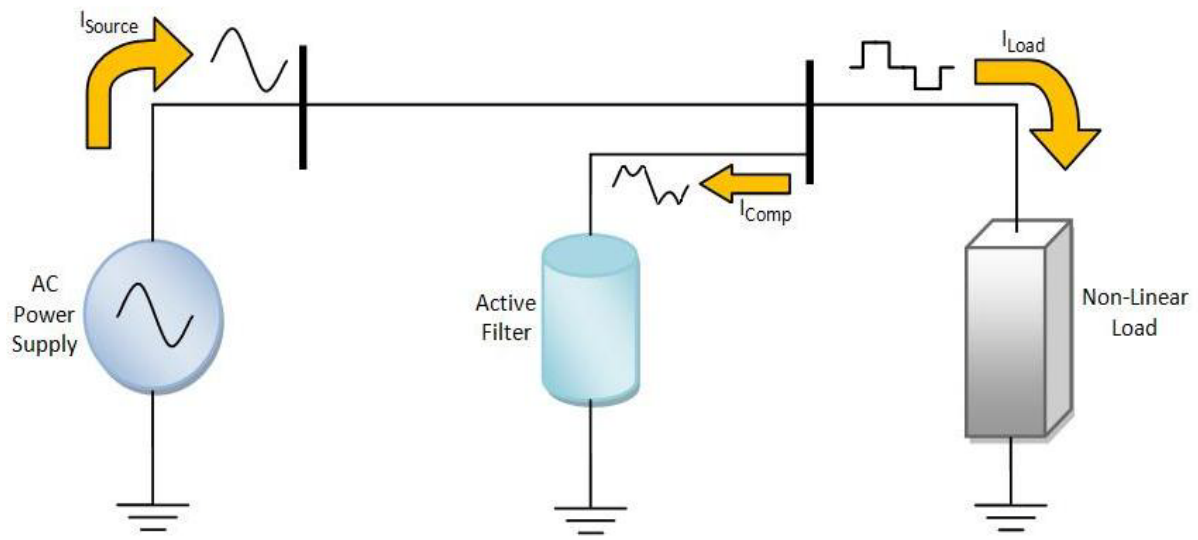

Fig. 1.2 Power system with a shunt compensator on the load side

1.4 Master dissertation Objectives

The first objective of this project is to go over the theorems and definitions of electric power concepts under non-sinusoidal conditions. In this manner we will see the harmonics causes and effects such as their flow in the power system and their contribution on the decrease of power indexes. In the second part we will survey different interpretation of active and reactive power and their ability to be used in the control algorithm of active filters. Then we will recall Akagi's theory of instantaneous power (p-q theory) and limitations of this approach. Moreover, we will make a study on the real-time harmonic and reactive compensation principles. Furthermore a brief study on active filters and their ability to actively clean the network from harmonics, to smooth reactive power and making a load balancing, will be done. Then a real-time modeling of an active filter in the MATLAB Simulink environment using Opal-RT block sets should be done. The last objective is to make Real-time implementation and control of an active filter using RT-lab simulator which dedicates the final part of the dissertation.

1.5 Methodology

At first we have review the concepts of electrical power definitions and their traditional approaches. The mechanism of harmonic generation and its effects on unbalanced systems is then studied. Consequently, the study of the instantaneous active and reactive power and the p-q theory of Akagi follow.

Different definitions of non-active power and compensable power theories found in the literatures are also compared. Moreover active filters and their compensation approaches are surveyed.

We will simulate the control block of an active filter in the Simulink environment to compensate the non-active power in balanced and unbalanced distorted conditions. In order to make the interfaces between physical instruments and the model in Simulink, the model will be modified with Opal-RT block sets. Then the model will be implemented in the real-time simulator to make the active filter controlled in real-time mode.

Finally conclusions and recommendations for future work are provided.

CHAPITRE 2 ELECTRIC POWER DEFINITIONS

2.1 Introduction

It has been generally accepted that classical definitions of electric power (active, reactive and apparent power) does not fulfill the conditions resulting from the existence of by harmonics and unbalances conditions. Consequently, various power definitions and calculation methods have been proposed in frequency domain and even in time domain to cover as much as the matter. Three main proposed definitions will be studied briefly in this chapter to give a better understanding of electrical powers definition in different situations. General power definition based on Budeanu, Depenbrock and Emanuel definitions will be presented, and finally the Czarnecki contribution on electrical powers will be studied.

In the same way many theories have been developed to control the active filters to achieve compensation of the unwanted harmonics from the network. The time domain approach due to Akagi Nabae under the name of “p-q theory” or “instantaneous power theory” is the most dominant theory for two or three phases and three or four wire but this method has some conceptual limitations which many contributors have attempted to resolve these limitations and associated problems that will be explained and clarified in the next chapter.

2.2 General powers definition

The commonly used definition of power established by Budeanu for a frequency domain analysis can be applied for a steady state analysis. That means for a steady state study voltages and currents could be decomposed in Fourier series to calculate harmonics and each parameter of the system like powers and power factors. It should be noticed that since the method use frequency domain it cannot be instantaneous in the time domain; therefore it should be clarified that each method is used for which domain of study.

2.2.1 Budeanu’s definition

Budeanu globally defines four types of power for a single phase case; apparent power (S), active power (P), reactive power (Q), and distorted power (D).

For single phase, the following powers can be derived from Budeanu's definitions:

Apparent power *S*:

$$S = VI = \sqrt{\sum_{k=1}^{\infty} V_k^2} \times \sqrt{\sum_{k=1}^{\infty} I_k^2} \tag{2-1}$$

Active power *P*:

$$P = \sum_{k=1}^{\infty} P_k = \sum_{k=1}^{\infty} V_k I_k \cos \varphi_k \tag{2-2}$$

Reactive power *Q*:

$$Q = \sum_{k=1}^{\infty} Q_k = \sum_{k=1}^{\infty} V_k I_k \sin \varphi_k \tag{2-3}$$

Distortion power *D*:

$$D = \sqrt{S^2 - P^2 - Q^2} \tag{2-4}$$

For the three-phase system the definitions are derived in the following sections.

2.2.2 Instantaneous power (W)

This definition in time-domain is common for all definitions with the unit of watt (W). It should be noticed that this power differs from the general active power in frequency domain which is an average of the instantaneous power in a cycle.

In three phase systems, with 3 or 4 wires the instantaneous voltages and currents are shown as an instantaneous space vector $\boldsymbol{v}$ and $\boldsymbol{i}$.

$$\boldsymbol{v} = \begin{bmatrix} v_{an} \\ v_{bn} \\ v_{cn} \end{bmatrix} \quad , \boldsymbol{i} = \begin{bmatrix} i_a \\ i_b \\ i_c \end{bmatrix} \tag{2-5}$$

v_{kn} - Phase to ground voltage.

i_k - Phase current.

The instantaneous active power is defined as:

$$p = \vec{v} \cdot \vec{\imath} = v_{an}\, i_a + v_{bn}\, i_b + v_{cn}\, i_c \tag{2-6}$$

For balanced three wire systems where $i_a + i_b + i_c = 0$, and it is possible to take one of the voltages as reference, and obtain the following relations:

$$p = (v_a - v_b) i_a + (v_b - v_b) i_b + (v_c - v_b) i_c \tag{2-7}$$

$$p = v_{ab}\, i_a + v_{cb}\, i_c = v_{ac}\, i_a + v_{bc}\, i_b = v_{ba}\, i_b + v_{ca}\, i_c \tag{2-8}$$

Where v_{ab}, v_{bc}, and v_{ca} are the instantaneous line-to-line voltages.

2.2.3 Active power (W)

Active power is the mean of the instantaneous power in the time period.

$$P = \frac{1}{kT}\int_{\tau}^{\tau+kT} v_i i_i dt \qquad i = a,b,c \tag{2-9}$$

The line-to-neutral voltages are as follows:

$$v_i = \sqrt{2}\sum_{h=1}^{n} V_{ih}\, sin(h\omega t + \alpha_h \pm 120^o h) \qquad i = a,b,c \tag{2-10}$$

The line currents have similar expressions:

$$i_i = \sqrt{2}\sum_{h=1}^{n} I_{ih}\, sin(h\omega t + \alpha_h \pm 120^o h) \qquad i = a,b,c \tag{2-11}$$

V and I are rms values.

For a general case in the frequency domain, using the Fourier series and sequence transformation, voltages and currents are decomposed in their rms values, and the active power is defined as follows:

$$P = \sum V_k I_k \cos(\theta_k) = \tag{2-12}$$

$$= V_{1d} I_{1d} \cos(\theta_{1d}) + V_{2d} I_{2d} \cos(\theta_{2d}) + V_{3d} I_{3d} \cos(\theta_{3d}) + \cdots$$

$$+V_{1i} I_{1i} \cos(\theta_{1i}) + V_{2i} I_{2i} \cos(\theta_{2i}) + \cdots$$

$$+V_{1o} I_{1o} \cos(\theta_{1o}) + V_{2o} I_{2o} \cos(\theta_{2o}) + \cdots$$

Where *d,i,o* are suffix for direct, inverse, and zero sequences.

2.2.4 Reactive power (var)

The reactive power is defined as follows:

$$Q = \sum V_k I_k \, sin(\theta_k) = \tag{2-13}$$

$$= V_{1d} I_{1d} \, sin(\theta_{1d}) + V_{2d} I_{2d} \, sin(\theta_{2d}) + V_{3d} I_{3d} \, sin(\theta_{3d}) + \cdots$$

$$+ V_{1i} I_{1i} \, sin(\theta_{1i}) + V_{2i} I_{2i} \, sin(\theta_{2i}) + \cdots$$

$$+ V_{1O} I_{1O} \, sin(\theta_{1O}) + V_{2O} I_{2O} \, sin(\theta_{2O}) + \cdots$$

2.2.5 Apparent power (VA)

It is possible to define two different apparent powers;

2.2.5.1 Arithmetic apparent power S_A

This definition is an extension of Budeanu's apparent power resolution for single-phase systems. S_A the sum of magnitude of apparent power for each phase:

$$S_a = \sqrt{P_a^2 + Q_a^2 + D_a^2} \tag{2-14}$$

$$S_b = \sqrt{P_b^2 + Q_b^2 + D_b^2} \tag{2-15}$$

$$S_c = \sqrt{P_c^2 + Q_c^2 + D_c^2} \tag{2-16}$$

The following arithmetic apparent power is obtained:

$$S_A = S_a + S_b + S_c \tag{2-17}$$

The power factor is obtained: $PF_A = {}^{P}/_{S_A}$ (2-18)

D_i is the Budeanu's **Distortion power** (var).

$$D = \sqrt{{S_A}^2 - P^2 - Q^2} \tag{2-19}$$

2.2.5.2 Vector apparent power S_V

S_V is the vector sum of phase apparent power:

$$\vec{S_V} = \vec{S_a} + \vec{S_b} + \vec{S_c} \tag{2-20}$$

$$|S_V| = \sqrt{P^2 + Q^2 + D^2} \tag{2-21}$$

Where

$$P = P_a + P_b + P_c \tag{2-22}$$

$$Q = Q_a + Q_b + Q_c \tag{2-23}$$

$$D = D_a + D_b + D_c \tag{2-24}$$

It is possible to separate the active and reactive power from distortion part:

$$S' = P + Q \tag{2-25}$$

$$|S'| = \sqrt{P^2 + Q^2} = \tag{2-26}$$

$$\sum |V_k|.|I_k| = \sum_{h=1}^{\infty} (|V_{hd}||I_{hd}| + |V_{hi}||I_{hi}| + |V_{hO}||I_{hO}|) \tag{2-27}$$

Budeanu's reactive power Q can be completely compensated with a simple capacitor; however this is not the case for the distortion power D. It is possible to demonstrate that P, Q, and D are two by two orthogonal, which is illustrated in figure 2.1.

So the power factor could be defined as follows: $PF_V = {|P|}/{|S_V|}$ (2-28)

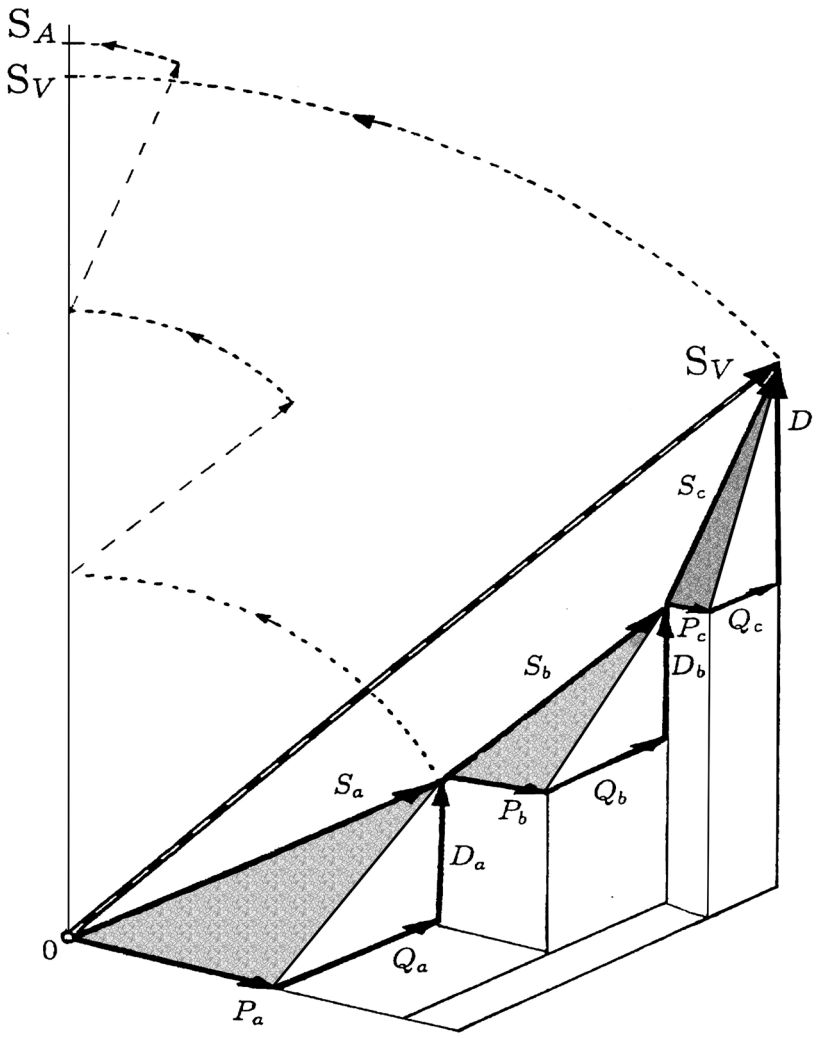

Fig. 2.1 Arithmetic S_A, and Vector S_V , apparent powers: Unbalanced nonsinusoidal conditions [6]

2.2.6 Author's contribution

If we suppose that: $|S| = |V|.|I|$ (2-29)

Where $|V| = \sum_h \sqrt{|V_{hd}|^2 + |V_{hi}|^2 + |V_{hO}|^2}$ (2-30)

$$|I| = \sum_h \sqrt{|I_{hd}|^2 + |I_{hi}|^2 + |I_{hO}|^2} \quad (2\text{-}31)$$

For a case without voltage distortion, that means: $V = V_{1d}$ (2-32)

It is possible to divide the apparent power into three main powers:

$$S^2 = S'^2 + D^2 + U^2 = \sqrt{|V_{1d}|^2} \times \sqrt{|I_{1d}|^2 + |I_{1i}|^2 + |I_{1O}|^2 + |I_{2d}|^2 + |I_{2i}|^2 + \cdots} \quad (2\text{-}33)$$

$$|S'| = \sqrt{P^2 + Q^2} = \sqrt{|V|^2 |I_{1d}|^2} \quad (2\text{-}34)$$

$$D = \sqrt{|V|^2 |I_{hd}|^2} \quad (2\text{-}35)$$

$$U = \sqrt{|V|^2 |I_i|^2 + |V|^2 |I_O|^2} \quad (2\text{-}36)$$

$$\begin{cases} |I_i|^2 = |I_{1i}|^2 + |I_{hi}|^2 \\ |I_O|^2 = |I_{1O}|^2 + |I_{hO}|^2 \end{cases} \quad (2\text{-}37)$$

Where suffix h is the number of harmonics, D is the distortion power, U is the power associated with the unbalances and is named the unbalance power, and S' is the fundamental apparent power. All these powers are two by two orthogonal; $D \perp S'$, $U \perp S'$, $D \perp U$.

2.3 Depenbrock and Emanuel definition

According to physical concepts of apparent power these two authors define the effective power (S_e) as the maximum transmittable active power for a given rms value of the voltage and the given rms value of the current. This equivalence leads to the definition of an effective line current I_{eff} and an effective line-to-neutral voltage V_{eff}.

$$V_{eff} = \sqrt{V_{eff\,1}^2 + V_{eff\,h}^2}\,, \qquad I_{eff} = \sqrt{I_{eff\,1}^2 + I_{eff\,h}^2} \tag{2-38}$$

Where for a four-wire system:

$$I_{eff} = \sqrt{\frac{I_a^2 + I_b^2 + I_c^2 + I_n^2}{3}} \tag{2-39}$$

$$V_{eff} = \sqrt{{}^1\!/_{18}\,[V_{ab}^2 + V_{bc}^2 + V_{ca}^2 + 3(V_a^2 + V_b^2 + V_c^2)]} \tag{2-40}$$

The I_n denotes the neutral current.

The apparent power is defined consequently:

$$S_{eff} = V_{eff} . I_{eff} \tag{2-41}$$

They divide the apparent power into two main partitions, the active power (P) and the non-active power (N).

$$P_{(W)} = P_1 + P_h \tag{2-42}$$

$$N_{(var)} = \sqrt{S_{eff}^2 - P^2} \tag{2-43}$$

The indice h defines the harmonic number.

$$P_1 = P_{1d} + (P_{1i} + P_{1O}) \tag{2-44}$$

$$P_h = \sum_{h\neq 1}^{\infty} V_{ih} I_{ih} \cos(\theta_{ih}) \qquad i = a, b, c \tag{2-45}$$

$$S_{1d} = P_{1d} + jQ_{1d} = 3V_{eff\ 1d} I_{eff\ 1d} \tag{2-46}$$

$$S_{eff\ 1}^2 = S_{1d}^2 + S_{U1}^2 \tag{2-47}$$

The $S_{eff\ 1}$ is the fundamental effective apparent power. The reactive power (Q_{1d}) is the conventional power to determine the amount of capacitor bank needed to compensate the conventional power factor.

The fundamental positive-sequence power factor (PF_1) is obtained from the following equation and plays the same significant role that the fundamental power factor does in non-sinusoidal single phase systems.

$$PF_1 = \frac{P_{1d}}{S_{1d}} \tag{2-48}$$

The load unbalance is evaluated by the fundamental unbalanced power (S_{U1}) from the following equation.

$$S_{U\ 1}^2 = \sqrt{(3V_{eff\ 1} I_{eff\ 1})^2 - (3V_{eff\ 1d} I_{eff\ 1d})^2} \tag{2-49}$$

The apparent power is divided into the fundamental effective apparent power ($S_{eff\ 1}$) and the non-fundamental effective apparent power ($S_{eff\ N}$).

$$S_{eff}^2 = S_{eff\ 1}^2 + S_{eff\ N}^2 \tag{2-50}$$

$$S_{eff\ N} = 3\sqrt{(V_{eff\ h} I_{eff\ h})^2 + (V_{eff\ h} I_{eff\ 1})^2 + (V_{eff\ 1} I_{eff\ h})^2} \tag{2-51}$$

The non-fundamental effective apparent power ($S_{eff\ N}$) is resolved into three distinctive terms:

the harmonic apparent power (VA) $\qquad S_{eff\ h} = 3.V_{eff\ h}.I_{eff\ h}$ (2-52)

the voltage distortion power (var) $D_{eff\ V} = 3.V_{eff\ h}.I_{eff\ 1}$ (2-53)

the current distortion power (var) $D_{eff\ I} = 3.V_{eff\ 1}.I_{eff\ h}$ (2-54)

and the harmonic apparent power itself is divided into active and reactive parts:

$$S_{eff\ h} = P_h + jQ_h \tag{2-55}$$

By defining the equivalent total harmonic distortions as follow:

$$THD_{eff\ V} = {V_{eff\ h}}/{V_{eff\ 1}}, \qquad THD_{eff\ I} = {I_{eff\ h}}/{I_{eff\ 1}} \tag{2-56}$$

The non-fundamental effective apparent power is also obtained from:

$$S_{eff\ N} = S_{eff\ 1}\sqrt{(THD_{eff\ V}THD_{eff\ I})^2 + THD_{eff\ V}{}^2 + THD_{eff\ I}{}^2} \tag{2-57}$$

So the general power factor under this approach is:

$$PF = \frac{P}{S_{eff}} \tag{2-58}$$

2.4 Czarnecki definition

Czarnecki introduced the concept of orthogonal decomposition of the current in a three phase nonlinear asymmetrical load with non-sinusoidal voltage source first in march 1988 for three phase cases, an extension of single phase with only an additional orthogonal component due to the asymmetry. It has been shown that the source current can be decomposed into five orthogonal components which contribute to different physical phenomena.

The admittance of an asymmetrical load excited with sinusoidal waveforms has an equivalent conductance (G_e) and an equivalent susceptance (B_e).

$$Y_e = G_e + jB_e \tag{2-59}$$

$$G_e = \frac{P}{\left|\vec{V}\right|^2} \quad , \quad B_e = \frac{-Q}{\left|\vec{V}\right|^2} \tag{2-60}$$

Where

$$P \triangleq \Re\{V_a I_a^* + V_b I_b^* + V_c I_c^*\} \quad , \quad Q \triangleq \Im\{V_a I_a^* + V_b I_b^* + V_c I_c^*\} \tag{2-61}$$

The norm $|V|$ of vector V can be considered as its generalized rms value, and the asterisk denotes the complex conjugate.

Let us suppose that the voltage (v) is composed of harmonics (h) from a number set of N_v. The source current is divided into two main parts; I_w, current composed of harmonics order h from set N_v , and I_g, composed of the rests of harmonics. Since these two current components are composed of harmonics of different frequencies, they are mutually orthogonal, hence:

$$I = I_w + I_g \tag{2-62}$$

$$|I|^2 = |I_w|^2 + \left|I_g\right|^2 \quad , \quad I_w = \sum_{h \in N_v} I_h \tag{2-63}$$

Now the equivalent admittance of harmonics with the equivalent conductance G_{he} and the equivalent susceptance B_{he} is defined as follow;

$$G_{he} = \frac{P_h}{\left|\overrightarrow{V_h}\right|^2} \quad , \quad B_{he} = \frac{-Q_h}{\left|\overrightarrow{V_h}\right|^2} \tag{2-64}$$

Where $$\left|\overrightarrow{V_h}\right|^2 = \sqrt{V_{ah}^2 + V_{bh}^2 + V_{ch}^2} \tag{2-65}$$

Each harmonic component I_h of the current I_w can be decomposed into three parts, active I_{hA}, reactive I_{hR}, and the term associated with the unbalances I_{hU};

$$I_w = \sum_{h \in N_v} (I_{hA} + I_{hR} + I_{hU}) \tag{2-66}$$

Where

$$I_{hA} \triangleq G_{he} v_h \tag{2-67}$$

$$I_{hR} \triangleq B_{he} \frac{dv_h}{d(h\omega t)} \tag{2-68}$$

$$I_{hU} = I_h - (I_{hA} + I_{hR}) \tag{2-69}$$

Consequently the current is decomposed into five mutually orthogonal parts. First, the active part (I_A) which is indispensable for active power transmission. Second, the reactive part (I_R) which reciprocates energy transmission between the source and the energy accumulating components. Its presence is related to the presence of the harmonic reactive power (Q_h) and has some relations with the reactive power defined by Budeanu in non-sinusoidal cases. Third, the component related to the load asymmetry (I_U) called the "unbalanced current". Fourth, I_S the scattered current, I_g which is composed of current harmonics caused by the load nonlinearity or the periodical variance of its parameters, means the harmonics which are not made by the harmonics of the voltage.

$$I = I_A + I_R + I_U + I_S + I_g \tag{2-70}$$

Where $$I_A \triangleq G_e v \tag{2-71}$$

$$I_R = \sum_{h \in N_v} I_{hR} \tag{2-72}$$

$$I_S = \left(\sum_{h \in N_v} I_{hA} \right) - I_A \tag{2-73}$$

$$I_U = \sum_{h \in N_v} I_{hU} \tag{2-74}$$

$$I_g = \sum_{h \in N_g} I_h \qquad (N_g = all\ harmonic\ orders - N_v) \tag{2-75}$$

Which rms values fulfill the relation:

$$\left|\vec{I}\right|^2 = \left|\vec{I}_A\right|^2 + \left|\vec{I}_R\right|^2 + \left|\vec{I}_U\right|^2 + \left|\vec{I}_S\right|^2 + \left|\vec{I}_g\right|^2 \tag{2-76}$$

Where

$$\left|\vec{I}_A\right| = G_e \left|\vec{V}\right| \tag{2-77}$$

$$\left|\vec{I}_R\right| = \sqrt{\sum_{h \in N_v} B_{he}^2 \left|\overrightarrow{V_h}\right|^2} \tag{2-78}$$

$$\left|\vec{I}_U\right| = \sqrt{\sum_{h \in N_v} [\left|\vec{I}_h\right|^2 - (G_{he}^2 + B_{he}^2) \left|\overrightarrow{V_h}\right|^2]} \tag{2-79}$$

$$\left|\vec{I}_S\right| = \sqrt{\sum_{h \in N_v} (G_{he} - G_e) \left|\overrightarrow{V_h}\right|^2} \tag{2-80}$$

$$\left|\vec{I}_g\right| = \sqrt{\sum_{h \in N_g} \left|\vec{I}_h\right|^2} \tag{2-81}$$

By multiplying the current decomposition by $|\vec{V}|^2$, we obtain the power resulted from each term.

$$S^2 = P^2 + Q^2 + D_U^2 + D_S^2 + D_g^2 \tag{2-82}$$

2.5 Summary

In this chapter, three main definitions of electrical power in three-phase systems have been presented; the general definition including Budeanu's one, which is the main and the most global definition of electrical power and the principal reference for the other contributors who came after. Then Depenbrock and Emanuel definition which is a Budeanu's developed definition followed by a brief definition proposed by the author of this dissertation. Czarnecki's contribution in power definition is shown in a manner to understand clearly his theory of orthogonal decomposition of current and power. Each author divided the power from his view point.

The Budeanu's is the most used definition but it does not cover all aspects of unbalanced and scattered phenomena, even the power factor in some situation does not cover all non-active parts.

Depenbrock and Emanuel proposed a more complex study on the Budeanu's definitions and developed it in order to cover some concealed parts of the power. Their definition is practical and simple to be used with measurement instruments. There are still many debates in the interpretation of the apparent power which can be considered as the maximum active power transmittable for a given voltage waveform and the rms value of the current. Every slight difference of the interpretation of power leads to a new definition and in fact, all the definitions endeavor to improve the comprehension of their theory to deal with all or nearly all aspects of electrical power.

Czarnecki proposed a more attractive definition in which the current is divided into some parts contributing to a significant power. But there is yet some incompetency in this definition.

The main problem of all the mentioned theories is that those are defined in frequency domain and even phasor representation; that is, for converting them into time domain equations, they need complicated calculations and some integrator elements, which will exclude them from being

instantaneous in the time domain, and this is the most important point in the control algorithm of active filters. In the instantaneous study (time domain), it is possible to observe some oscillating powers which are not visible in phasor study. These differences will be discussed and clarified in the next chapter, focused on time domain approaches and particularly Akagi's theory.

J. L. Willems and G. D. Marques are other authors, who made some important contributions in this field. Willems theory has a great similarity with Emanuel. Marques uses G. Darrieus's theory of reactive power [23] to make the Active filter controller. Darrieus theory is much complicated and uses many integral equations to detect the reference current for his compensation current which make the controller more complex and gives it more undesired impact, hence it is more theoretical than practically useful compared to Akagi's theory.

CHAPITRE 3 INSTANTANEOUS POWER THEORIES AND SIMULATIONS

3.1 Introduction

It has been shown that classical definitions of electric power; active, reactive and apparent power do not fulfill the conditions caused by harmonics. Consequently, various power definitions and calculation methods have been proposed to cover the matter as much as possible. Accordingly some power definitions were discussed and compared for non-sinusoidal conditions from the literature in the previous chapter.

For single phase power systems, the concepts such as active and reactive power, active and reactive current, and power factor are well defined. Various attempts have been proposed to generalize these concepts to the three phase case with unbalanced and distorted currents and voltages, some of them were studied in the previous chapter.

This chapter is consecrated to Akagi's theory and other contributors to this theory. In the p-q theory, Akagi introduces the concept of instantaneous reactive power to generalize the classical reactive power concept for single phase sinusoidal systems to the three-phase non-sinusoidal situation.

The Akagi's concept is very interesting for practical purposes, in particular to analyze the instantaneous compensation of reactive power without energy storage. Then the Generalized theory, which is a more complex theory based on vector calculations applicable to multiple phase systems, is presented. This theory is the newest one for instantaneous compensations found in the literature. After that the Willems solution, which is a simple and efficient way for reducing the calculation process, is presented. The Willems theory is based on the p-q theory and the orthogonal decomposition of currents. Finally these three calculation methods are compared.

In the next phase of the project the theoretical knowledge is used to simulate an active filter in MATLAB-Simulink and then in the RT-Lab environment. The simulations have been tested to insure the effectiveness of the model.

3.2 Instantaneous p-q Theory

Akagi introduces this concept first at the Japanese conference in 1982. After that, many authors developed the idea and made their contribution to this domain. Today, most active filters of industrial scale use this theory for their control blocks. The time domain approach proposed by Akagi Nabae under the name of "p-q theory" or "instantaneous power theory" is the most widely spread theory for two or three phase and three or four wire systems. Between various theories on three and four wire instantaneous reactive power of three and four wire systems, the Akagi theory is the most attractive method. Indeed, this approach, compared to others, uses simple calculations, without involving integration or any passive filters to compensate harmonics in the system.

The "p-q theory" of Akagi uses the Clark transformation to transform voltages and currents from three phases 'abc' to two phase system 'αβ0', and then defines *instantaneous active* and *reactive power*. Hence, these two instantaneous powers differ from conventional active and reactive power definitions such as Budeanu definition defined for the frequency domain. This method is applicable to two or three phase systems with or without ground wire and can be applied to some extent to multi-phase system compensation.

In a three-phase with 3 or 4 wires system, the instantaneous voltages and currents can be described as instantaneous space vector *v* and *i* as mentioned in the previous chapter, and using the Clark transformation, they become in αβ0 coordinates:

$$\boldsymbol{i}_{\alpha\beta 0} = \begin{bmatrix} i_\alpha \\ i_\beta \\ i_0 \end{bmatrix} = \underbrace{\sqrt{\frac{2}{3}} \begin{bmatrix} 1 & -1/2 & -1/2 \\ 0 & \sqrt{3}/2 & -\sqrt{3}/2 \\ 1/\sqrt{2} & 1/\sqrt{2} & 1/\sqrt{2} \end{bmatrix}}_{\boldsymbol{C}} \times \begin{bmatrix} i_a \\ i_b \\ i_c \end{bmatrix} \tag{3-1}$$

$$\boldsymbol{v}_{\alpha\beta 0} = \begin{bmatrix} v_\alpha \\ v_\beta \\ v_0 \end{bmatrix} = \boldsymbol{C} \times \begin{bmatrix} v_{an} \\ v_{bn} \\ v_{cn} \end{bmatrix} \tag{3-2}$$

Additionally by multiplying the Clark matrix into the sequence transformation matrix, a third matrix is obtained. This matrix relates the sequence components to the αβ0 components.

$$\boldsymbol{T} = \frac{1}{3}\begin{bmatrix} 1 & \delta & \delta^2 \\ 1 & \delta^2 & \delta \\ 1 & 1 & 1 \end{bmatrix} \qquad (\delta = e^{j\left(\frac{2\pi}{3}\right)}) \tag{3-3}$$

$$\boldsymbol{M} = \boldsymbol{C} \times \boldsymbol{T}^{-1} = \sqrt{\frac{2}{3}}\begin{bmatrix} 0 & {}^{3}/_{2} & {}^{3}/_{2} \\ 0 & {}^{3}/_{2}\, e^{-j\pi/2} & {}^{3}/_{2}\, e^{j\pi/2} \\ {}^{3}/_{\sqrt{2}} & 0 & 0 \end{bmatrix} \tag{3-4}$$

$$\boldsymbol{V}_{\alpha\beta 0} = \boldsymbol{M} \times \boldsymbol{V}_{seq} = \boldsymbol{M} \times \begin{bmatrix} V_+ \\ V_- \\ V_0 \end{bmatrix} \tag{3-5}$$

In the p-q theory, instantaneous powers are defined as follow:

$$\begin{bmatrix} p \\ q \\ p_0 \end{bmatrix} = \underbrace{\begin{bmatrix} v_\alpha & v_\beta & 0 \\ v_\beta & -v_\alpha & 0 \\ 0 & 0 & v_0 \end{bmatrix}}_{\boldsymbol{B}} \begin{bmatrix} i_\alpha \\ i_\beta \\ i_0 \end{bmatrix} \tag{3-6}$$

In fact the instantaneous active power is the same as what was described in the past chapter. The instantaneous active power can be rewritten in the αβ0 coordinates.

$$p_{3\varphi} = \vec{v} \cdot \vec{\imath} = v_{an}\, i_a + v_{bn}\, i_b + v_{cn}\, i_c = v_\alpha i_\alpha + v_\beta i_\beta + v_0 i_0 = p + p_0 \tag{3-7}$$

The instantaneous active power is equal to the sum of real power p and the zero-sequence power p_0. In the case of a three-phase three wire system, p_0 doesn't exist and the $p_{3\varphi}$ is equal to p.

The reactive power defined by Akagi is different from the reactive power defined in the past chapters (Akagi named this power as *imaginary power q*). This power is a time domain and some terms, which are eliminated in the frequency domain, are present here. Thus they should not be confused together.

$$q = v_\beta\, i_\alpha - v_\alpha\, i_\beta \tag{3-8}$$

For a three-phase with three wire circuit where p_0 is absent and zero-sequence components are excluded, we can define the apparent power as follow:

$$v = v_\alpha + jv_\beta \qquad i = i_\alpha + ji_\beta \tag{3-9}$$

$$s = v.i^* = p + jq = \left(v_\alpha i_\alpha + v_\beta i_\beta\right) + j(v_\beta i_\alpha - v_\alpha i_\beta) \tag{3-10}$$

The current can be obtained in reverse sequences, from the two powers. Hence the current could be decomposed into two parts; active and reactive currents.

$$\begin{bmatrix} i_\alpha \\ i_\beta \end{bmatrix} = \frac{1}{{v_\alpha}^2 + {v_\beta}^2} \begin{bmatrix} v_\alpha & v_\beta \\ v_\beta & -v_\alpha \end{bmatrix} \begin{bmatrix} p \\ q \end{bmatrix} \tag{3-11}$$

So each current in orthogonal axis is decomposed into active and reactive part.

$$\begin{bmatrix} i_\alpha \\ i_\beta \end{bmatrix} \triangleq \overbrace{\begin{bmatrix} i_{\alpha p} \\ i_{\beta p} \end{bmatrix}}^{i_p} + \overbrace{\begin{bmatrix} i_{\alpha q} \\ i_{\beta q} \end{bmatrix}}^{i_q} = \frac{1}{{v_\alpha}^2 + {v_\beta}^2} \begin{bmatrix} v_\alpha & v_\beta \\ v_\beta & -v_\alpha \end{bmatrix} \begin{bmatrix} p \\ 0 \end{bmatrix} + \frac{1}{{v_\alpha}^2 + {v_\beta}^2} \begin{bmatrix} v_\alpha & v_\beta \\ v_\beta & -v_\alpha \end{bmatrix} \begin{bmatrix} 0 \\ q \end{bmatrix} \tag{3-12}$$

Instantaneous active currents on the α and β axis are obtained ($i_{\alpha p}, i_{\beta p}$), as well as instantaneous reactive currents ($i_{\alpha q}, i_{\beta q}$).

If we suppose a balanced source voltage ($v_0 = 0$), for a three-phase system with or without ground wire, the instantaneous reactive power (which should be compensated) from p-q theory is:

$$\boldsymbol{i}_{q\ (p-q\ theory\ )} = \frac{1}{\sqrt{3}} \begin{bmatrix} i_0 \\ i_0 \\ i_0 \end{bmatrix} + \boldsymbol{C}^{-1} \times \begin{bmatrix} i_{\alpha q} \\ i_{\beta q} \\ 0 \end{bmatrix} \tag{3-13}$$

Where i_0 is the zero-sequence component and:

$$i_{\alpha q} = \frac{v_\beta}{{v_\alpha}^2 + {v_\beta}^2} \times q_{(p-q\ theory\ )} = \frac{\sqrt{6}\left(-\frac{v_{an}}{4} - \frac{v_{bn}}{4}\right)(v_{an} i_b - v_{bn} i_a)}{{v_{an}}^2 + {v_{bn}}^2 + v_{an} v_{bn}} \tag{3-14}$$

$$i_{\beta q} = \frac{-v_\alpha}{{v_\alpha}^2 + {v_\beta}^2} \times q_{(p-q\ theory\ )} = \frac{\frac{3v_{an}}{\sqrt{2}}\ (v_{an} i_b - v_{bn} i_a)}{{v_{an}}^2 + {v_{bn}}^2 + v_{an} v_{bn}} \tag{3-15}$$

The active portions are obtained as follow:

$$i_{\alpha p} = \frac{v_\alpha}{{v_\alpha}^2 + {v_\beta}^2} \times p = \frac{\sqrt{\frac{3}{2}}(2{v_{an}}^2 i_a + 2v_{an} v_{bn} i_b + v_{an} v_{bn} i_a + {v_{an}}^2 i_b)}{{v_{an}}^2 + {v_{bn}}^2 + v_{an} v_{bn}} \tag{3-16}$$

$$i_{\beta p} = \frac{v_\beta}{{v_\alpha}^2 + {v_\beta}^2} \times p = \frac{\frac{1}{\sqrt{2}}(2v_{bn} + v_{an})(2v_{an} i_a + 2v_{bn} i_b + v_{bn} i_a + v_{an} i_b)}{{v_{an}}^2 + {v_{bn}}^2 + v_{an} v_{bn}} \tag{3-17}$$

By mean of the previous decomposition, the power on each axis is obtained. The instantaneous active and reactive powers (as named by Akagi) in α and β axis are established. Note that Akagi call the $p_{\alpha q}$ and $p_{\beta q}$ as reactive powers and they should not be confused with the "q", which Akagi named it as the imaginary power.

$$p = v_\alpha i_{\alpha p} + v_\alpha i_{\alpha q} + v_\beta i_{\beta p} + v_\beta i_{\beta q} = \tag{3-18}$$

$$\frac{{v_\alpha}^2}{{v_\alpha}^2 + {v_\beta}^2} p + \frac{v_\alpha v_\beta}{{v_\alpha}^2 + {v_\beta}^2} q + \frac{{v_\beta}^2}{{v_\alpha}^2 + {v_\beta}^2} p + \frac{-v_\beta v_\alpha}{{v_\alpha}^2 + {v_\beta}^2} q = \tag{3-19}$$

$$p_{\alpha p} + p_{\alpha q} + p_{\beta p} + p_{\beta q} = p_{\alpha p} + p_{\beta p} \qquad (p_{\alpha q} + p_{\beta q} = 0) \tag{3-20}$$

As demonstrated, the sum of the two reactive powers $p_{\alpha q}$ and $p_{\beta q}$ is zero. They don't have a contribution to the active power, and consequently they can be compensated without disturbing the active power transmission and the energy flow from the source to the load. The unit of all these four powers is watt (W) because each power is defined by the product of the voltage and a part of instantaneous current on the same axis.

In presence of both voltage and current zero-sequences, for a three phase with four wire system, the p_0 will not be absent. Akagi proposes not to compensate the zero-sequence power. This suggestion was based on some reasons like the need of a storage element for compensating the p_0. The formulas become as follows:

$$\boldsymbol{B}^{-1} = \begin{bmatrix} \frac{v_\alpha}{{v_\alpha}^2 + {v_\beta}^2} & \frac{v_\beta}{{v_\alpha}^2 + {v_\beta}^2} & 0 \\ \frac{v_\beta}{{v_\alpha}^2 + {v_\beta}^2} & \frac{-v_\alpha}{{v_\alpha}^2 + {v_\beta}^2} & 0 \\ 0 & 0 & \frac{1}{v_0} \end{bmatrix} \tag{3-21}$$

$$= \frac{1}{{v_0}^2({v_\alpha}^2 + {v_\beta}^2)} \begin{bmatrix} {v_0}^2 v_\alpha & {v_0}^2 v_\beta & 0 \\ {v_0}^2 v_\beta & -{v_0}^2 v_\alpha & 0 \\ 0 & 0 & v_0({v_\alpha}^2 + {v_\beta}^2) \end{bmatrix}$$

Moreover the current are divided as follow:

Instantaneous active current $\boldsymbol{i}_p(\alpha\beta 0) = \boldsymbol{B}^{-1} \times \begin{bmatrix} p \\ 0 \\ p_0 \end{bmatrix} \rightarrow \ \boldsymbol{i}_p = \boldsymbol{C}^{-1} \times \boldsymbol{i}_p(\alpha\beta 0)$ (3-22)

Instantaneous reactive power $\boldsymbol{i}_q(\alpha\beta 0) = \boldsymbol{B}^{-1} \times \begin{bmatrix} 0 \\ q \\ 0 \end{bmatrix} \rightarrow \boldsymbol{i}_{q\ (p-q\ theory)} = \boldsymbol{C}^{-1} \times$ (3-23)

$\boldsymbol{i}_q(\alpha\beta 0)$

Equivalent functions of the above powers for a general case including distortion and unbalances in the voltages and currents in time can be derived by the transformation matrix $\boldsymbol{M}$ from the sequence phasors. Hence, rewriting the harmonic currents and voltages in αβ0 coordinates in terms of symmetrical components in the time domain, yields the following expressions:

$$\begin{cases} v_\alpha = \sqrt{3} \sum_{h=1}^{\infty} [V_{hd}\, sin(h\omega t + \alpha_{hd}) + V_{hi}\, sin(h\omega t + \alpha_{hi})] \\ v_\beta = \sqrt{3} \sum_{h=1}^{\infty} [-V_{hd}\, cos(h\omega t + \alpha_{hd}) + V_{hi}\, cos(h\omega t + \alpha_{hi})] \\ v_0 = \sqrt{6} \sum_{h=1}^{\infty} V_{h0}\, sin(h\omega t + \alpha_{h0}) \end{cases} \tag{3-24}$$

The *d, i, 0* notice the direct, inverse and zero-sequence, and *h*, the harmonic order. Similar equations are written for currents.

The powers are as follow:

$$\bar{p}_0 = \sum_{h=1}^{\infty} 3V_{h0} I_{h0}\, cos(\alpha_{h0} - \delta_{h0}) \tag{3-25}$$

$$\bar{p} = 3\sum_{h=1}^{\infty} V_{hd} I_{hd}\, cos(\alpha_{hd} - \delta_{hd}) + V_{hi} I_{hi}\, cos(\alpha_{hi} - \delta_{hi}) \tag{3-26}$$

$$\bar{q} = 3\sum_{h=1}^{\infty} V_{hd} I_{hd}\, sin(\alpha_{hd} - \delta_{hd}) - V_{hi} I_{hi}\, sin(\alpha_{hi} - \delta_{hi}) \tag{3-27}$$

$$\tilde{p}_0 = 3\left\{\sum_{\substack{g=1 \\ h\neq g}} \left[\sum_{h=1}^{\infty} V_{g0} I_{h0}\, cos\big((\omega_g - \omega_h)t + \alpha_{g0} - \delta_{g0}\big)\right] - \sum_{g=1} \left[\sum_{h=1}^{\infty} V_{g0} I_{h0}\, cos\big((\omega_g - \omega_h)t + \alpha_{g0} - \delta_{g0}\big)\right]\right\} \tag{3-28}$$

$$\begin{aligned}\tilde{p} = 3\Bigg\{&\sum_{\substack{g=1 \\ h\neq g}} \left[\sum_{h=1}^{\infty} V_{gd} I_{hd}\, cos\big((\omega_g - \omega_h)t + \alpha_{gd} - \delta_{hd}\big)\right] \\ &- \sum_{g=1} \left[\sum_{h=1}^{\infty} V_{gd} I_{hi}\, cos\left(\big(\omega_g + \omega_h\big)t + \alpha_{gd} + \delta_{hi}\right)\right] \\ &+ \sum_{\substack{g=1 \\ h\neq g}} \left[\sum_{h=1}^{\infty} V_{gi} I_{hi}\, cos\big((\omega_g - \omega_h)t + \alpha_{gi} - \delta_{hi}\big)\right] \\ &- \sum_{g=1} \left[\sum_{h=1}^{\infty} V_{gi} I_{hd}\, cos\left(\big(\omega_g + \omega_h\big)t + \alpha_{gi} + \delta_{hd}\right)\right]\Bigg\}\end{aligned} \tag{3-29}$$

$$\tilde{q} = 3\left\{\sum_{\substack{g=1 \\ h\neq g}}\left[\sum_{h=1}^{\infty} V_{gd} I_{hd}\, sin\big((\omega_g - \omega_h)t + \alpha_{gd} - \delta_{hd}\big)\right]\right. \tag{3-30}$$

$$-\sum_{g=1}\left[\sum_{h=1}^{\infty} V_{gd} I_{hi}\, sin\left(\big(\omega_g + \omega_h\big)t + \alpha_{gd} + \delta_{hi}\right)\right]$$

$$-\sum_{\substack{g=1 \\ h\neq g}}\left[\sum_{h=1}^{\infty} V_{gi} I_{hi}\, sin\big((\omega_g - \omega_h)t + \alpha_{gi} - \delta_{hi}\big)\right]$$

$$\left.+\sum_{g=1}\left[\sum_{h=1}^{\infty} V_{gi} I_{hd}\, sin\left(\big(\omega_g + \omega_h\big)t + \alpha_{gi} + \delta_{hd}\right)\right]\right\}$$

Where ω is the angular frequency ($\omega_h = h.\omega$) and the δ is the current phase. These generic expressions elucidate the instantaneous powers in term of conventional equations in time domain.

Since The imaginary power q, does not contribute to the total energy flow between the source and the load, it can be compensated without disturbing the active power. The imaginary power is proportional to the quantity of energy that is being exchanged between phases, and its unit is defined as “Volt-ampere imaginary (vai)” by Akagi.

The figure 3.1 tries to give a physical meaning to instantaneous powers. The total instantaneous energy flow per time unit (p) from the source to the non linear load, and the energy exchanged between the phases without transferring energy to the load (q) are presented.

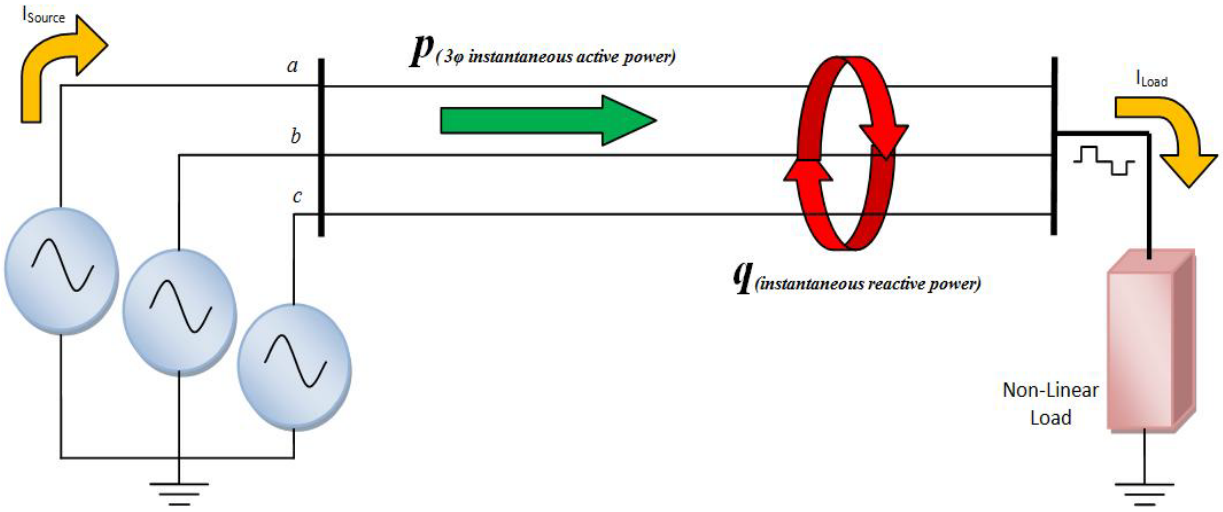

Fig. 3.1 Schema to better understand the physical meaning of the instantaneous powers

It has been demonstrated that by compensating the reactive part of the current not only a major part of harmonics are compensated, furthermore a unity conventional power factor is also obtained ($\cos \emptyset \cong 1$). The figure 3.2 demonstrates a compensation of the whole reactive power for a distorted current with an angle of $\pi/6$ radian. The result of this compensation is shown in the table 3.1.

Table 3.1 Instantaneous reactive compensation

	Load	**Source**
Total current (*I*)	1.1964 A	0.969 A
Fundamental (I_1)	1.15 A	0.955 A
Harmonic currents (I_h)	0.3299 A	0.1572 A
THD (C_{dis})	0.2869	0.16464

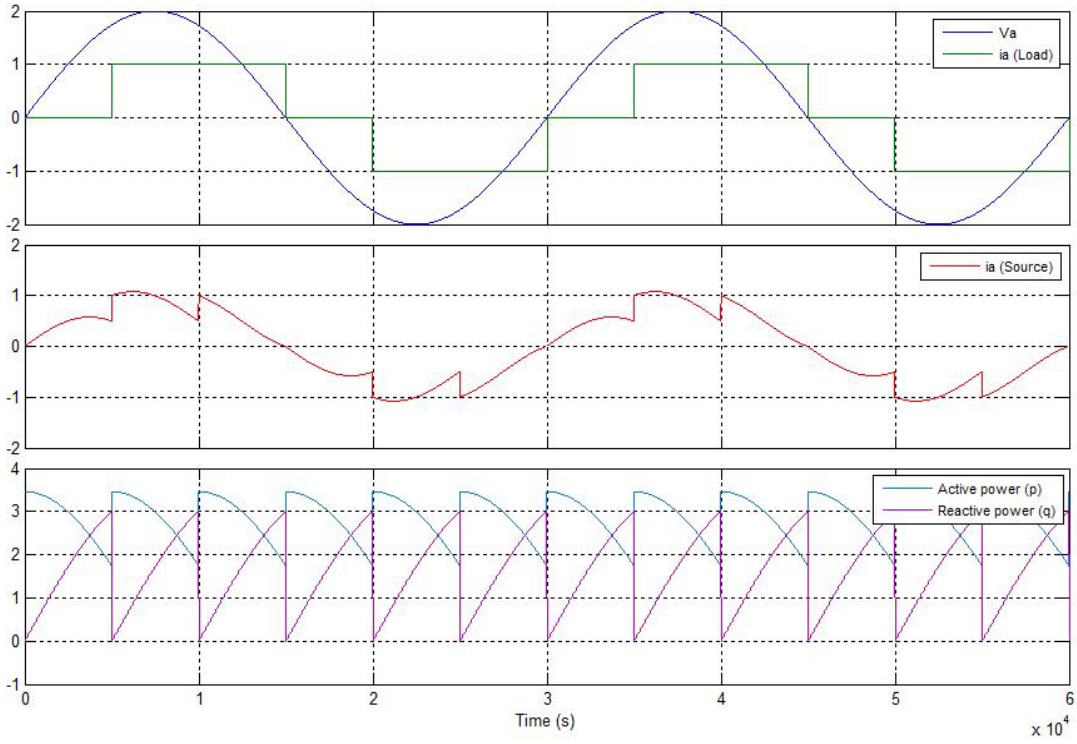

Fig. 3.2 Load voltage and current, source current, Instantaneous powers

The only problem caused by this compensation is the generation of some higher harmonics order. The problem of appearance of hidden harmonics is solved by compensating all the non active power which will be clarified. The quality of this compensation depends on the oscillating active power ($\tilde{p}$) which is not compensated.

The result of the simulation for a three phase three wire system, using the Opal-RT real-time simulator is shown in figure 3.3. It is possible to observe a better shape of current after compensation. The figure shows that a complete compensation of the imaginary power result to a smoother current, and the angle between voltage and current is eliminated and $\cos \emptyset \cong 1$ is achieved.

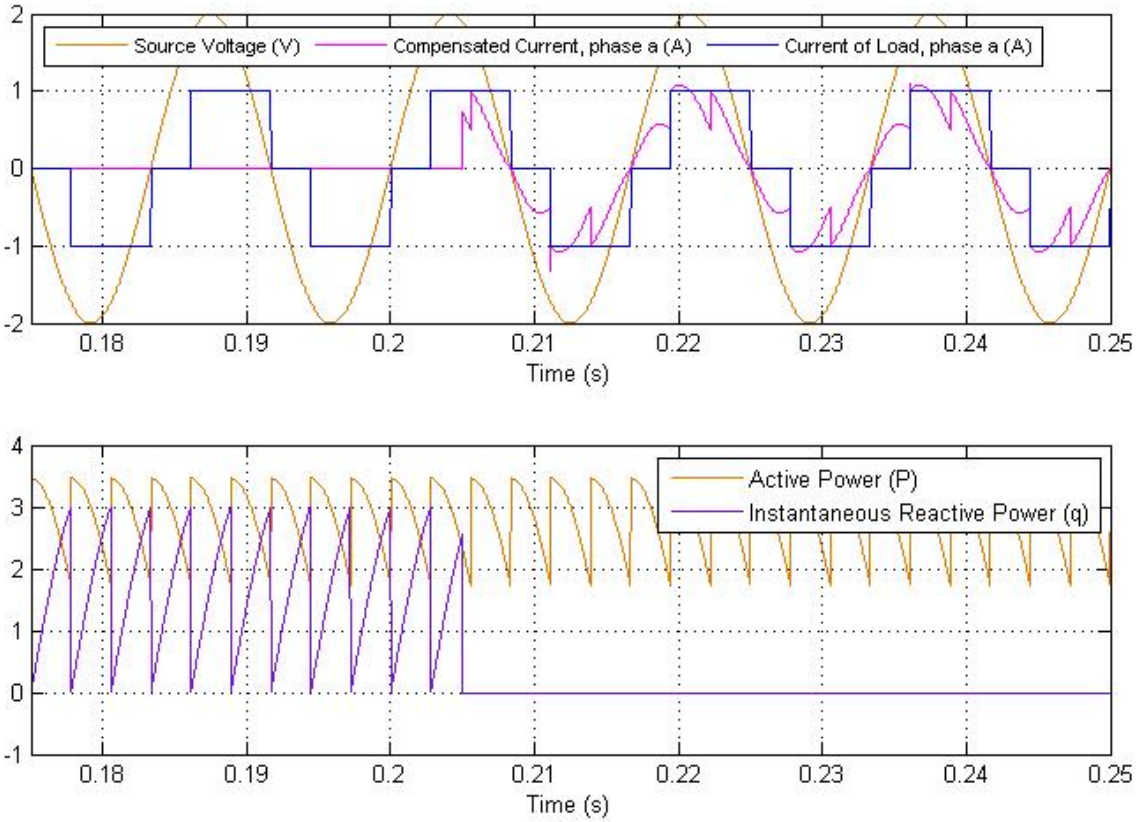

Fig. 3.3 Instantaneous reactive compensation (q)

The active filter starts to process the data (voltages and currents) at 0.205 s and at the same instant the PWM inverter begins to inject harmonic cancellation currents. The frequency of the source is 60 Hz and the load is a controlled rectifier with a thyristor firing angle α of 30°. As shown in Fig. 3.3, the response is immediate and a good transient response is achieved. The active filter does not compensate the oscillating active power ($\tilde{p}$), so it is possible to observe some harmonics in phase 'a' current. However, the harmonic currents are greatly reduced. The instantaneous voltage and current of the source are in phase, and the compensation objective of a unity displacement power factor is met.

Both active and reactive powers can be divided into a constant amplitude component and an oscillating component: $p = \bar{p} + \tilde{p}$ and $q = \bar{q} + \tilde{q}$. The effects of compensating the imaginary power were studied. For a full compensation of harmonics, without power factor compensation, only the oscillating part of the two powers should be compensated. In order to completely compensate all non active powers, the total imaginary power and the oscillating part of the active

power should be compensated. With this compensation, a sinusoidal wave form and unity power factor is achieved.

Finally from the Akagi theory it is possible to extract three types of compensation;

- The sinusoidal compensation, in which the $(\tilde{p} + \tilde{q})$ should be compensated. The sinusoidal current alternative implies a balanced sinusoidal voltage source. This case requires the utilization of a passive filter in order to obtain the components of the instantaneous active power and a PLL is also needed to extract the balanced fundamental component of the three-phase system. These fundamental voltages are then used by the controller as voltage references.
- The instantaneous imaginary power compensation, the imaginary power (q) is totally compensated. This compensation has been studied formerly.
- Instantaneous non-active power compensation requires the compensation of the instantaneous imaginary power and oscillating part of the instantaneous active power $(\tilde{p} + q)$. The sum of these two powers contributes to build the instantaneous non-active power.

For a four wire system, where the zero-sequence current exists, depending on whether the source voltage has a zero-sequence, the compensation approach changes. If the source voltage contains zero-sequence, this voltage imbalances and the load zero-sequence initiates the zero-sequence power p_0. If the active filter is designed with no energy storage devices, it could not compensate the zero-sequence power. But if the active filter is built with energy storage devices, it will be able to compensate the zero sequence power. The zero-sequence power contains an oscillating part associated to an average value. In the case of an optimal power flow to the source the zero sequence power (p_0), imaginary (reactive) power (q), oscillating part of the active power $(\tilde{p})$, should be compensated to keep only the average of the active power $(\bar{p})$. In a four wire system it is possible to distinguish six kinds of instantaneous power shown in the table 3.2.

Table 3.2 Instantaneous powers

	Constant value	**Oscillating Value**
Instantaneous active power ($p = \bar{p} + \tilde{p}$)	$\bar{p}$	$\tilde{p}$
Instantaneous imaginary power ($q = \bar{q} + \tilde{q}$)	$\bar{q}$	$\tilde{q}$
Instantaneous zero-sequence power ($p_0 = \bar{p}_0 + \tilde{p}_0$)	$\bar{p}_0$	$\tilde{p}_0$

Each power is divided in its average and oscillating portion. It should be noticed that the zero-sequence power could be interpreted as a single phase system between the source and the load. As known in a single phase system, if the instantaneous power contains an oscillating portion, it is not possible to compensate it without compensating its average one. Consequently if the active filter must compensate the zero sequence power, it must be able to compensate the average power of this one, which requires a storage element in the active filter.

In the absence of the voltage zero-sequence ($p_0 = 0$), and for the first objective, similar results are obtained for a three-phase, four-wire system. The main difference is that the neutral current i_0 of the load is totally compensated by the active filter and the source does not provide any zero-sequence current. The compensation is instantaneous and a good transient response is obtained. The absence of any passive filter or PLL in the current and voltage measurement paths explains the absence of any delay and the immediate response of the controller.

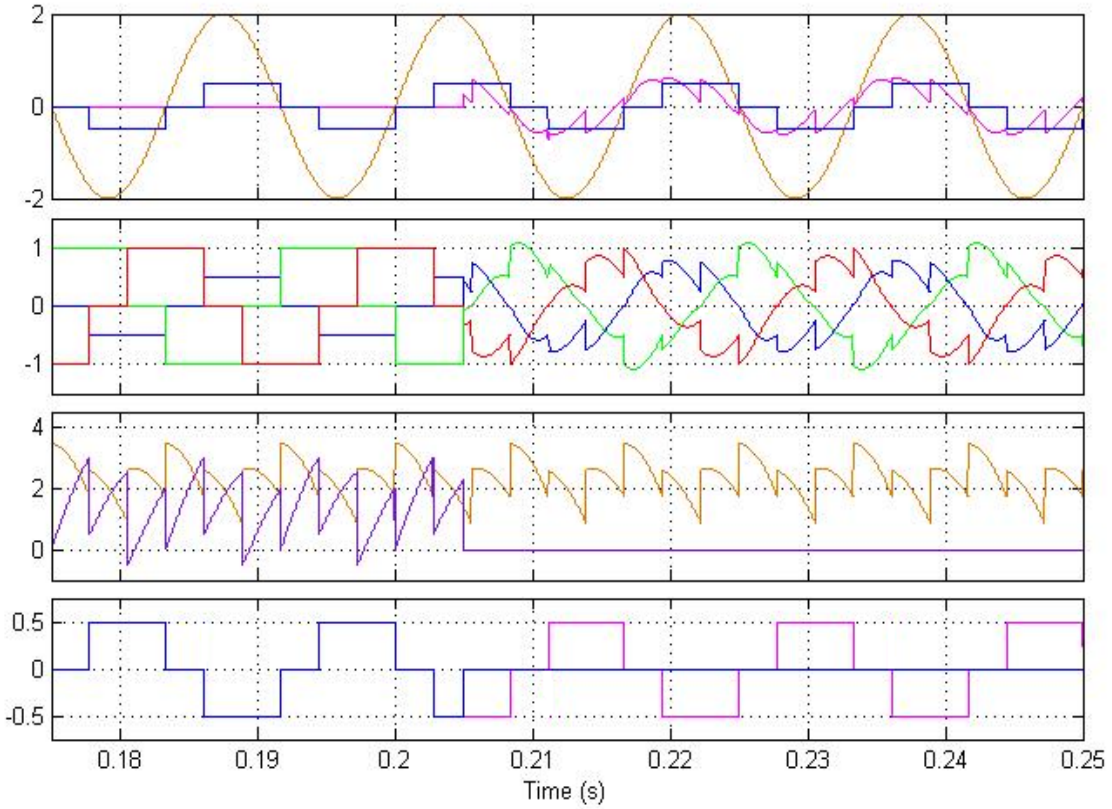

Fig. 3.4 Phase "a" voltage and current of load and source, source currents, instantaneous active and reactive power, load and source zero sequence current (i_0)

Two other different objectives can be assigned to the active filter: the three-phase source should supply constant power or the source currents should be perfectly sinusoidal. The constant power case requires to totally compensating the non-active power, which is: $\tilde{p} + q$ while the sinusoidal current alternative implies, in the case of a balanced sinusoidal voltage source, a perfect sinusoidal current waveform and unity power factor. Both of these cases require the utilization of a passive filter in order to obtain the components of the instantaneous active power and, in the second case, a PLL is also needed to extract the balanced fundamental component of the three-phase system. These fundamental voltages are then used by the controller as voltage references.

In both cases, the response is sluggish. The problem is present for both three and four wire systems.

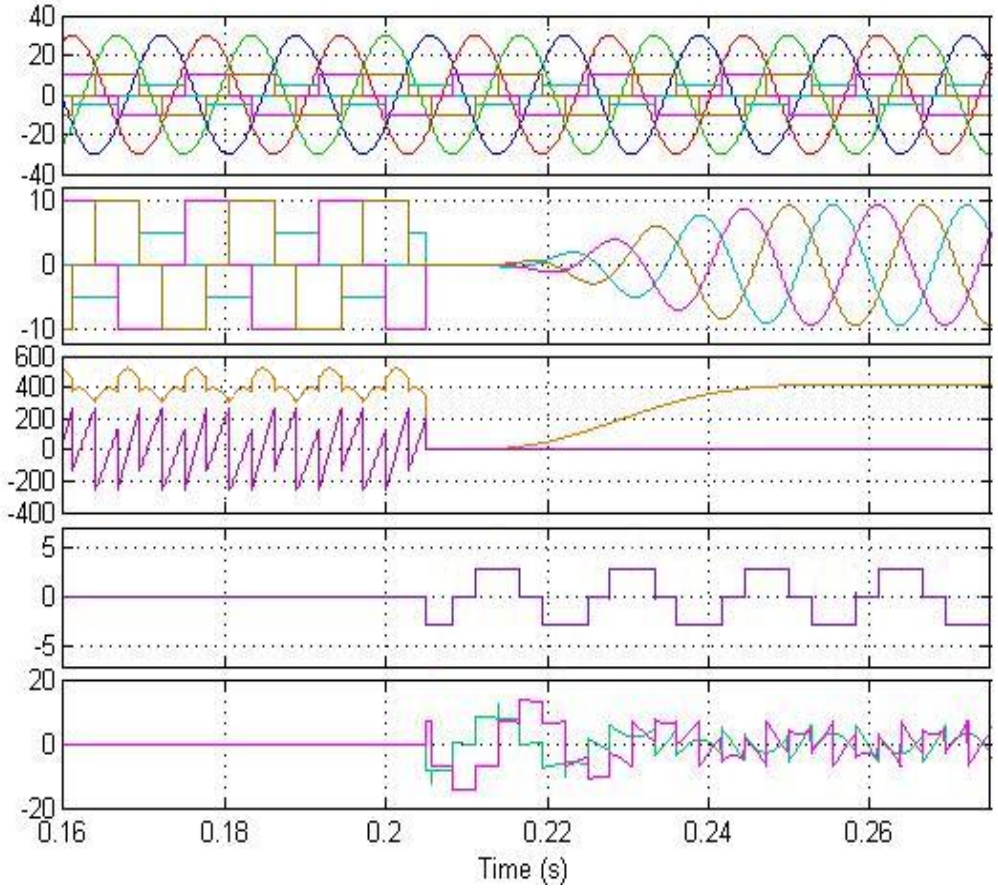

Fig. 3.5 a) load voltages and currents b) source currents c) instantaneous active and reactive power d) active filter zero-sequence current (i_0), e) compensation currents ($i_{C\alpha}, i_{C\beta}$)

Figure 3.5 depicts the constant power compensation case. The active filter starts acting at 0.205 s. At this particular instant, the controller begins to read the input data and the PWM inverter is turned on. Contrarily to the first implementation, a delay exists between the instant when the controller is activated (0.205s) and the instant when the source provides the desired constant power (0.24 s). The presence of a passive filter inside the active filter to separate the constant power component ($\overline{p}$) from its oscillating counterpart ($\widetilde{p}$) explains this poor response of the active filter.

In this case, a fifth-order Bessel low pass filter with a cutoff frequency of 25 Hz is used to extract $\tilde{p}$ from the instantaneous active power (p). The difference between the average value of the instantaneous active power ($\bar{p}$) obtained from the Bessel filter and the exact $\bar{p}$ becomes one of the inputs of the active filter. Therefore, it is important to take some precaution in order to avoid that the active filter supplies all the active power of the load at the turn on instant. The

power signal derived from the Bessel low pass filter slowly increases to reach its final value after 2 to 3 cycles. The problem exists, but is less serious, in the case of a sudden load variation.

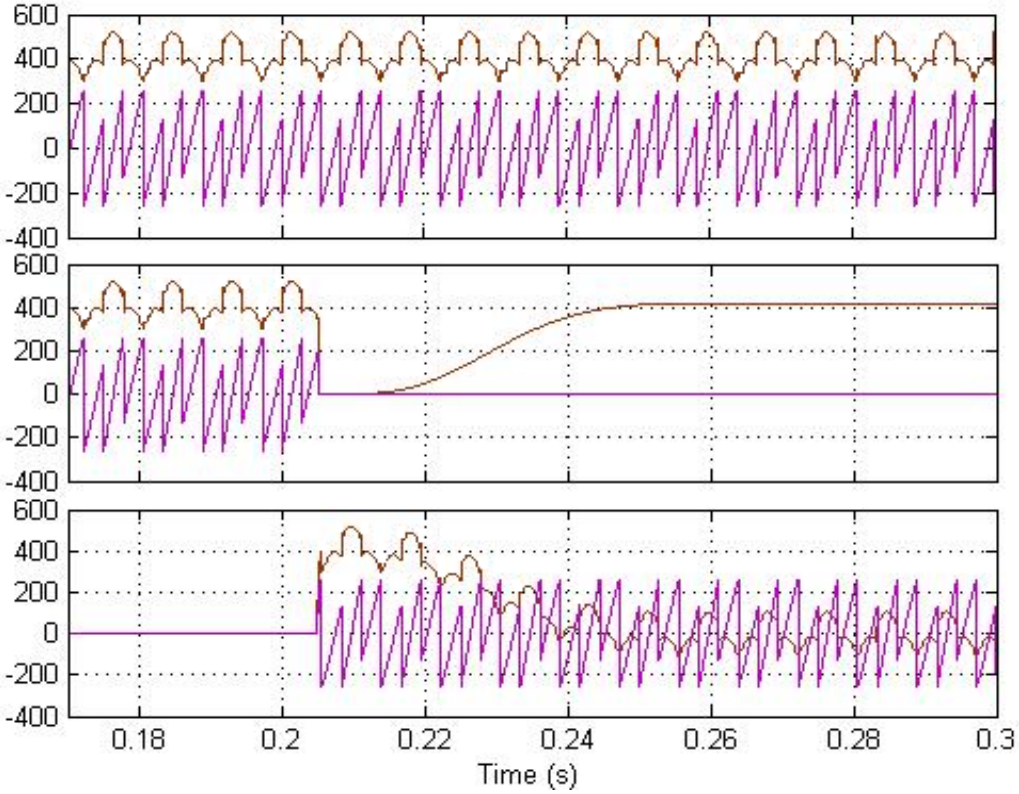

Fig. 3.6 Load, source, and active filter instantaneous active and reactive power

In figure 3.6 it is possible to observe the power supplied by each component. The third graph shows the active filter active and reactive powers. At the beginning, the active filter must supply all the active Power ($\tilde{p}$). In steady state, the active filter provides only the oscillating component. Since the active filter structure for a three or a four-wire system is similar, the problem exists in both situations. A structure of a three-phase three-wire active filter is showed in the figure 4.15.

3.3 Generalized instantaneous reactive power

The Generalized theory of instantaneous reactive power is based on vector calculations. This theory tries to introduce a global multiphase definition. F. Z. Peng and X. Dai are the main authors who contributed to this theory in [13, 28]. Their approaches are quite simpler than the p-q theory, but still some important considerations should be taken into account when using this theory for the controller. This method has the same abilities than the p-q theory. It should be kept in mind that zero sequence voltages is introduced in calculations and manipulating homopolar mode (zero-sequence) with non-homopolar components can produce undesirable effects. The p-q theory suggests compensating the zero-sequence current completely but, using the generalized theory, this power is even divided into the active and the reactive power depending on the presence of the zero-sequence voltage.

Accordingly, as mentioned before, the instantaneous voltages and currents are described as instantaneous space vector *v* and *i*. Their corresponding vectors in *αβ0* coordinates are obtained by the use of Clark's transformer matrix. The generalized powers are defined as follows; the active power remains the same as described previously:

$$p_{3\varphi} = \vec{v} \cdot \vec{\imath} = v_{an} i_a + v_{bn} i_b + v_{cn} i_c = v_\alpha i_\alpha + v_\beta i_\beta + v_0 i_0 = p + p_0 \tag{3-31}$$

The reactive power which is the purpose of this theory is defined as follows:

$$\vec{q} \triangleq \vec{v} \times \vec{\imath} \tag{3-32}$$

Where "·" is the internal product of vectors and "×" denotes the external products of vectors.

$$\vec{q}_{abc} = [q_a \quad q_b \quad q_c]^T = \vec{v}_{abc} \times \vec{\imath}_{abc} = \begin{bmatrix} v_{bn} i_c - v_{cn} i_b \\ v_{cn} i_a - v_{an} i_c \\ v_{an} i_b - v_{bn} i_a \end{bmatrix} \tag{3-33}$$

And also for the αβ0 coordinates:

$$\vec{q}_{\alpha\beta 0} = [q_\alpha \quad q_\beta \quad q_0]^T = \vec{v}_{\alpha\beta 0} \times \vec{\imath}_{\alpha\beta 0} = \begin{bmatrix} v_\beta i_0 - v_0 i_\beta \\ v_0 i_\alpha - v_\alpha i_0 \\ v_\alpha i_\beta - v_\beta i_\alpha \end{bmatrix} \tag{3-34}$$

These two powers are related together as follows:

$$\boldsymbol{q}_{\alpha\beta 0} = \boldsymbol{C} \times \boldsymbol{q}_{abc} \tag{3-35}$$

Even more the concept of instantaneous reactive power from the p-q theory could be considered as a special case of the concept above. For an n-phase system, the voltages and currents are a (n by 1) dimensional matrix so the Clark's transformation matrix for a multiphase system should be calculated and a (n, n) matrix is obtained. Thus the powers for this n-phase system are obtained by the same formulas described above.

It is possible to observe the following relation between these two theories:

$$Sum(\boldsymbol{q}_{abc}) = q_a + q_b + q_c = \boldsymbol{q}_{\alpha\beta 0}(3) = q_0 = q_{(p-q\ theory)} \tag{3-36}$$

Both active and reactive powers can be divided into a constant amplitude component and an oscillating component: $p = \bar{p} + \tilde{p}$ and $q = \bar{q} + \tilde{q}$

It should be noticed that the generalized instantaneous reactive power differs from the instantaneous non-active power. The oscillating portion of the instantaneous active power ($\tilde{p}$) and the instantaneous reactive power together contribute to build the non-active power.

So it is possible to divide the current into two parts: $i = i_p + i_q$ (3-37)

Instantaneous active current: $i_p = \frac{p \times \overrightarrow{v_s}}{\overrightarrow{v_s} \cdot \overrightarrow{v_s}}$ (3-38)

Instantaneous reactive current: $i_q = \frac{\vec{q} \times \overrightarrow{v_s}}{\overrightarrow{v_s} \cdot \overrightarrow{v_s}}$ (3-39)

Where $\vec{v}_s$ is the source voltage.

By using the Lagrange's formula it is possible to demonstrate that the sum of the two parts equal to the whole current:

$$i_p + i_q = \frac{p \times \overrightarrow{v_s}}{\overrightarrow{v_s} \cdot \overrightarrow{v_s}} + \frac{\vec{q} \times \overrightarrow{v_s}}{\overrightarrow{v_s} \cdot \overrightarrow{v_s}} = \frac{(\vec{v}.\vec{\imath}) \times \vec{\imath} + (\vec{v} \times \vec{\imath}) \times \vec{\imath}}{\underbrace{\vec{v}.\vec{v}}_{|\vec{v}|^2}} \tag{3-40}$$

$$= (Lagrange^{'}s\ simplification)$$

$$= \frac{(\vec{v}.\vec{\imath}) \times \vec{v} + [-(\vec{\imath}.\vec{v}) \times \vec{v} + (\vec{v}.\vec{v}) \times \vec{\imath}]}{\vec{v}.\vec{v}} = \frac{(\vec{v}.\vec{v}) \times \vec{\imath}}{\vec{v}.\vec{v}} = \vec{\imath} = i$$

By compensating the reactive portion of current, a unity conventional power factor ($\cos \emptyset \cong 1$) will be achieved, so it will be possible to observe that between the voltage wave form and the current, there would not be any phase shifting.

$$if\ i_q = 0 \xrightarrow{yields} i = i_p \rightarrow S = P \rightarrow \lambda\ or\ PF = 1$$

These formulas are valid in both *abc* or *αβ0* coordinates. Fig. 3.7 shows the decomposition of current.

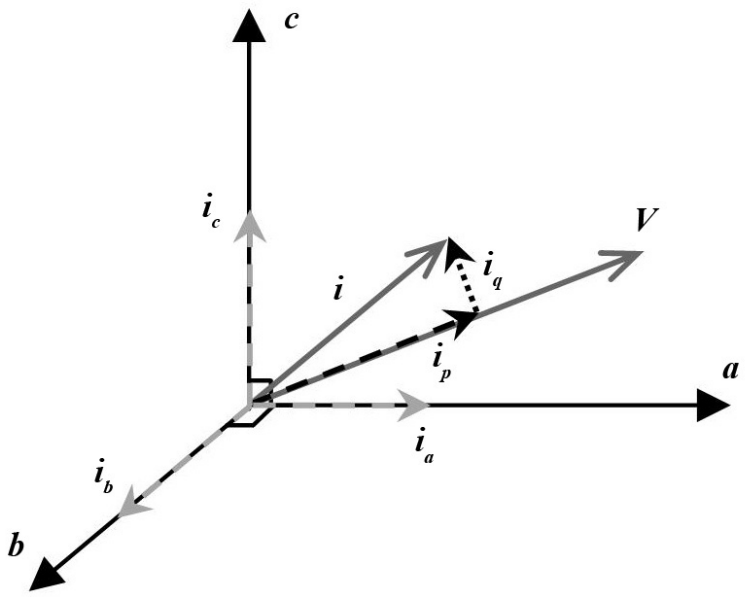

Fig. 3.7 Decomposition of current in a 3D space

If the voltage of the source is supposed to be balanced ($v_0 = 0$) then the reactive powers are simplified as follows:

$$\vec{q}_{\alpha\beta 0} = [q_\alpha \quad q_\beta \quad q_0]^T = \begin{bmatrix} v_\beta i_0 \\ -v_\alpha i_0 \\ v_\alpha i_\beta - v_\beta i_\alpha \end{bmatrix} = \begin{bmatrix} \frac{1}{\sqrt{2}}(v_b - v_c) i_0 \\ \frac{-1}{\sqrt{6}}(2v_a - v_b - v_c) i_0 \\ \frac{1}{\sqrt{3}} Sum(\boldsymbol{q}_{abc}) \end{bmatrix} \tag{3-41}$$

3.4 Willems approach on reactive power compensation

Willem proposes a simple solution to compensate the reactive portion of instantaneous power. He proposes to subtract the active part from the whole current, consequently the reactive part will be obtained [33, 34]. The instantaneous active power which is the same as other definitions is used to obtain the active part of the current.

The instantaneous power transmitted to the load is the scalar product of the voltage and current vectors, which can be demonstrated as multi-elements matrix:

$$p_{(t)} = \boldsymbol{v}_{(t)}{}^{T}\boldsymbol{i}_{(t)} \tag{3-42}$$

As shown in the figure 3.7 let $i_p(t)$ be the orthogonal projection of the vector $i(t)$ on the vector $v(t)$. Explicitly we have:

$$\boldsymbol{i}_p(t) = \frac{\boldsymbol{v}_{(t)}{}^{T}\boldsymbol{i}_{(t)}}{\left|\boldsymbol{v}_{(t)}\right|^2}\,\boldsymbol{v}_{(t)} \tag{3-43}$$

Where the $|.|$ denotes the length of a vector. The above equation can be derived from linear algebra by considering the projection of the vector $\boldsymbol{i}(t)$ on the vector $\boldsymbol{v}(t)$.

Moreover the reactive portion of the current

$$\boldsymbol{i}_q(t) = \boldsymbol{i}(t) - \boldsymbol{i}_p(t) \tag{3-44}$$

is orthogonal to the $\boldsymbol{v}(t)$, such that

$$\boldsymbol{v}(t)^{T}\boldsymbol{i}_q(t) = 0 \tag{3-45}$$

From the definition it follows that

$$|\boldsymbol{i}(t)|^2 = |\boldsymbol{i}_a(t)|^2 + |\boldsymbol{i}_b(t)|^2 + |\boldsymbol{i}_c(t)|^2 = \left|\boldsymbol{i}_p(t)\right|^2 + \left|\boldsymbol{i}_q(t)\right|^2 \tag{3-46}$$

The proposed decomposition has the limitation that it does not give the ability to have a sinusoidal current to the user. By compensating only the reactive part of the power, a unity power factor and a bulk of harmonic will be compensated but a sinusoidal balanced current is not

possible. To achieve a complete compensation, the controller should be able to separate and compensate the oscillating portion of the active power, which the Willems method is unable to do.

3.5 Comparison of approaches

In this section the differences of the theories are compared with the help of symbolic calculations in the Matlab environment.

Running the program in the Appendix-I for a three-phase with three-wires (3ph-3w) gives results show that there is a complete concordance between the Willems's and Akagi's (p-q theory) in both active and reactive parts of the currents.

$$i_p(Willems) = i_p(p-q\ Theory) \tag{3-47}$$

$$= \begin{bmatrix} \frac{va}{2}\left(\frac{2.va.ia + 2.vb.ib + vb.ia + va.ib}{va^2 + vb^2 + vb.va}\right) \\ \frac{vb}{2}\left(\frac{2.va.ia + 2.vb.ib + vb.ia + va.ib}{va^2 + vb^2 + vb.va}\right) \\ \frac{-(va+vb)}{2}\left(\frac{2.va.ia + 2.vb.ib + vb.ia + va.ib}{va^2 + vb^2 + vb.va}\right) \end{bmatrix}$$

$$i_q(Willems) = i_q(p-q\ Theory) = \boldsymbol{C}^{-1} \times \begin{bmatrix} i_{\alpha q} \\ i_{\beta q} \\ 0 \end{bmatrix} \tag{3-48}$$

$$= \begin{bmatrix} -\frac{1}{2}\left(\frac{-2.vb^2.ia - va.ia.vb + 2.vb.ib.va + va^2.ib}{va^2 + vb^2 + vb.va}\right) \\ \frac{1}{2}\left(\frac{2.va^2.ib + vb.ib.va - 2.va.ia.vb - vb^2.ia}{va^2 + vb^2 + vb.va}\right) \\ -\frac{1}{2}\left(\frac{vb^2.ia - va.ia.vb + va^2.ib - vb.ib.va}{va^2 + vb^2 + vb.va}\right) \end{bmatrix}$$

For the General cases for three phases and four wires, results are quite different from the previous section. By running the program in Appendix-II the active portion of the p-q theory differs from the active current of Willems theory. This difference comes from the transformation

matrix. As for the p-q theory we have separated the zero-sequence power, the equation in front of the matrix became different.

In the p-q theory the gain is $\frac{1}{{v_0}^2({v_\alpha}^2+{v_\beta}^2)}$ while in the Willems theory the gain is $\frac{1}{{v_0}^2+{v_\alpha}^2+{v_\beta}^2}$. So the results differ from each other and $i_p(Willems) \neq i_p(p-q\ theory)$.

When the voltages are balanced ($v_0 = 0$), the two currents are equal:

$$v_c = -v_a - v_b \xrightarrow{yields}$$

$$i_p(Willems) = i_p(p-q\ theory)$$

$$i_q(Willems) = i_q(p-q\ Theory) = \boldsymbol{C}^{-1} \times \begin{bmatrix} i_{\alpha q} \\ i_{\beta q} \\ i_0 \end{bmatrix} \tag{3-49}$$

The only limitation to this case is that while using the p-q theory for compensation, as for $v_0 = 0$ the division $\frac{1}{v_0}$ (or even $\frac{1}{{v_0}^2({v_\alpha}^2+{v_\beta}^2)}$) becomes infinite ($\infty$). This is one of the simple limitations of the conventional Akagi's theory. So if the Active filter uses this theory it should decide whether to keep the zero-sequence power or to compensate it, because as we demonstrated, it is crucial to know the objectives of the compensation to prevent hazard results.

For the Generalized theory and Willems the program in Appendix-III gives accurate results. This program illustrates that the two methods give the same results and a complete coherence exists between them.

$$p_{(Generalized\ \ theory)} = p_{(Willems)} \xrightarrow{yields} i_p(Generalized\ theory) = i_p(Willems)$$

And so

$$i_q(Generalized\ theory) = i_q(Willems)$$

The problem of the infinite result from the p-q theory has disappeared in the Generalized theory. But the generalized theory compared with the p-q theory is much more complex.

The generalized theory is expandable for multi-phase systems, but the p-q theory is specified to three phase with three or four wire systems.

The results of the simulation confirm the result of symbolic calculations. The case of the three phases - four wires system shows a good coherence between the p-q theory of Akagi and the Willems method of compensation. In these simulations, the amplitude and frequency of waves are considered as arbitrary values; of course this assumption do not influence the compensation method nor the shape of the compensated currents and they do not have a significant value. Two cases are simulated, the first one with a unity power factor and the second one with a 30 degree phase angle between voltages and currents.

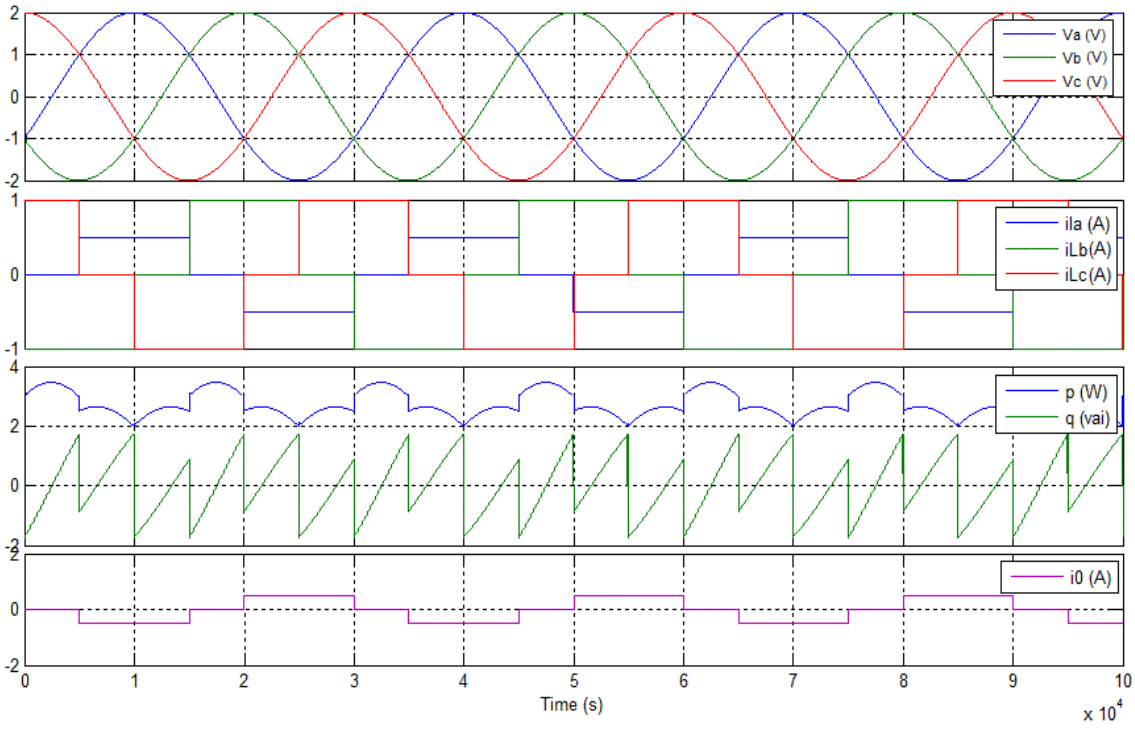

Fig. 3.8 a) source voltages b) load currents c) instantaneous powers d) zero-sequence current of the load, for the case with zero phase degree

The figure 3.8 shows an unbalanced system with distorted currents. The phase “a” has half the magnitude than the two other phases, so this unbalance will cause a zero-sequence current flowing into the fourth wire. In these simulations, the source voltage is supposed to be sinusoidal and balanced. The instantaneous reactive power is the subject of compensation in these cases. The two instantaneous powers are demonstrated. Of course, in the absence of zero-sequence voltage the instantaneous zero-sequence power does not exist.

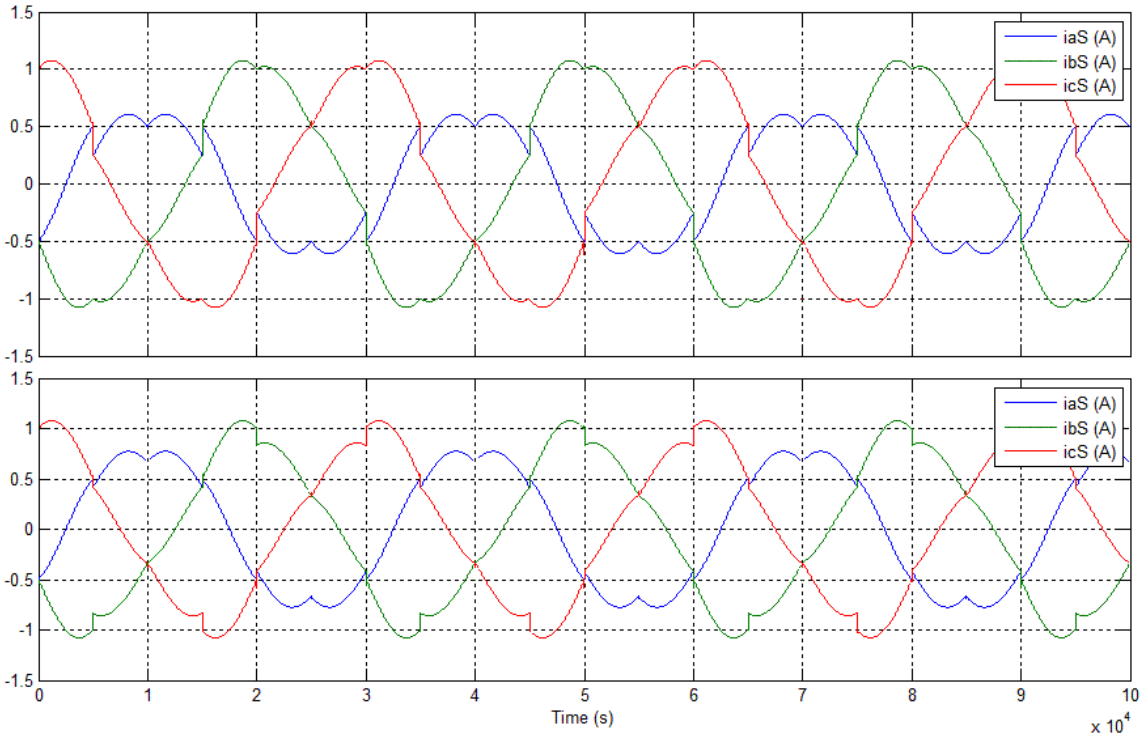

Fig. 3.9 Source currents a) without zero-sequence compensation b) with zero-sequence compensation for the case with zero phase degree

The figure 3.9 shows the source current compensated by the p-q method where the reactive current is totally compensated without compensating the zero-sequence current. The second part demonstrates a total compensation of the reactive and zero-sequence currents. The shape of current has changed while in the second case the zero-sequence component is absent. In the both cases the oscillating portion of the active power has not been compensated. The lack of compensating the oscillating portion of the active power causes the current waveform to still have a distorted shape. But bulks of harmonics are compensated.

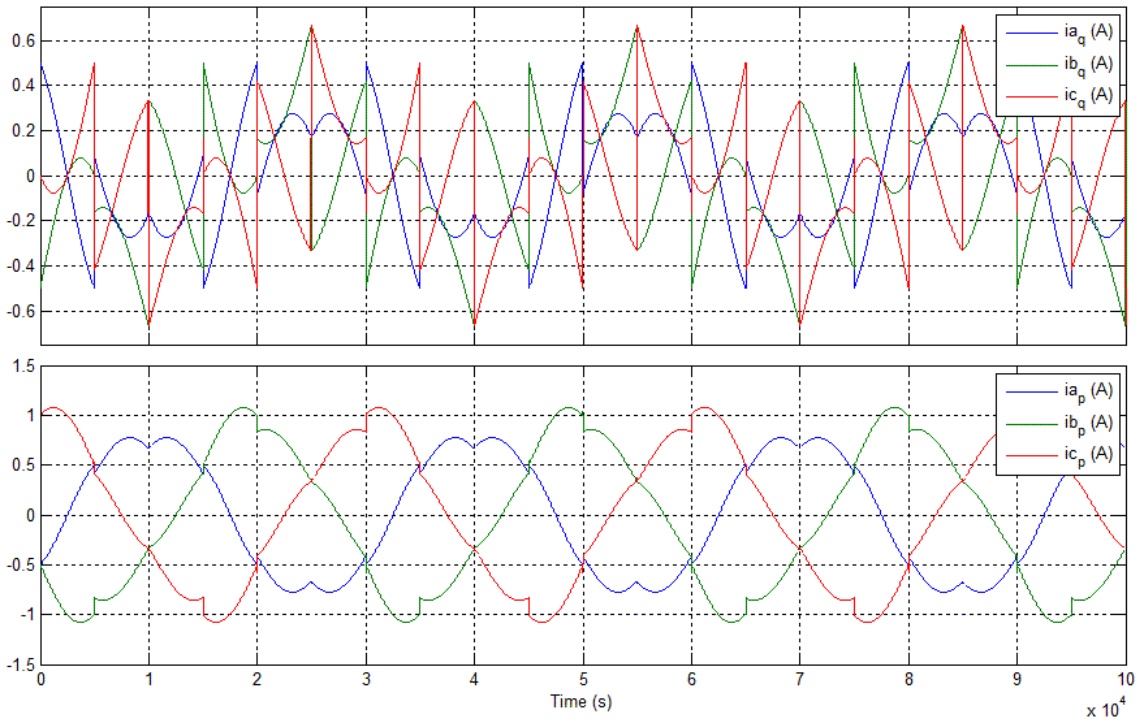

Fig. 3.10 Compensating current injected by the active filter, source currents for the case with zero phase degree

The figure 3.10 shows the compensation of the reactive part of the current based on the Willems theory. The first part of this figure shows the inverse of the compensating current which is the reactive current calculated by the Willems method, then the opposite of these shapes will be added to the load current. These currents are the sum of reactive current and zero-sequence current based on the p-q theory. The second part is the active part of the current based on the Willems method. It is clear that the result obtained by the Willems method is exactly same as the result of compensating the reactive and zero-sequence currents by the p-q theory of Akagi. So these simulations demonstrate the exactitude of the recent calculations in the comparison chapter.

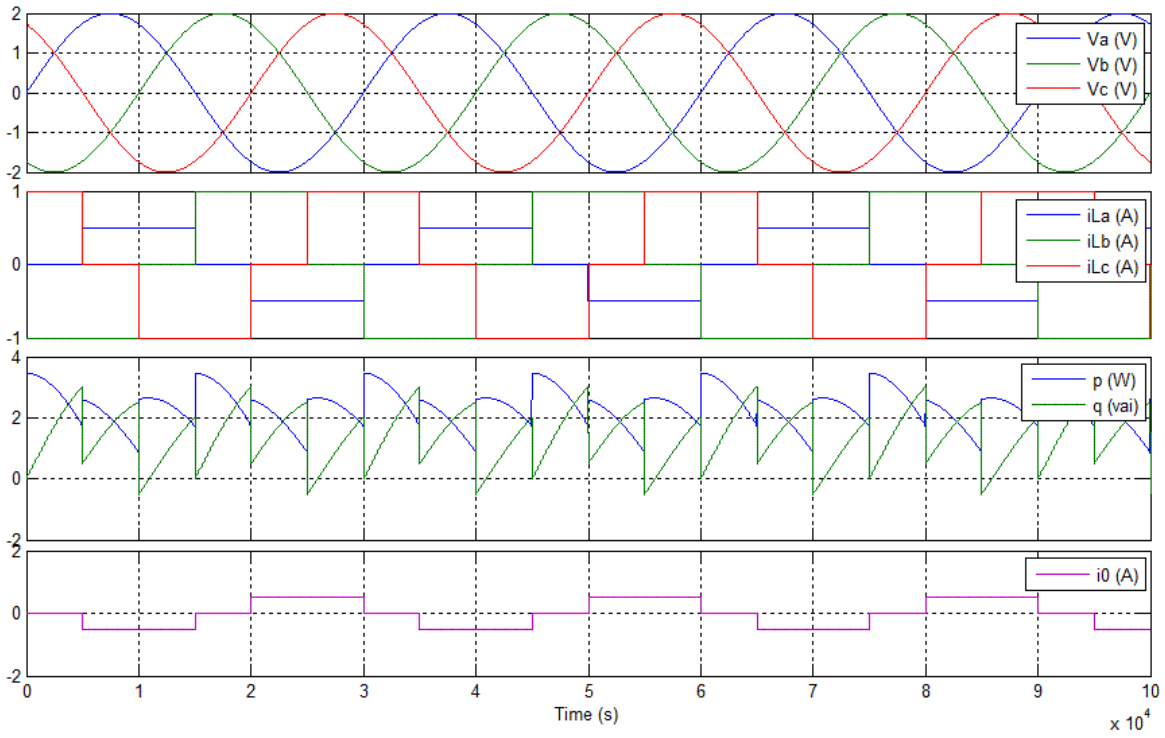

Fig. 3.11 a) Source voltages, b) load currents, c) instantaneous powers, d) zero-sequence current of the load for the case with 30 phase degree

The figure 3.11 shows a case where the currents lag $\pi/6$ degrees behind the voltages. In this case, the currents are not only unbalanced and distorted but they also have a $\cos\theta \neq 1$. The same simulations are done, with compensation by the p-q theory then by the Willems one.

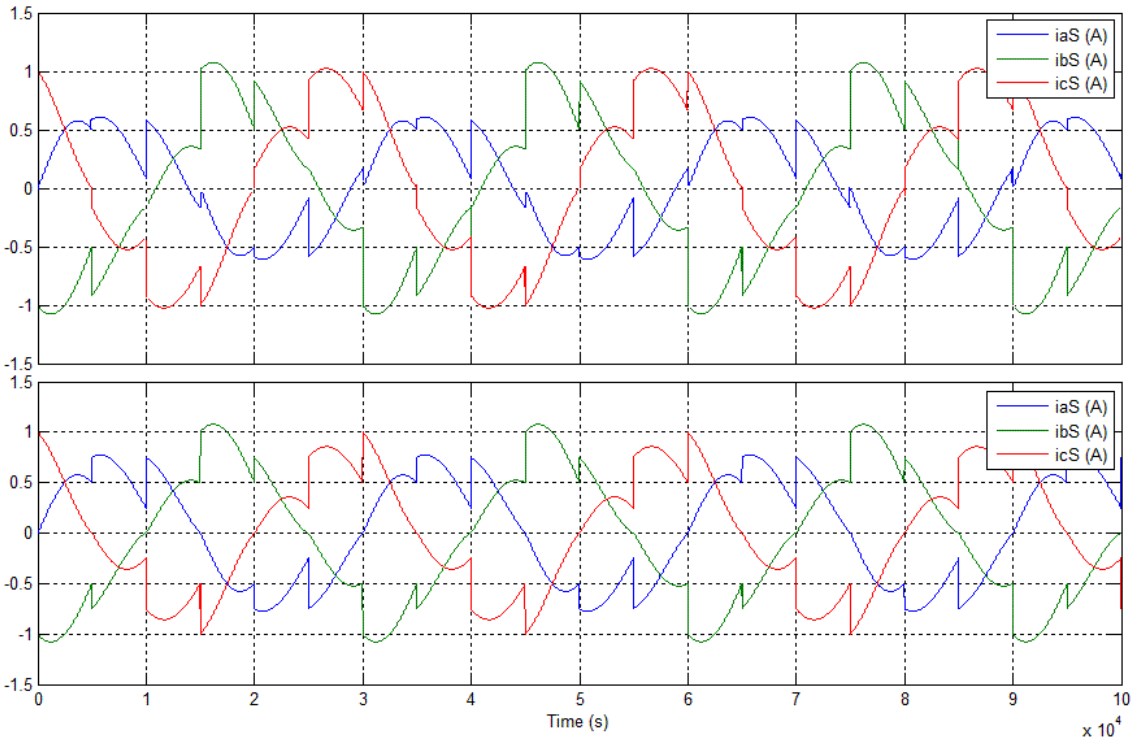

Fig. 3.12 Source currents a) without zero-sequence compensation b) with zero-sequence compensation for the case with 30 phase degree

The figure 3.12 is the results of compensating the reactive power in the first part and the reactive part added with the zero-sequence current, in the second part. For such situations where the voltage zero-sequence is absent, Akagi suggests compensating the zero-sequence part of the current and he considered this part as a non active part of current. Consequently the current will have a better shape and without zero-sequence components. In all the simulations, the active power, comprising its oscillating and average part have not been compensated. This will cause the current to have a unity power factor and distorted, but with less harmonic distortion.

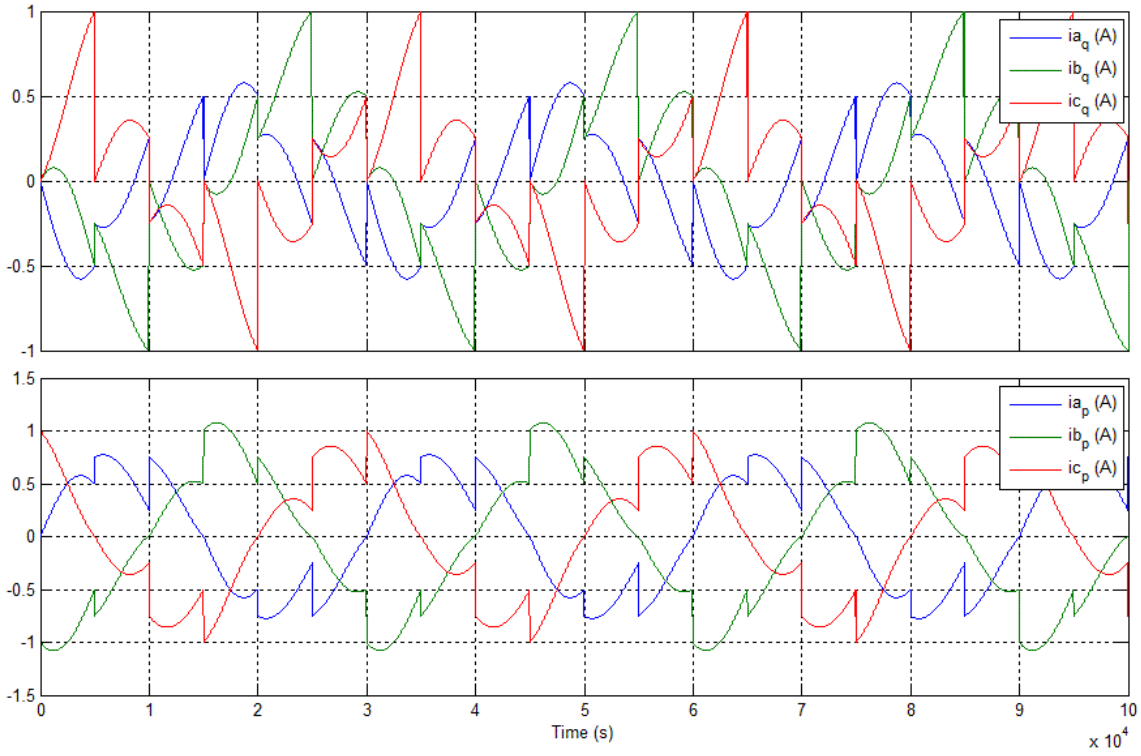

Fig. 3.13 Compensating current injected by the active filter, source currents for the case with 30 phase degree

Figure 3.13 shows the results of the compensating current and the active part of the current. These shapes are exactly the same as in last figure. Therefore, the simulations confirm that whether using the p-q theory of Akagi by including the zero-sequence component in the compensating current, or the Willems method, the result will be the same. The difference will be in the compensation of the oscillating part of the active power, where the Willems method does not give the opportunity for a sinusoidal compensation while the Akagi's method has the flexibility to do more. But if the goal is only getting a unity power factor and compensating some order of harmonics but not eliminating all of them, the Willems method seems to be a good choice because of its simplicity and less calculation to separate currents. But for more complex applications the Akagi's method is preferable.

The result for a sinusoidal current objective which implies additionally the compensation of the oscillating portion of the active instantaneous power is presented in the figure 3.5.

3.6 Summary

In this chapter three main instantaneous power definitions are presented. Akagi's p-q theory of instantaneous powers, which is the first and principal theory for the instantaneous calculation of powers, was presented. Unfortunately this approach is limited to three phase systems. Although the calculations presented by this theory are simple, they don't give a clear physical meaning of the different powers. As demonstrated in section 3.5, this theory has some other conceptual limitations. The condition of the compensation should be specified at the beginning to tune up the controller. The inaccuracy of this method depends on the probability to obtain an infinite value in different step in the control algorithm, which leads to a faulty result. By now, the dominant controller methods used in industrial active filter seems to be based on this theory because of its rapidity.

The Generalized theory of instantaneous power tries to extend the Akagi's theory to systems with more phases. By using vector algebraic systems they extend the Akagi's idea to multi phase systems, and give a more physical interpretation to instantaneous powers concepts. The wicked point of this theory is the complexity of calculations. The differences of this method and the original p-q theory is widely discussed and argued in [3]. Moreover, many unwanted components appear in the compensating current, which makes this theory less practical than the p-q theory.

For systems with more than three phases, the Generalized and the Willems theory could be used, but if the objective is to obtain a sinusoidal current or compensating the whole non-active power, we have no other choice than the Generalized theory. The Willems theory is the best choice if the objective is only compensating the reactive (imaginary) power. The Willems method insures a unity power factor and compensates the major part of harmonics present in the current. This method is useful for three phases and more, but in the presence of the zero sequence current or even the zero-sequence power it should be revised to take into account the compensation purpose.

As a conclusion, it was demonstrated in this chapter that each author divides the powers from his own point of view by taking into account the application they think more important in the compensation target. To allow comparison with results found in the literature, the original p-q theory will be used for the real-time implementation of the active filter controller.

CHAPITRE 4 LABORATORY REAL TIME CONTROL OF THE ACTIVE FILTER

4.1 Introduction

Based on the theories studied in the past chapters and the simulations presented in third chapter, a real-time controller has been realized and implemented on an Opal-RT real-time simulator. The real converter and loads are connected to the simulator and the whole set-up becomes a hardware in the loop (HIL) system. The real time controller was then used to eliminate harmonics of a nonlinear three-phase three-wire load. The equipments used for these tests are presented in this chapter and the laboratory set up is reviewed. Finally the experimental results is shown and analyzed.

Regarding the Clark transformation on a three phase system, the p-q theory introduced by Akagi sounds a good departure to realize an instantaneous compensator for the reactive power but in the case of the whole non-active power compensation, other methods should be used. For instance, one may combine PLL, Butterworth or passive filter with the controller to do so. Of course, the hypothesis will be refuted if the results of real-time tests show a non instantaneous compensation or a non sinusoidal wave form in the current supplied by the source. The method proposed for a real-time test is to simulate the active filter on an Opal-RT simulator and then connecting it to the physical system.

The objective of this project is to review the theorems and definitions of electric power concepts under non-sinusoidal conditions and compare different control algorithms found in the literature. In this manner we will recall Akagi's Theory of instantaneous power (*p-q Theory*) which is the best approach till nowadays. For the same reason, this theory was chosen for implementation in the real-time controller.

Finally the model was implemented in the laboratory on a RT-Lab real-time Simulator connected to a three phase 120/240 V system and to a three phase rectifier as a non-linear load. Experimental results are also compared with simulation results.

4.2 Equipments and ambitions

The physical equipments needed for this project were provided by the Power System Laboratory of the École Polytechnique de Montréal. An overview of the laboratory environment is presented in figure 4.1.

Fig. 4.1 Power System laboratory at École Polytechnique de Montréal

The controller was modeled using the Opal-RT block sets in Simulink and then after compilation was loaded into the real-time simulator for the next step. For the non-linear load a three phase rectifier with a resistive load was used to produce the distorted current. On the dc side two parallel diode bridges were used to increase the load currents. The two bridges produce a 77 V dc.

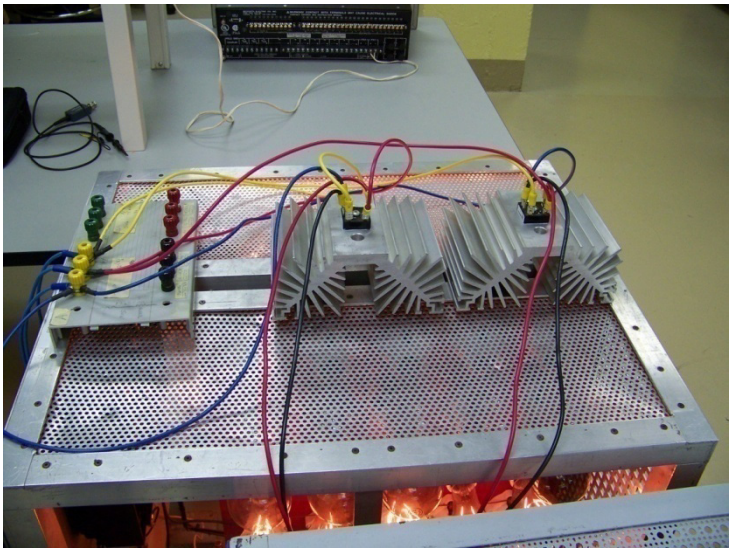

Fig. 4.2 Two diode bridges connected in parallel

The load is connected to a laboratory power source through a three phase autotransformer. The autotransformer is used to control the dc output of the bridges and to limit the dc voltage applied to the lamps used as resistive load. For the same reason, the nonlinear load could not be connected directly to the source. The figure 4.2 displays the two diode bridges connected in parallel as rectifier.

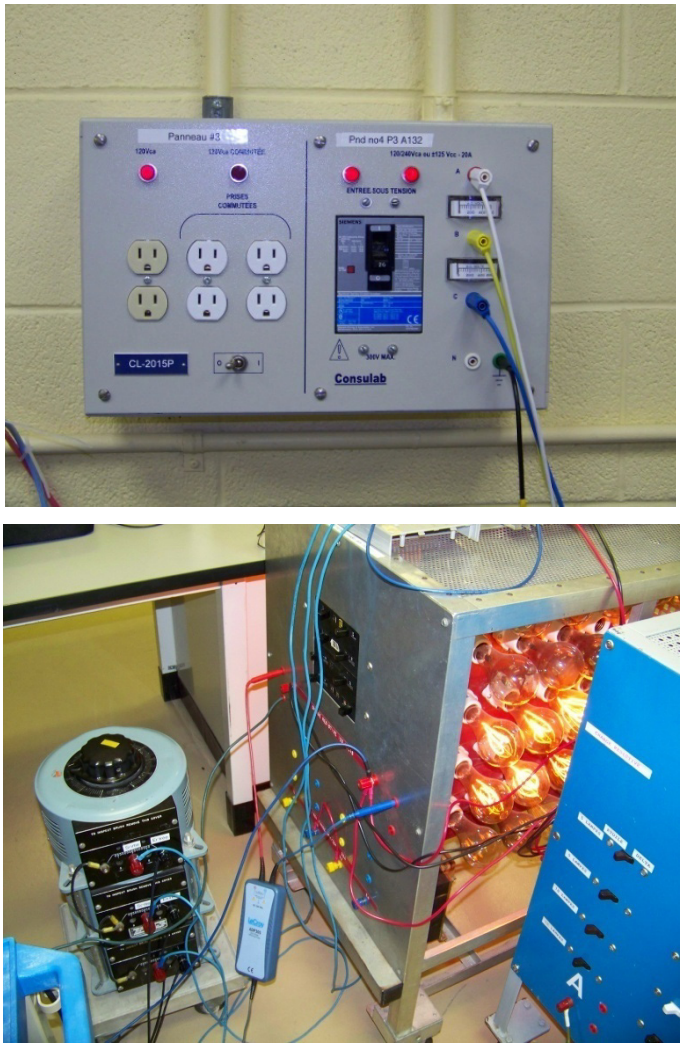

Fig. 4.3 The three phase source panel, the resistive load and the autotransformer

Figure 4.3 shows the source panel and the autotransformer between the load and the source. The dc voltage of the diode bridge is nearly $\sqrt{6}$ times greater than the rms value of the phase to ground voltage on the input side. So, in order to keep the dc voltage at 75 V the ac side should have 30 V phase to ground voltage. Since the source voltage is 240 V line-line (≈ 133V ph-n), the autotransformer will adjust the voltage to maintain 30 V at the input of the diode bridges.

The voltage and current probes are connected to the source side of the transformer. Since the transformer distorts the current due to its magnetization current (hysteresis characteristics), this decision was made to compensate all the distortion made by the non-linear load and the autotransformer. In fact the non-linear load that the active filter is supposed to compensate consists of a transformer and a resistive rectifier. Figure 4.3 shows the current and voltage probes

connected by a Db25 connector to the patch panel. The patch panel transfers the data directly to the analog input of the Mx-Station (the Opal-RT real-time simulator).

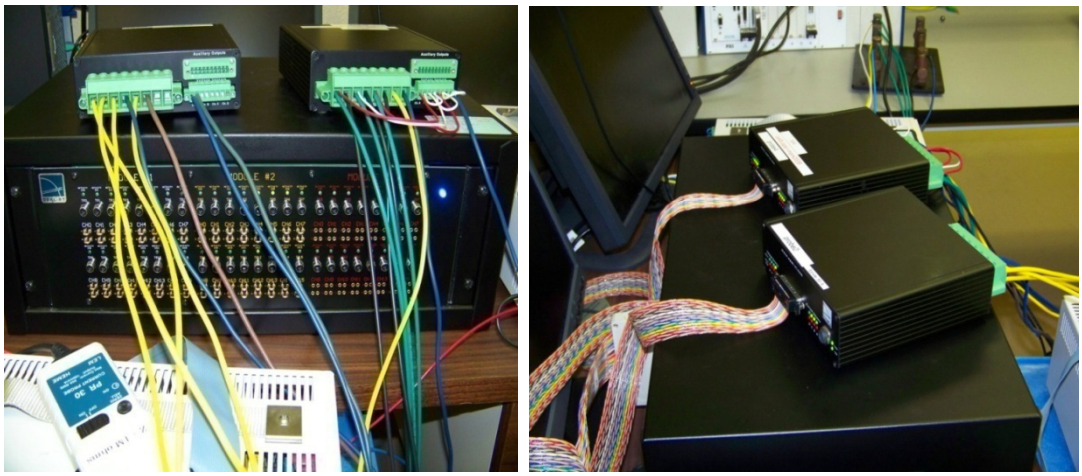

Fig. 4.4 The Probes and the patch panel, the probes and connection cables (front view)

The probes supplied by Opal-RT do not introduce any delay and they have a great sensitivity even for low inputs. They can be adjusted to different voltage levels (100V ~ 600V). The output is a 10 V analog signal. But for the current probes the gain is fixed and for a 25 A current a 5 V signal will appear at the output of the probe. These probes present a good sensitivity, current of a few mA at the inputs are measurable.

The main part of the system is the real-time simulator. The Mx-Station is a commercial real-time simulator produced by the Opal-RT. This real-time simulator has the capability of 10 µs time steps. The figure 4.5 displays the simulator and the two I/O cards at the rear. The I/Os are composed of digital inputs/outputs and analog inputs/outputs. In this work, the analog inputs are used to read the data from the probes and the digital card is used to output the PWM signal for the inverter.

Fig. 4.5 The real time simulator (MX-station), the analog card (left), the digital cards (right)

The real time simulator is connected to a PC. The models are simulated, compiled and then transferred by the PC to the target. During the operation the data are transferred to the PC to be acquired and monitored. The figure 4.6 shows the PC and scopes during a real-time operation of the active filter.

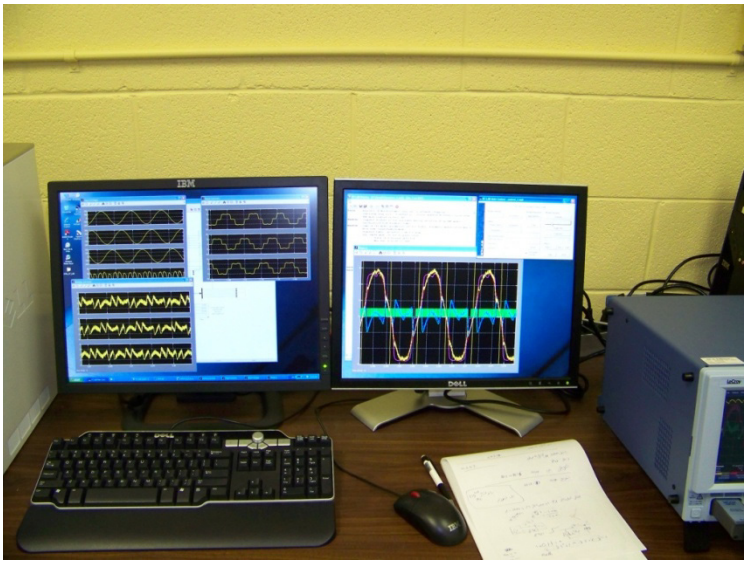

Fig. 4.6 The Probes and the patch panel, the probes and connections cables (front view)

After loading and executing the model into the simulator, the simulator starts reading data as explained previously. The simulator instantaneously sends out the six PWM impulsions to the external inverter as shown in the figure 4.7. The simulator reads, processes (including calculations), and produces the output signals with a step time of 10 µs.

The inverter is a commercial one from the Semikron company. This inverter has a capability to produce up to 50 A.

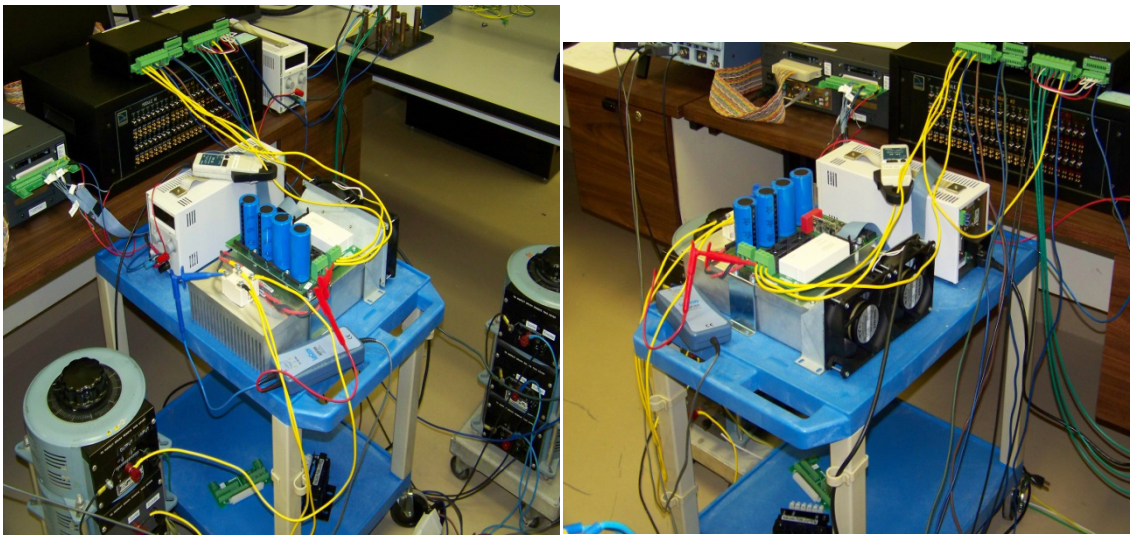

Fig. 4.7 The three phase inverter, source for the electronic boards

The inverter has also an integrated rectifier to produce the required dc voltage. The IGBTs of the inverter could function with a frequency up to 12 kHz. This frequency is high enough for the laboratory tests. The firing signal for the inverter came directly from the real-time simulator as 12V digital signals.

4.3 Laboratory tests

Based on the p-q theory, a model for the controller was built in the Simulink environment. Then some modifications are made on the model to be compatible with the real-time simulator. An overview of the model is presented in the figure 4.8. The parameter of the model could be changed during the execution, but the model could not be changed. Once a change is made in the model, it should be recompiled and reloaded to the real-time simulator.

Different tests have been done. A single non-linear load was used because of the limitations in the laboratory installation. The control block has been changed from the Akagi to Willems and they were compared and as predicted in the previous chapter, results are exactly the same for a reactive compensation strategy. But for the sinusoidal current strategy, the need to compensate the oscillating portion of the instantaneous active current necessitates the use of the p-q theory in the controller.

The model as shown in the figure 4.8 was divided into two parts. The first part is the calculations block and the second one combines the oscilloscopes to visualize the waveforms and signals. The Sm_1 block is loaded into the processor after being successfully compiled. Any mistake in the model would cause the compilation to fail. Moreover, during the execution, the number of detected overruns is important to insure a correct operation of the Simulator.

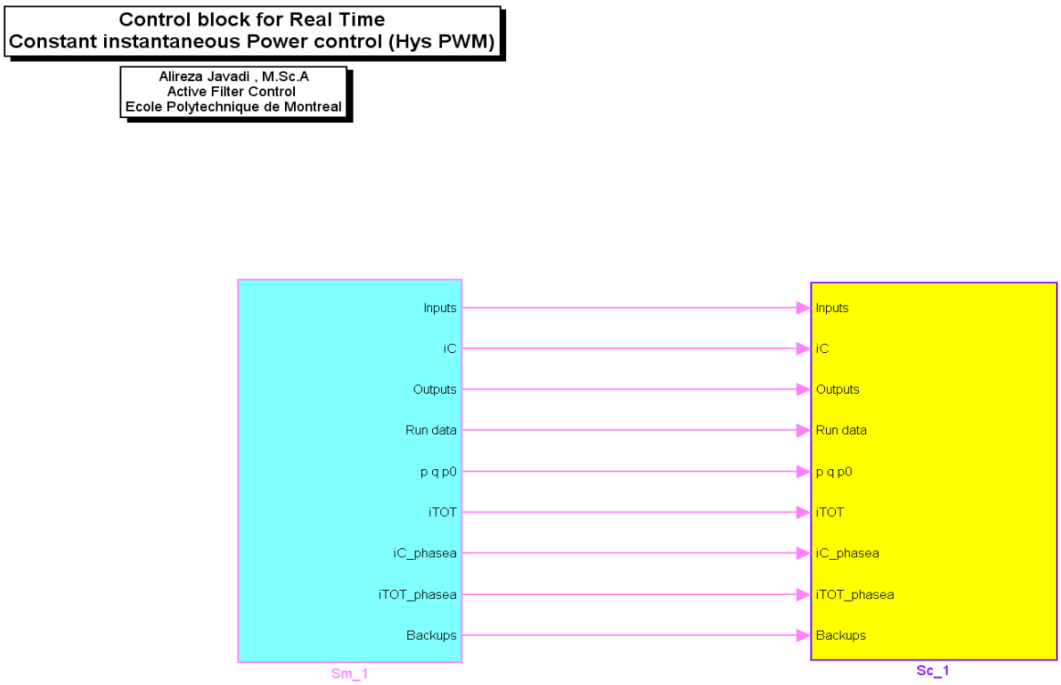

Fig. 4.8 Schematic of the control of the active filter controller

It is possible to take a look at the internal structure of the first block of the figure 4.8 as it appears in figure 4.9 the inputs came from the analog I/O. The control block calculates the active and reactive current and extracts the part to be compensated.

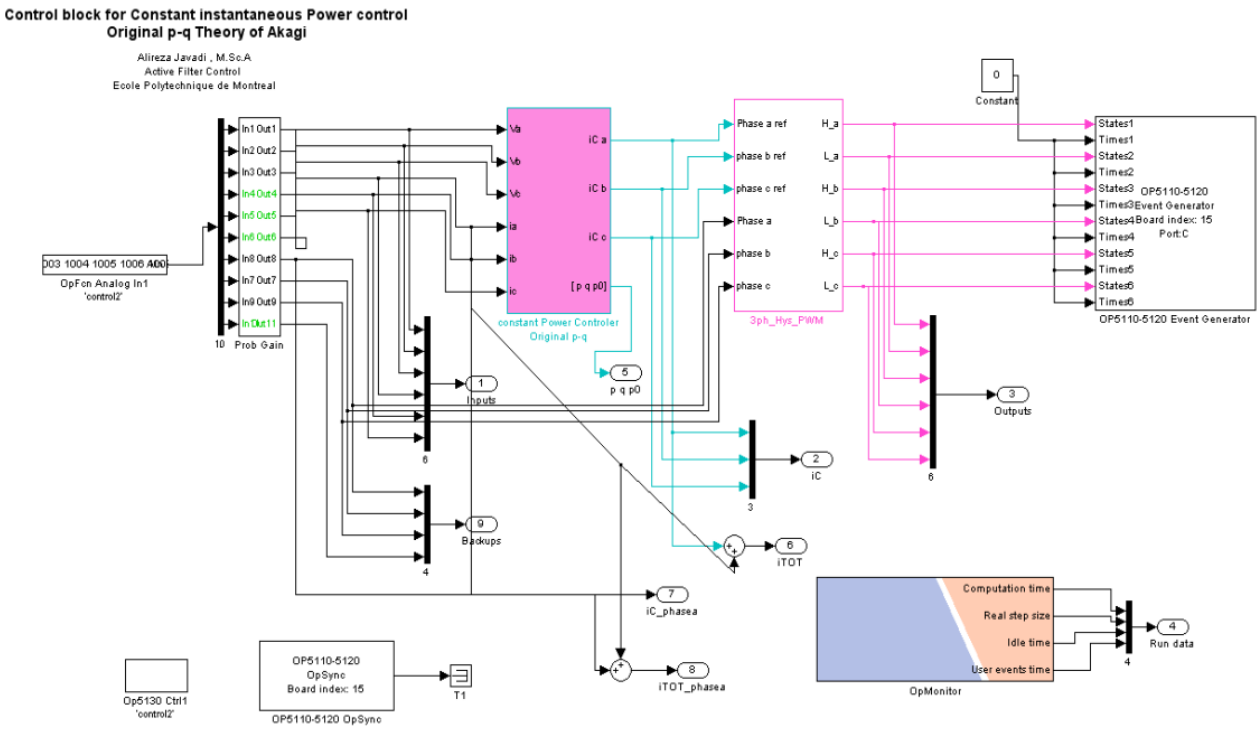

Fig. 4.9 Under mask of the active filter controller block

The compensation currents are then entered into the Hysteresis PWM block. Then this block produce the impulsions for an inverter with three wire system. The hysteresis block takes the hysteresis band width for modulation as shown in the figure 4.10. Half of the tolerance band is the distance that the backup current could diverge from the compensation current as shown in the figure 4.11. In a hysteresis current control method, the current is compared with the reference with a band width tolerance and each time it reach this limit an impulsion is generated to control it. The step size and the maximum frequency supported by the inverter are the factors that limit the tolerance band width.

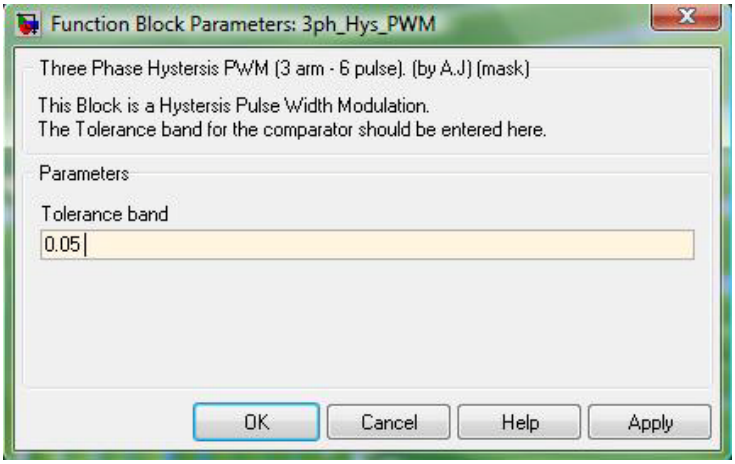

Fig. 4.10 Hysteresis Block parameters

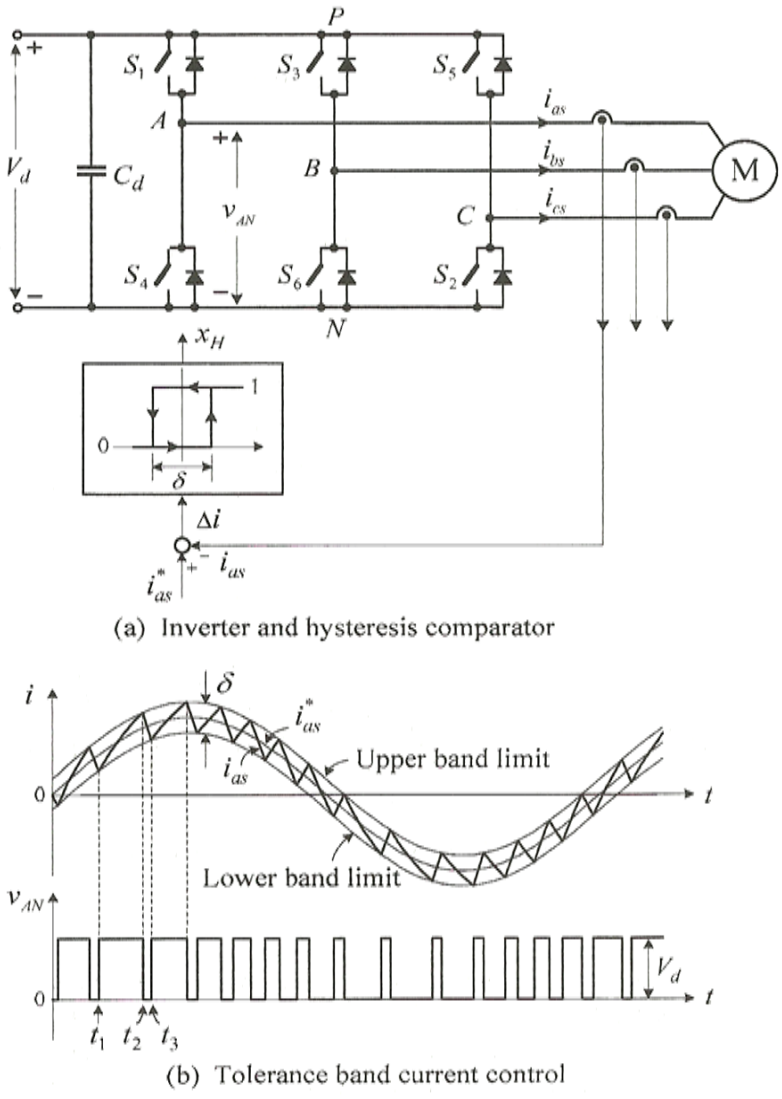

Fig. 4.11 Current-regulated voltage source inverter [36]

The six impulsions are produced instantaneously at the digital outputs of the real-time simulator. The inverter takes these impulsions and produces the desired current. The inverter model used in this test was a VSC (voltage source converter) inverter module, but the application is a current control based one and a CSC was needed. In order to overcome this problem, an inductance is needed in series with the inverter terminal in each phase to convert the voltage to current, and then a backup of this current is taken for the calculations. By this simple solution the VSC could be used like a CSC (current source converter). The other important limitation is that this inverter could not be used for four wire systems; this limitation prevents the compensation of the zero-sequence current and power.

The model was first built with a PWM six pulse module, as shown in figure 4.12. The results of that control method were compared with the Hysteresis PWM. Of course for this application, where the waveform has a great importance, the hysteresis solution seems to be a better choice.

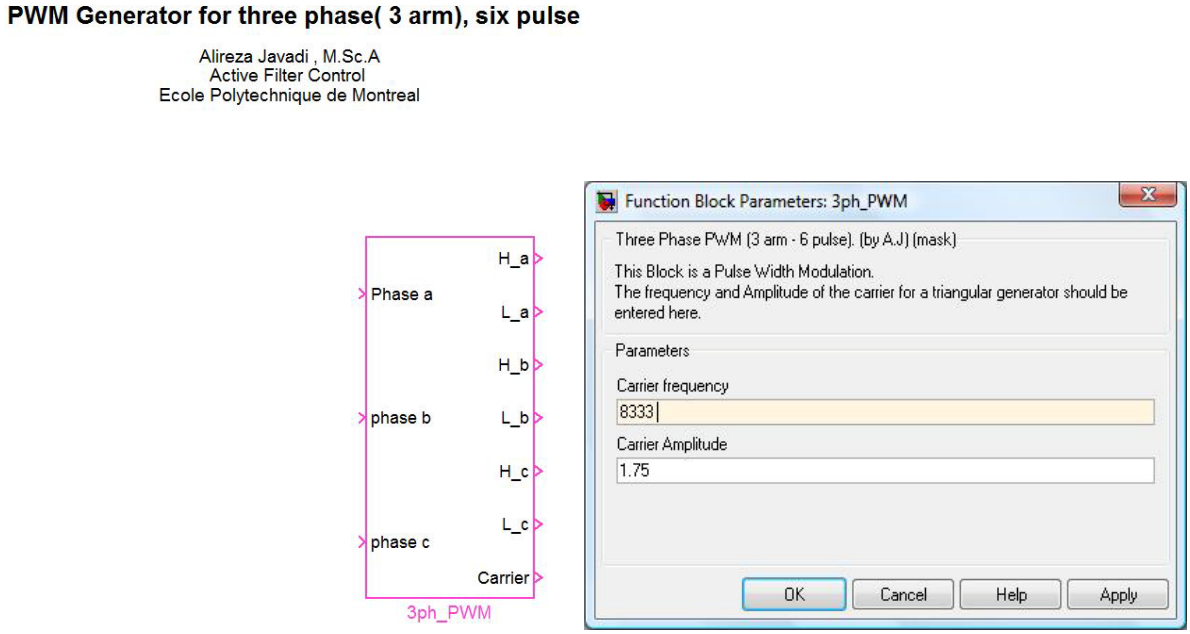

Fig. 4.12 Pulse width modulation (PWM) block, block parameters

The PWM is useful where there is no need to obtain a perfect current shape. The model produces a triangular signal to be compared with the input signal to create the firing angles. The frequency and the amplitude of the carrier are adjustable from the block parameter window.

It should be noticed that the simulator functions in discrete time steps and any block which uses the variable step cannot be used in the controller. For all the tests the step size is configured

to 10 µs to have the best performance for the compensation. The oscilloscopes are all synchronized together. This hardware in the loop (HIL) application demonstrates the reliability of such real-time simulators. Some overviews of the window during the execution are showed in the figure 4.13.

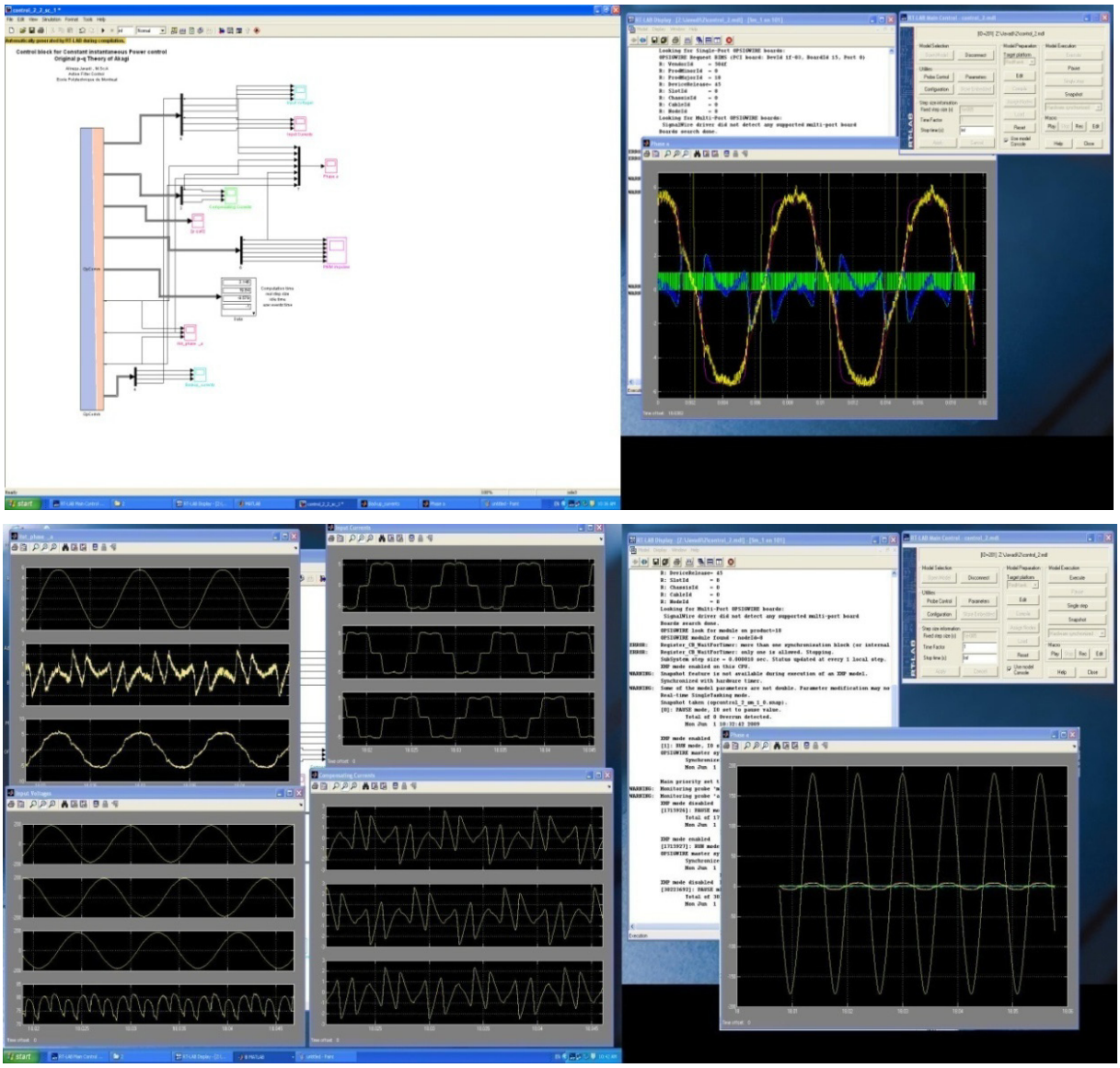

Fig. 4.13 Oscilloscopes view during the execution of the test

A schema of the circuit realized in the laboratory is shown in the figure 4.14. These block diagrams illustrate the elements described previously. The exact connections are not shown in this schema.

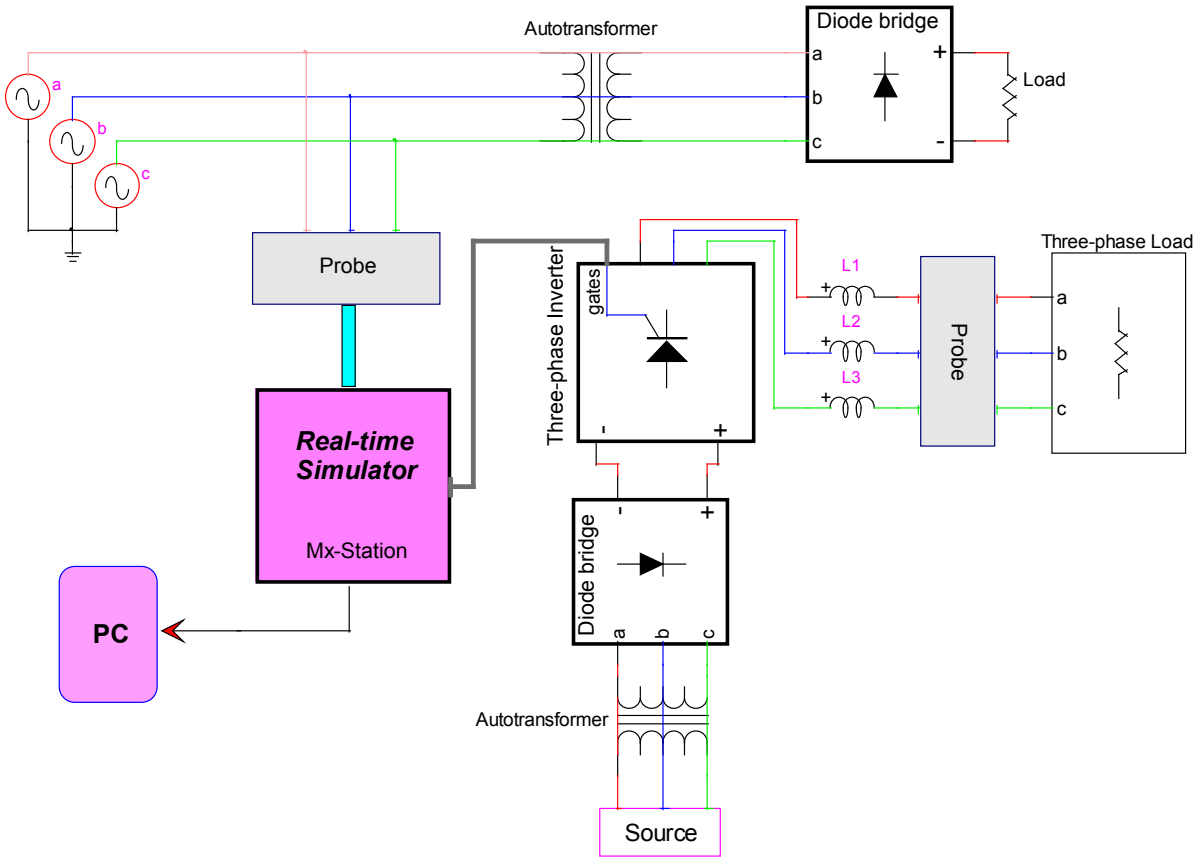

Fig. 4.14 Laboratory circuit block diagram

In an industrial implementation, an active filter is connected to the nonlinear load in parallel as shown in the figure 4.15. The difference between this configuration and the one used in these laboratory tests is that, the active filter does not inject the compensation current into the system directly. In this project, the compensation current produced by the three phase inverter is injected into a three phase resistive load instead of injecting it to the three phase system. The absence of an inverter with a capacitance in the dc side was the reason of such configuration. As explained the inverter used in this test was build with an integrated voltage source as shown in the figure 4.14, this voltage source was created by a rectifier.

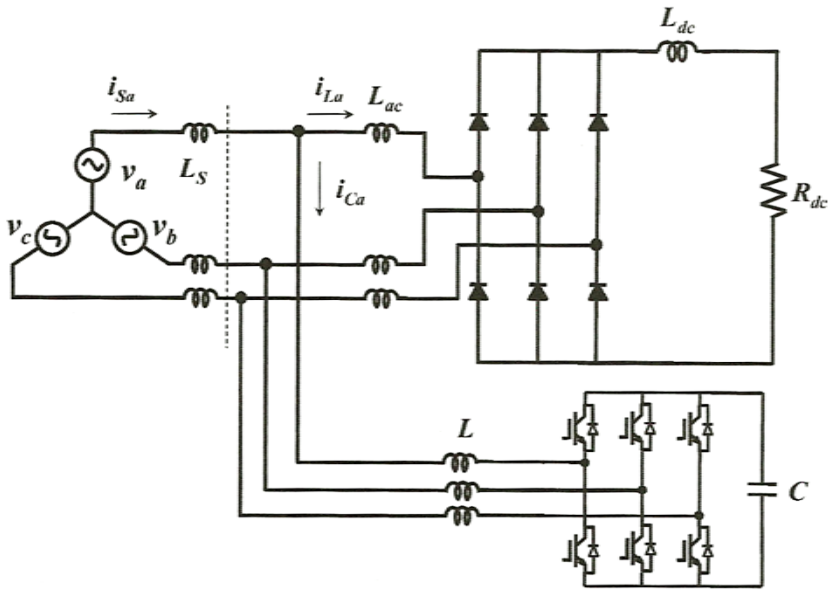

Fig. 4.15 Industrial active filter implementation block diagram with an energy storage component

By protection measures, it was not possible to connect the output terminals of the three phase inverter to the system composed of the source and the non linear load, with the equipment available in the laboratory. Any unwanted problem during the control process would have led to a disaster by making a short circuit between two sources if the outputs of the present inverter have been connected to the nonlinear load. This important limitation make was solved by connecting the outputs to a resistive load. So to demonstrate the effect of the active filter, the compensation current produced by the inverter was added with the non linear load by the real-time simulator. These current were read by the probes instantaneously and added mathematically in the simulator. This method make it feasible to observe the exact effect if the inverter were connected directly to the nonlinear load without confronting security troubles.

4.4 Real-time Results

The results of different tests are presented in this section. Three tests were done, each with different parameters. Before the start of tests, the simulator has been tested to insure a real-time simulation in both, Software synchronized and Hardware synchronized modes. Both the analog and the digital I/Os were tested to produce signals and receive signals from external sources. The inverter was tested for different switching frequencies. An external four channel oscilloscope has confirmed the results.

The first test was made with a simple PWM module. The second part is consecrated to the controller to generate the firing angles to the hysteresis pulse width modulation block. In this section, different tests were performed and compared. Then the controller is verified for different conditions. For instance, some changes are applied to the load to insure the reliability and efficiency of this controller. These real-time tests presented in this chapter represent only some sample of the tests done in the laboratory. The step size of the real time simulator for all the test was set to 10 μs.

4.4.1 Control using pulse width modulation (PWM)

The results of this section demonstrate the real-time operation of the controller when based on the p-q theory. In this test a PWM block generates the signals to fire each IGBT of the inverter. As explained before the power inverter used in the laboratory has three legs. The figure 4.16 shows the results of such control methods. The instantaneous active and imaginary powers are shown. Since the system is a three phase three wire one, the zero-sequence current is null; however in cases where the zero-sequence power was present, the controller has the ability to compensate it depending on the application. The figure shows the presence of both mean value and oscillating part in the instantaneous powers.

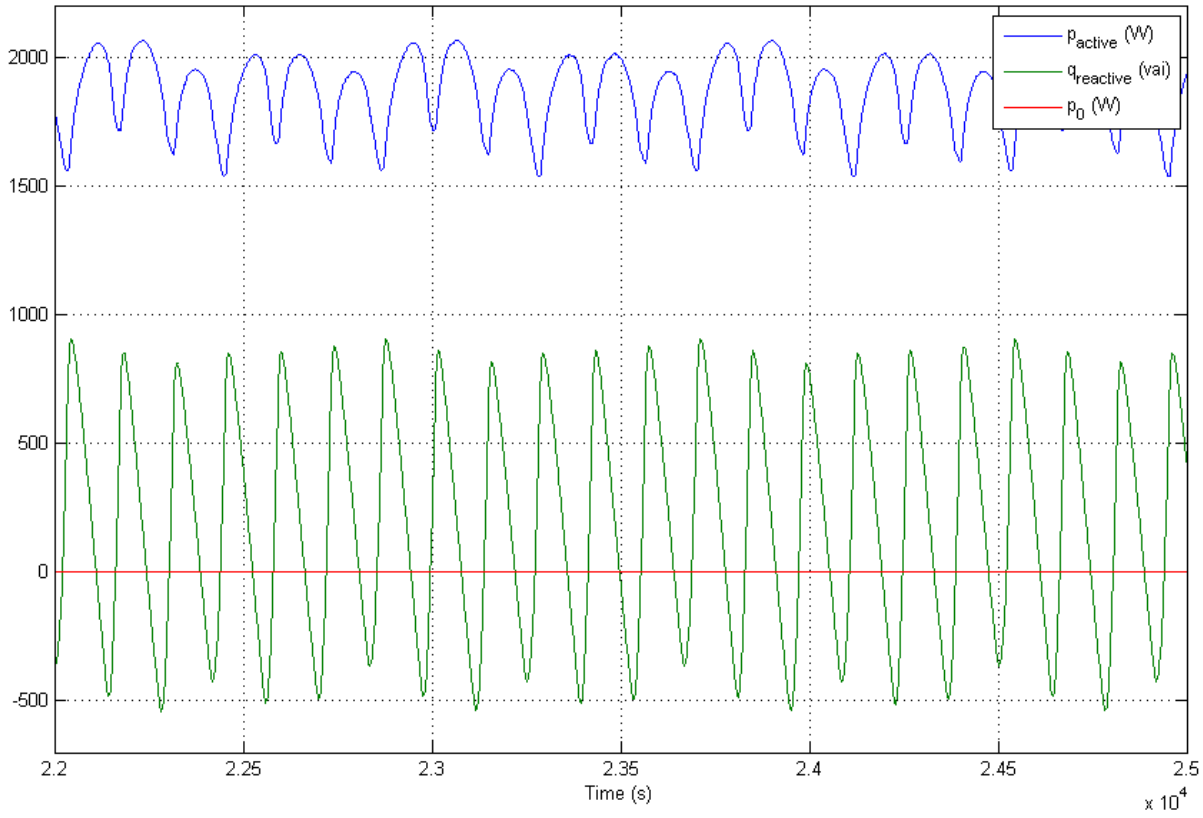

Fig. 4.16 Instantaneous active, reactive and zero-sequence power of the non-linear load

The next figure shows the instantaneous compensating currents calculated by the controller and the carrier signal generated from the simulator to be used in the PWM. These currents are calculated instantaneously without any delay, and it demonstrates the capability of the control methods and real-time components.

The frequency of the carrier could be changed. In this essay the frequency is set to 8.33 kHz. The amplitude of the carrier is 1.5 to have an over modulation. The figure 4.17 shows this parameter.

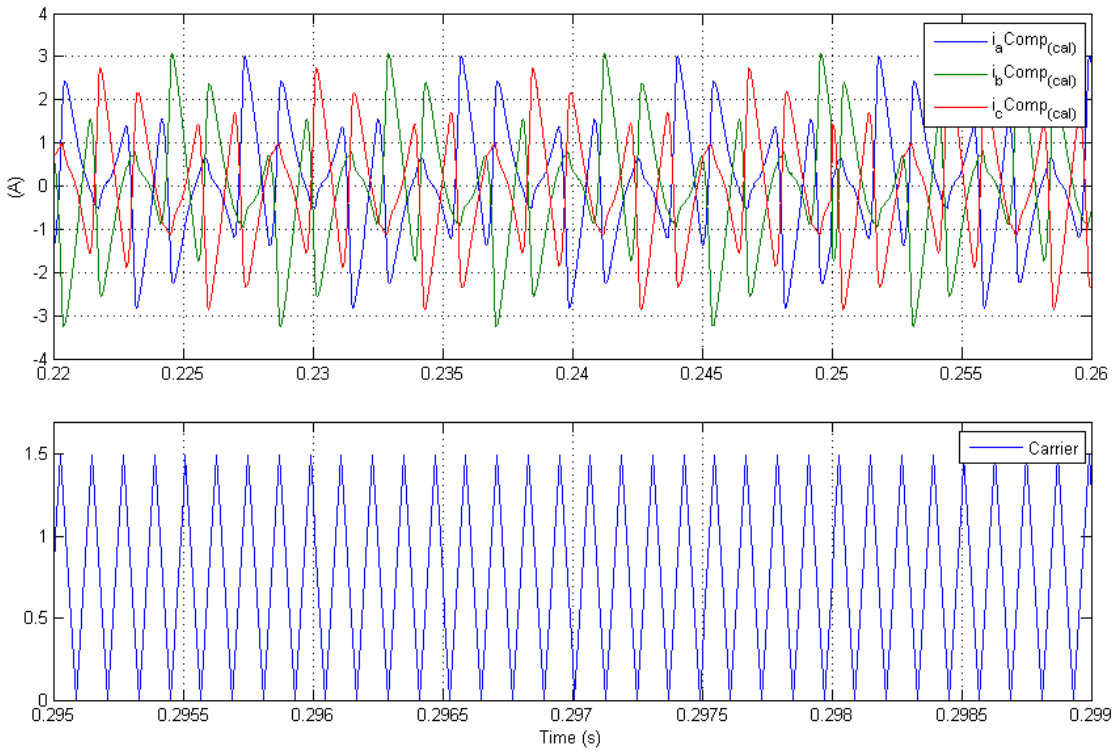

Fig. 4.17 Instantaneous calculated compensating currents, carrier signal

The result of the test is shown in the figure 4.18. The figure shows the calculated currents and the real produced currents.

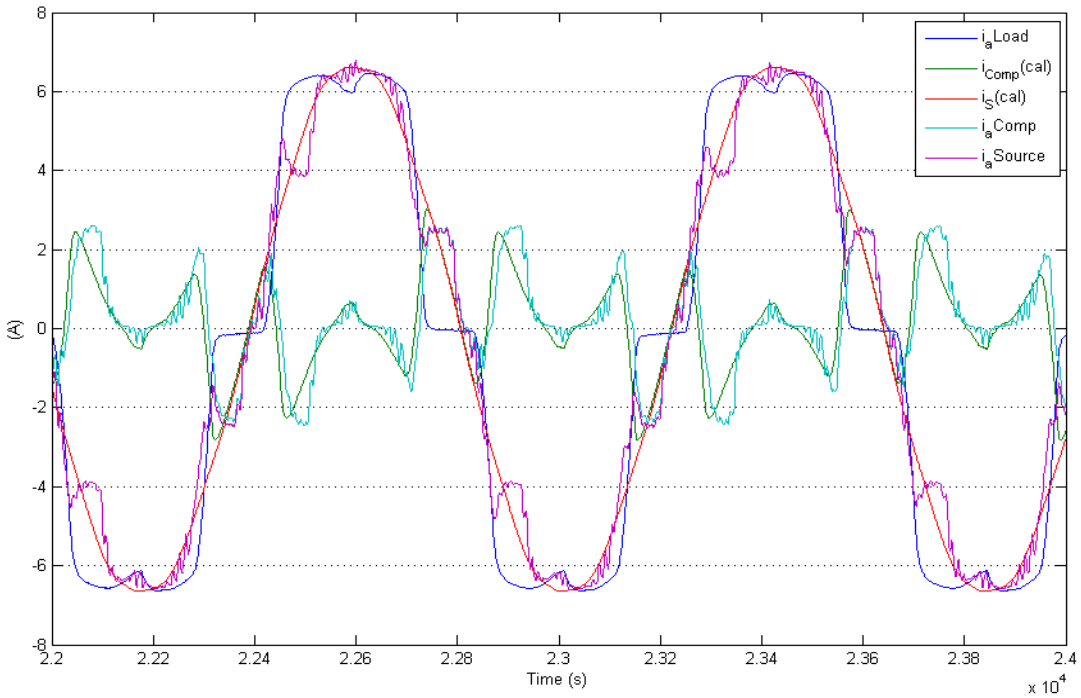

Fig. 4.18 Instantaneous load, source, compensating and calculated currents

The current produced by the inverter follows the reference current which is supposed to be generated. The sum of this current and the load current has a better shape. But some errors are present, they are caused by the strong slope which makes it hard to follow exactly the calculated compensating current.

The PWM introduces many undesired spikes, and the control method is not able to control these noises. However, the results demonstrate that the controller work perfectly and the inverter inject a current wave form as intended from this control method. The weak point of this method is the fact that if a fault occurs in the inverter causing undesired current, the controller is not able to detect them.

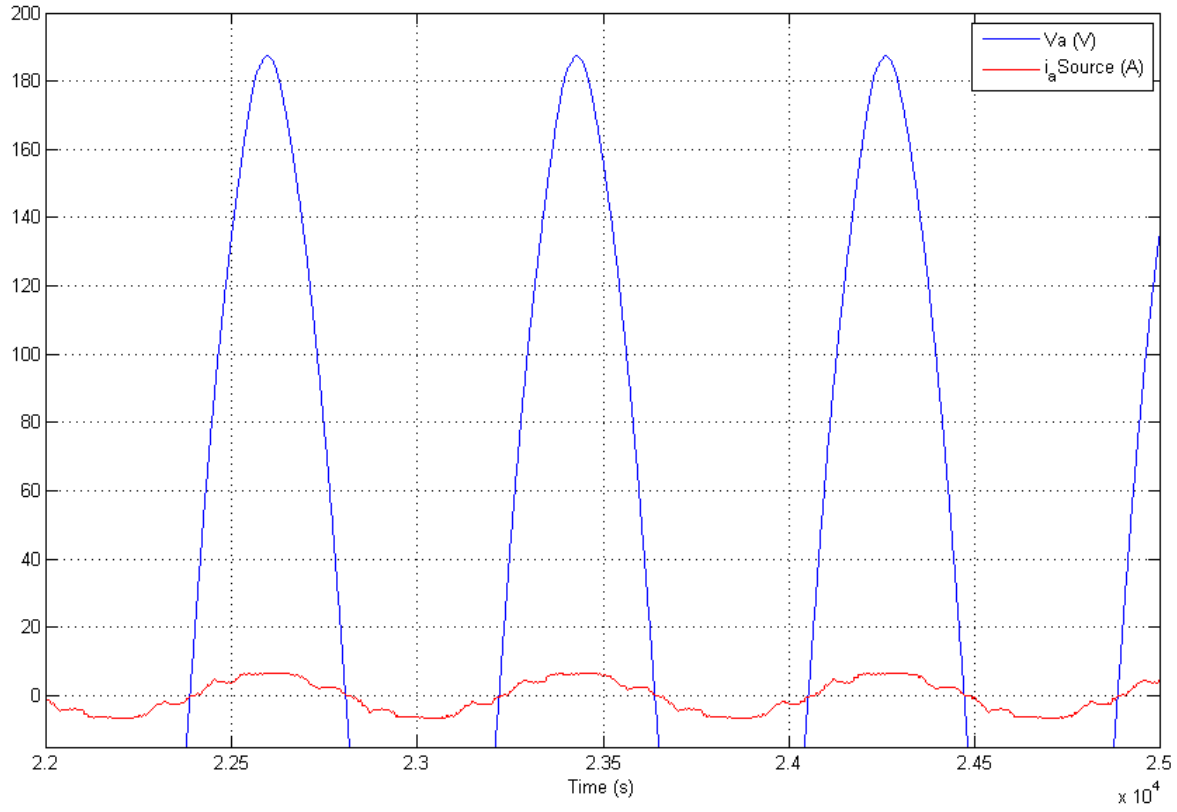

Fig. 4.19 The first phase (“a”) source voltage and current

The figure 4.19 shows the source voltage and the current. In accordance with the calculations and simulations, the real-time result shows that after compensation, a sinusoidal waveform and a unity power factor could be obtained.

4.4.2 Control using Hysteresis PWM generation

In this section three different tests are done. The control strategy is the same as in the previous section, the difference lies in the switching impulses that are imposed to the inverter. The impulses are generated by the hysteresis pulse width modulation technique. This control method implies the use of more laboratory equipments and some modification in the controller in addition to the replacement of the PWM block by a hysteresis one. All of these blocks were made by the author as they could not be found in the Simulink block sets. The algorithm of the hysteresis PWM was adapted for an inverter with three legs [36].

The hysteresis method is more complex than the simple PWM and needs more calculations, which may have some impacts on the real-time tests. This method gives the capability to have a better control on the injected currents. In this method the backup currents were measured by a second probe and compared with the reference currents. Then the current is compared with the reference one and each time it reaches the specified margins an appropriate signal is generated to keep the current inside the margins. By this method six pulses are generated for each switch of the inverter. So the real-time simulator could control the current with an excellent precision.

The following figures shows the results for the second case, obtained for such control strategy. A 90 V dc is imposed to the inverter, and a 3 mH inductance in series with the inverter terminals is used to realize a current source topology.

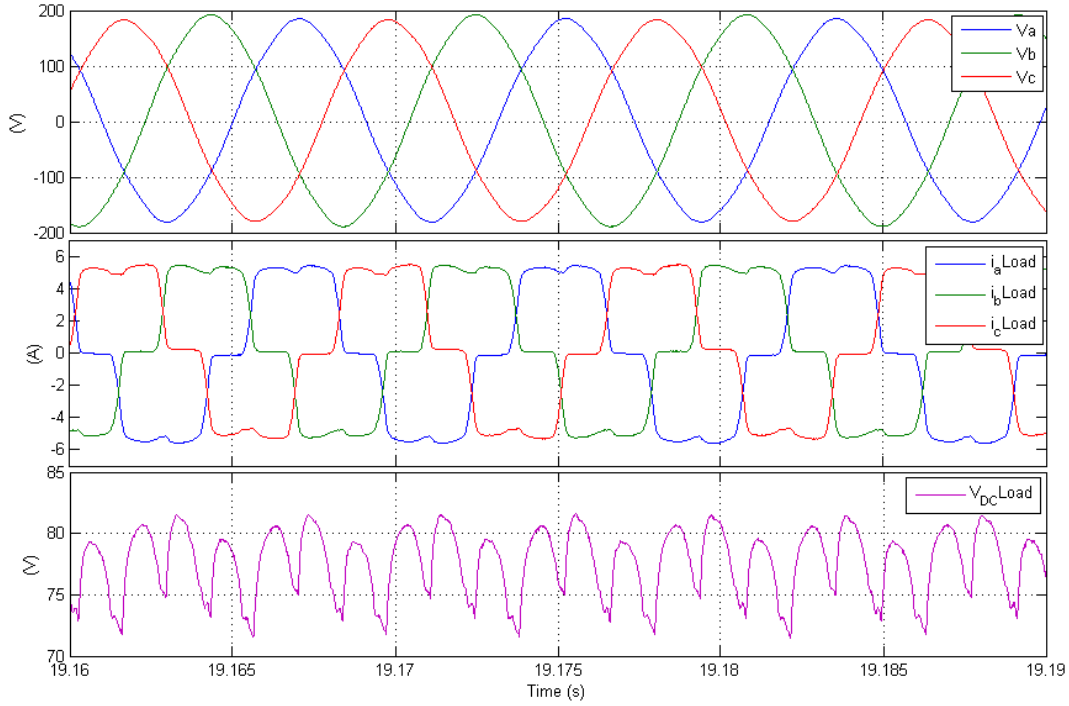

Fig. 4.20 The three phase voltages and currents, the dc voltage of the non-linear load

The figure 4.20 shows the three phase voltage and the three phase currents of the non-linear load and the dc voltage after the two rectifiers. This figure illustrates distorted currents.

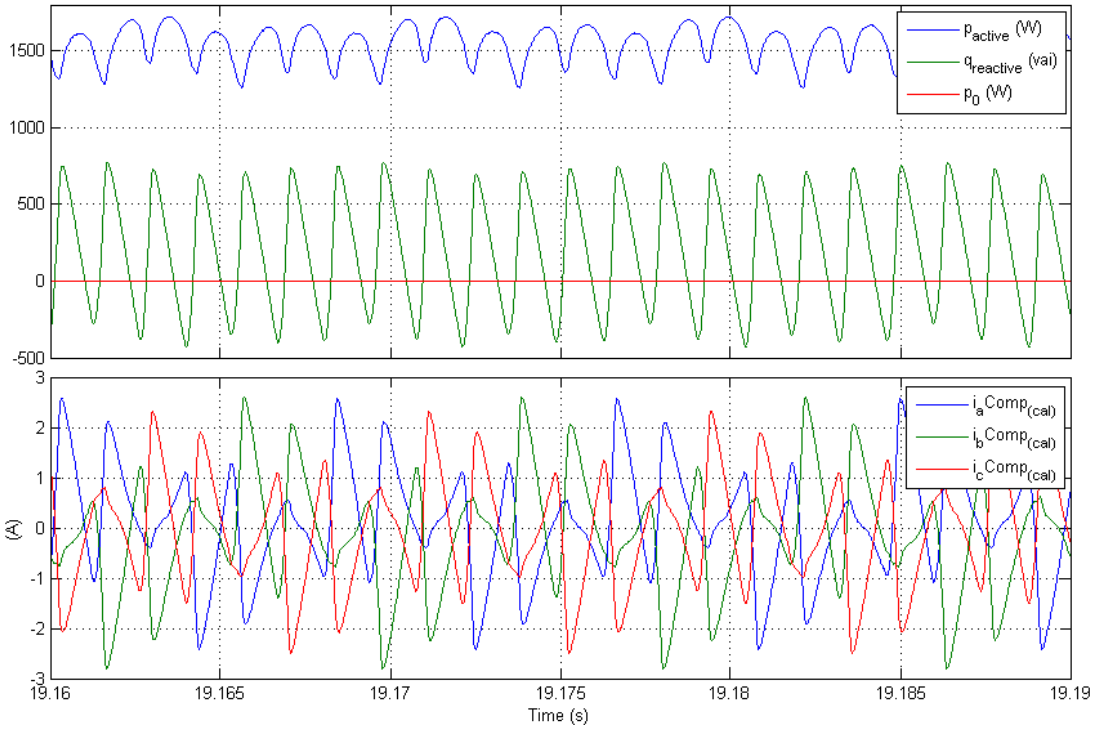

Fig. 4.21 Instantaneous active, reactive and zero-sequence powers, calculated compensation currents

The figure 4.21 illustrates the instantaneous powers and the calculated currents to be compensated. These currents are taken as reference for the hysteresis PWM to be compared with the backup currents.

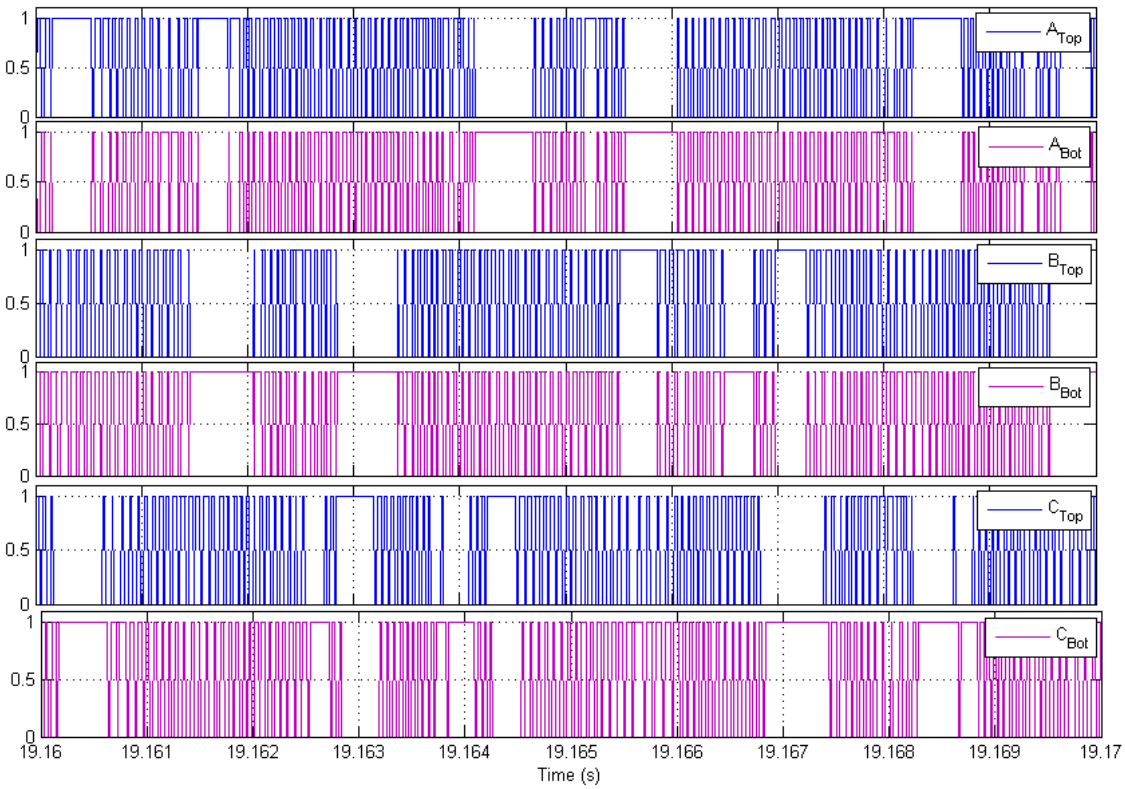

Fig. 4.22 Hysteresis PWM impulsions

The figure 4.22 shows the generated impulsions for the inverter. These impulsions are applied to the digital output of the real-time simulator providing 12 V signals sent to the inverter. The digital I/O of the simulator considers a voltage between 0 V~5 V as logical zero and 10V~14V as logical one signals.

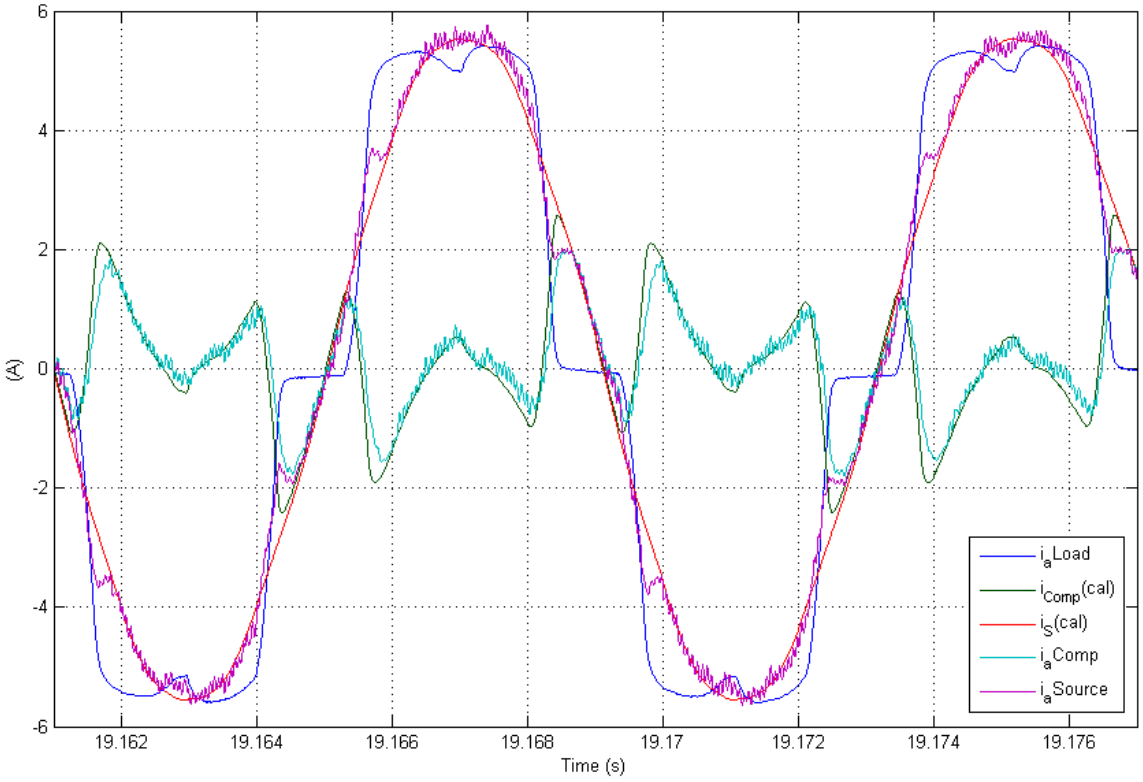

Fig. 4.23Instantaneous load, source, compensating and calculated currents for the second case

The figure 4.23 shows how much the source current became sinusoidal with little spikes caused by the inverter switching. These negligible high order harmonics have the frequencies around the switching frequency of the inverter and could be easily filtered by a simple small passive filter at the output of the inverter.

It is visible that the produced current follows with a high precision the reference current, and it can be observed that the reference current has an excellent sinusoidal wave form. This result demonstrates that the controller calculates and produces instantaneously a correction current, in manner that by adding them the source current becomes sinusoidal. The result is exactly what is intended from this test considering the simulation results of the past chapters.

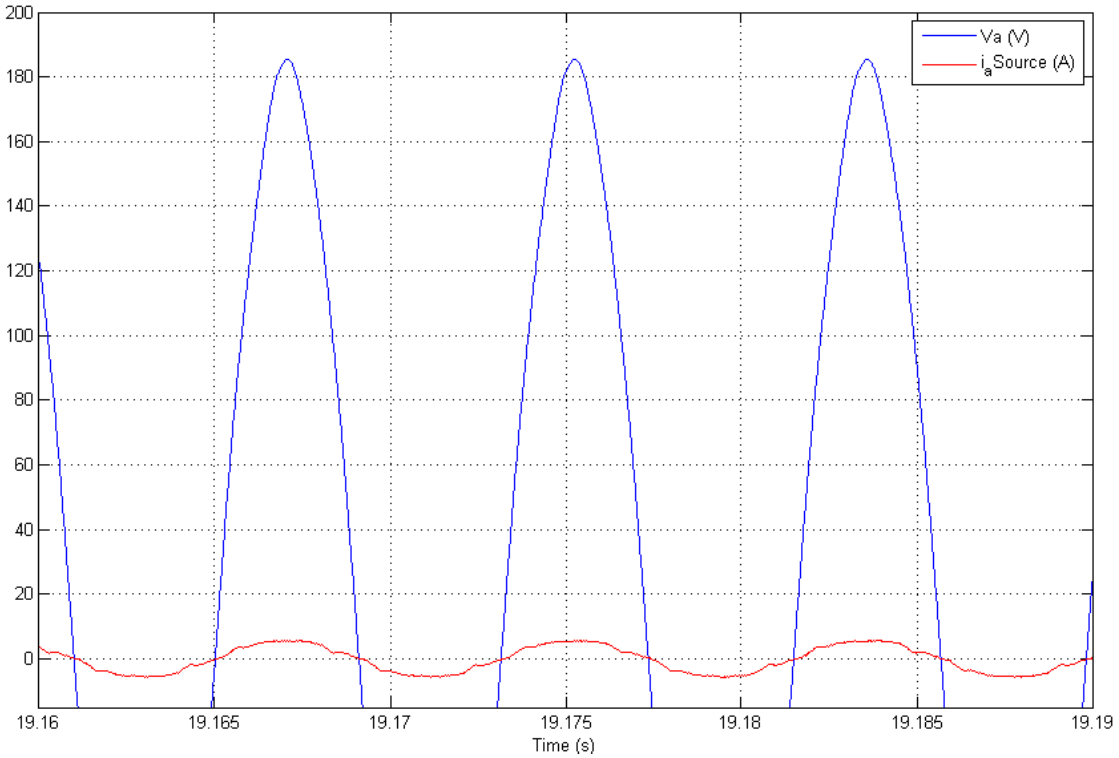

Fig. 4.24 The phase "a" source voltage and current for the second case

This figure shows that by such compensation, the source current could have a sinusoidal shape with a unity power factor.

The case three ; the results for the same control strategy with a 130 V dc for the inverter with a 3 mH inductance connected in series to the inverter terminals are presented in the figures 4.25 to 4.28.

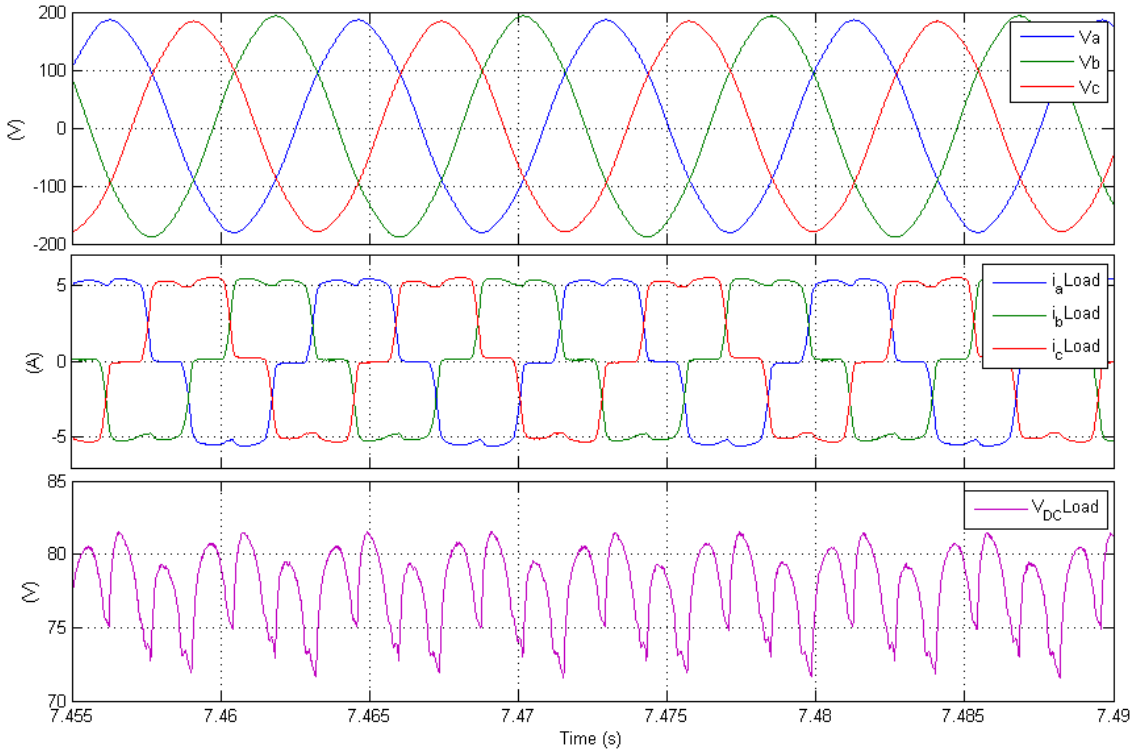

Fig. 4.25 The three phase voltages and currents, the dc voltage of the non-linear load

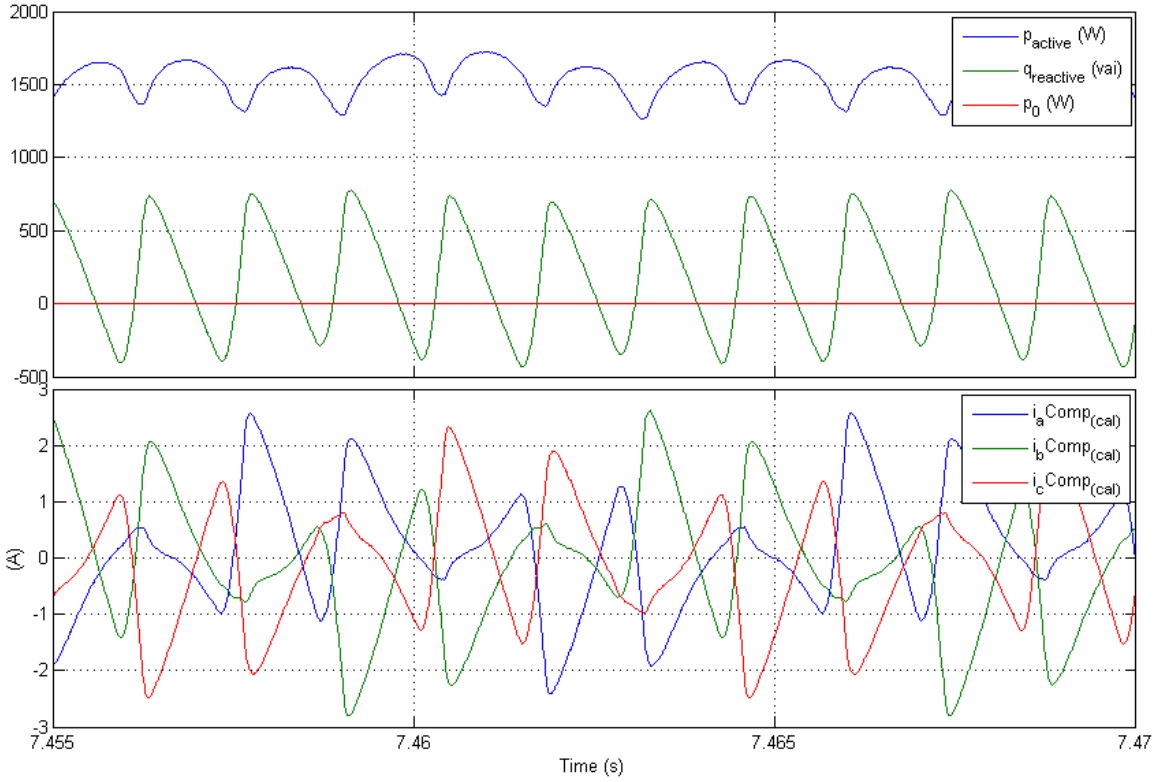

Fig. 4.26 Instantaneous active, reactive and zero-sequence powers, calculated compensation currents for the third case

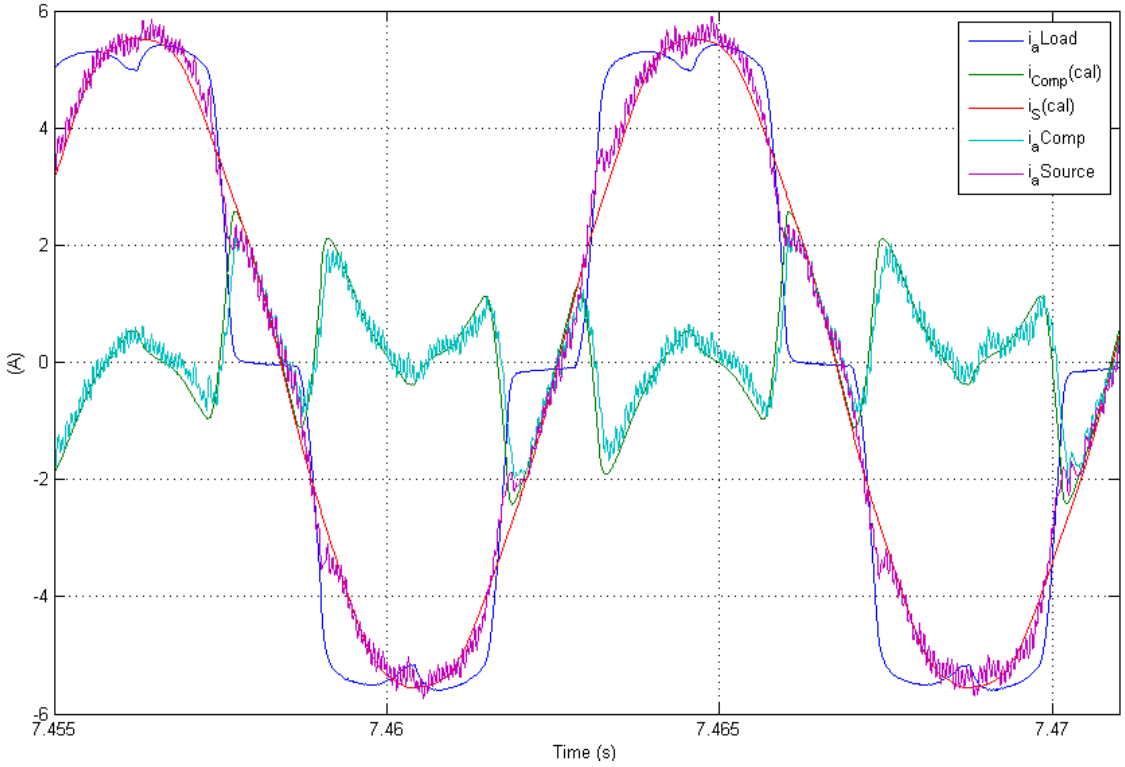

Fig. 4.27 Instantaneous load, source, compensating and calculated currents for the third case

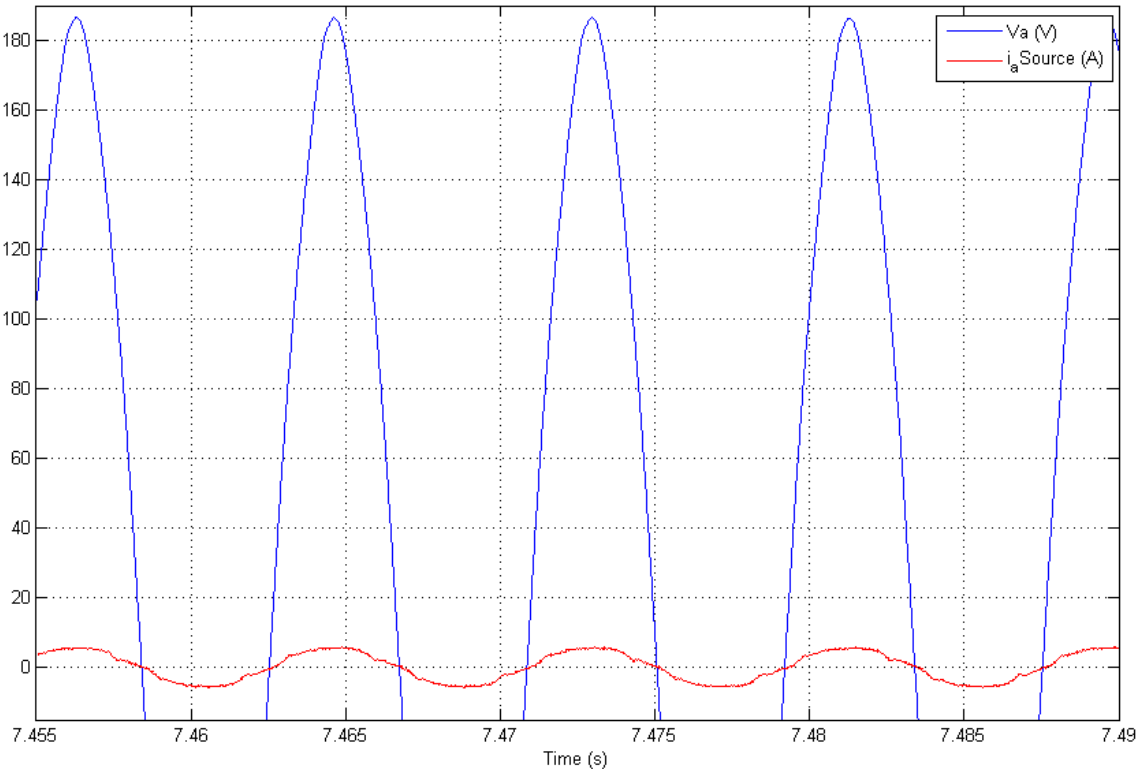

Fig. 4.28 The first phase “a” source voltage and current for the third case

Last figures show the real-time test for the compensation of harmonics for a non-linear load. The particular difference in this experiment is the change in the voltage in the dc side of the inverter which has been increased from 90 V to 130 V.

This voltage increase makes the current to have a better dynamic response, faster slope and a better ability to follow the reference current. The weak point is the increase in the high order harmonics produced by the switching frequency. As mentioned before, these harmonics could be easily eliminated by a small passive filter. The other way to reduce these harmonics is to decrease the hysteresis PWM band.

The factors which limit the decrease of the margin in the hysteresis PWM are the maximum switching frequency of the inverter, the minimum step size supported by the real-time simulator (MX-station), and the inductance used in series at the output terminals of the inverter. These three factors are such that they should be adjusted accordingly to each set of conditions.

The decrease of the inductance has the same impact as the increase of the dc voltage and both improve the dynamic response of the active filter. The following condition should be satisfied for the time step:

$$Step\ size \leq minimum\ time\ for\ the\ current\ to\ increase\ whith\ in\ the\ hystersis\ dead\ band$$

To calculate the minimum margins the author suggests the following method:

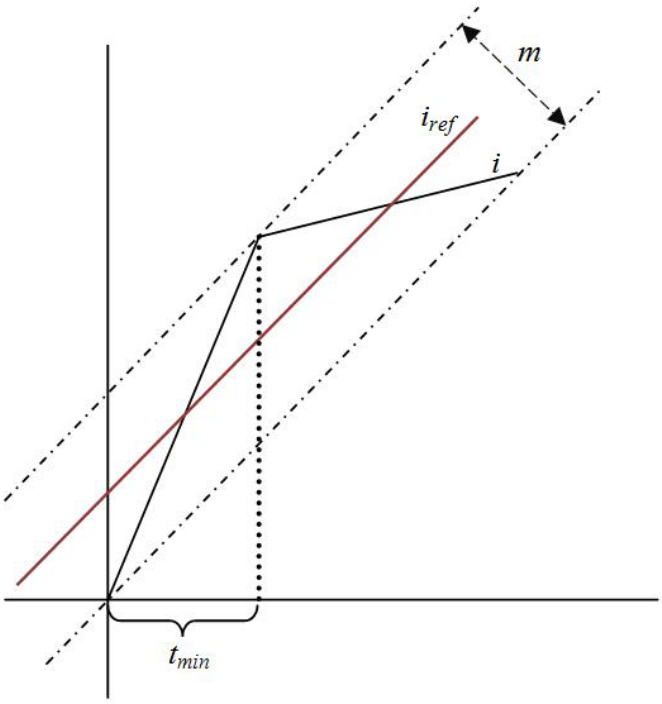

Fig. 4.29 The minimum margin calculation

$$tan\left(\theta_{i_{ref}}\right).t + m = tan(\theta_i).t \xrightarrow{yields} t = {m}\Big/{\left(tan(\theta_i) - tan\left(\theta_{i_{ref}}\right)\right)} \quad (4\text{-}1)$$

$$So: \quad t_{min} \geq Step\ size \quad (4\text{-}2)$$

The case four: the following results show the same control strategy for a 200 V dc voltage and a 3 mH inductance.

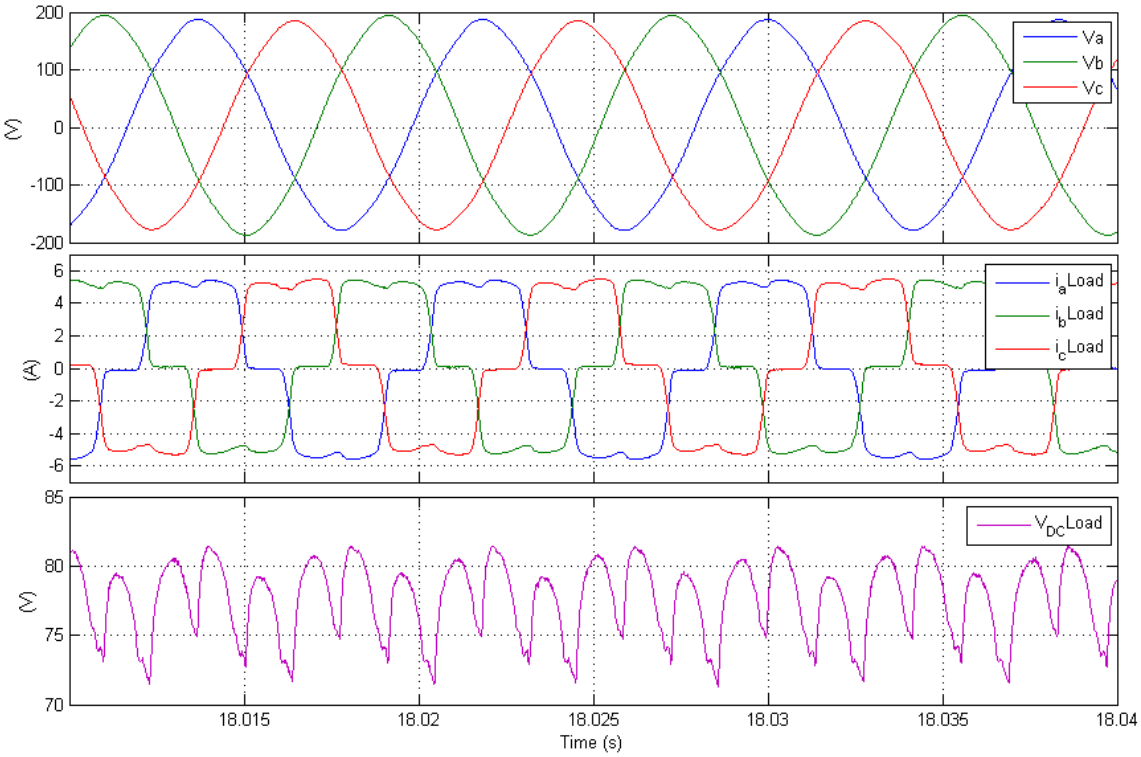

Fig. 4.30The three phase voltages and currents, the dc voltage of the non-linear load

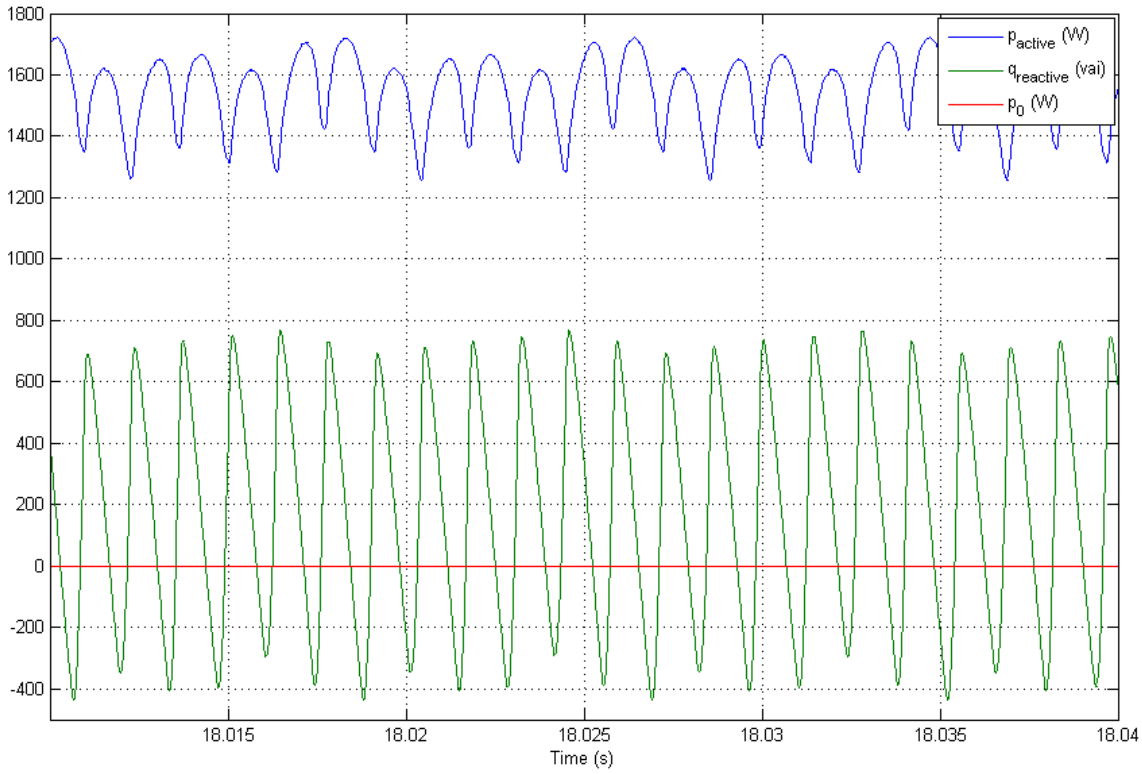

Fig. 4.31 Instantaneous active, reactive and zero-sequence powers

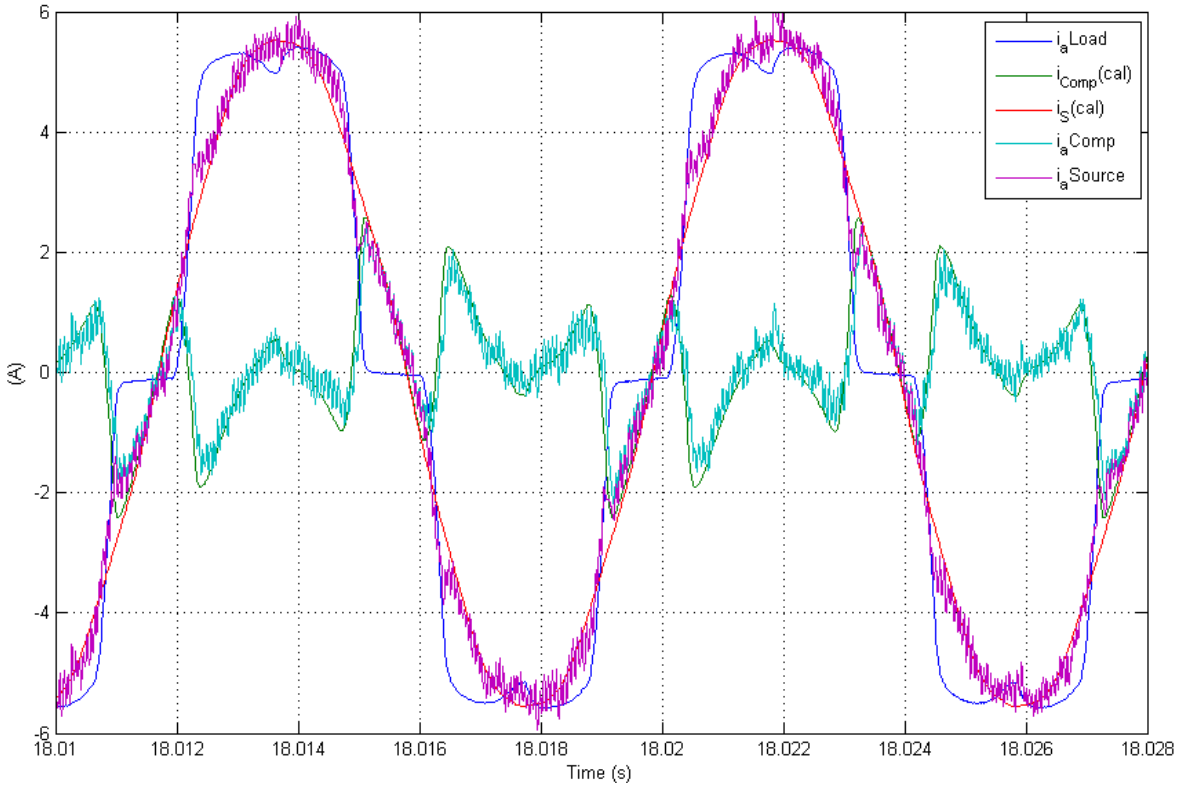

Fig. 4.32 Instantaneous load, source, compensating and calculated currents for the case four

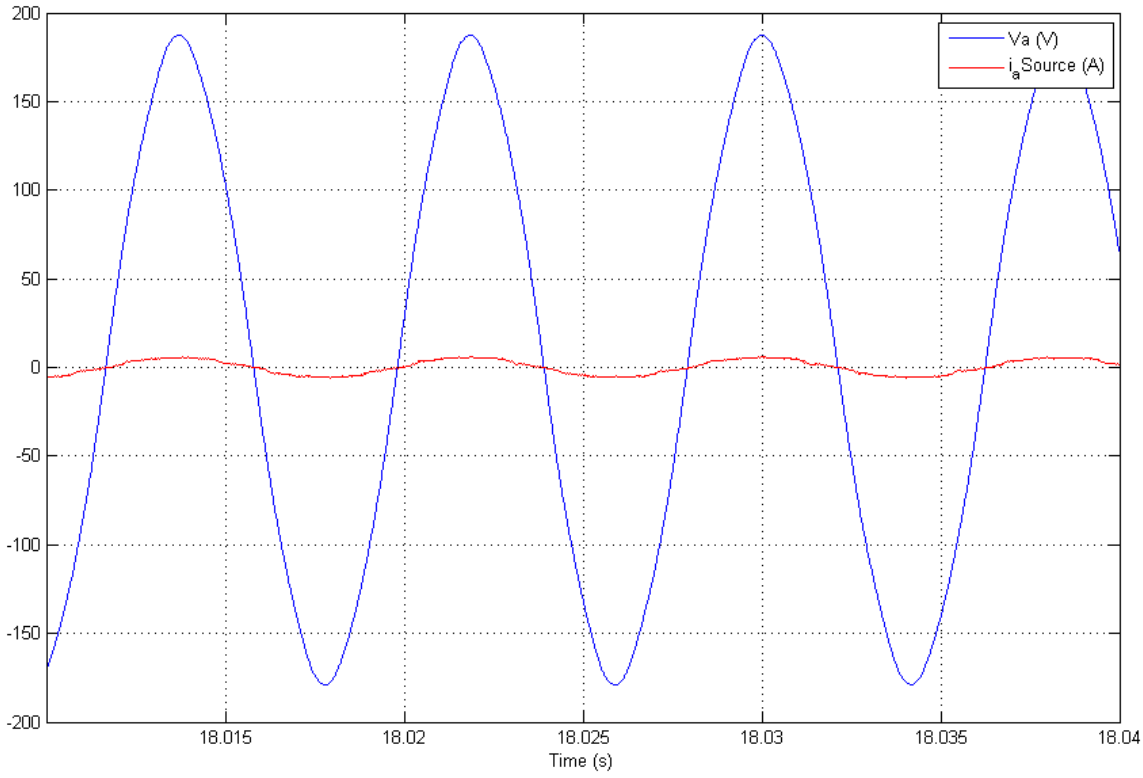

Fig. 4.33 The phase “a” source voltage and current for the case four

These results confirm the hypothesis explained previously. The increase in the dynamic response of the active filter has increased the amplitude of spikes. While trying to improve the dynamic ability of the active filter the increase in the amplitude of switching harmonics should be taken into account.

As described, the increase of the inductance has the effect of decreasing the dynamic response. This reduction in dynamic response will reduce the amplitude of spikes.

Case five: the following figures show the results for a test with 150 V on the dc side of the inverter and a 15 mH inductance connected to the inverter terminals in series.

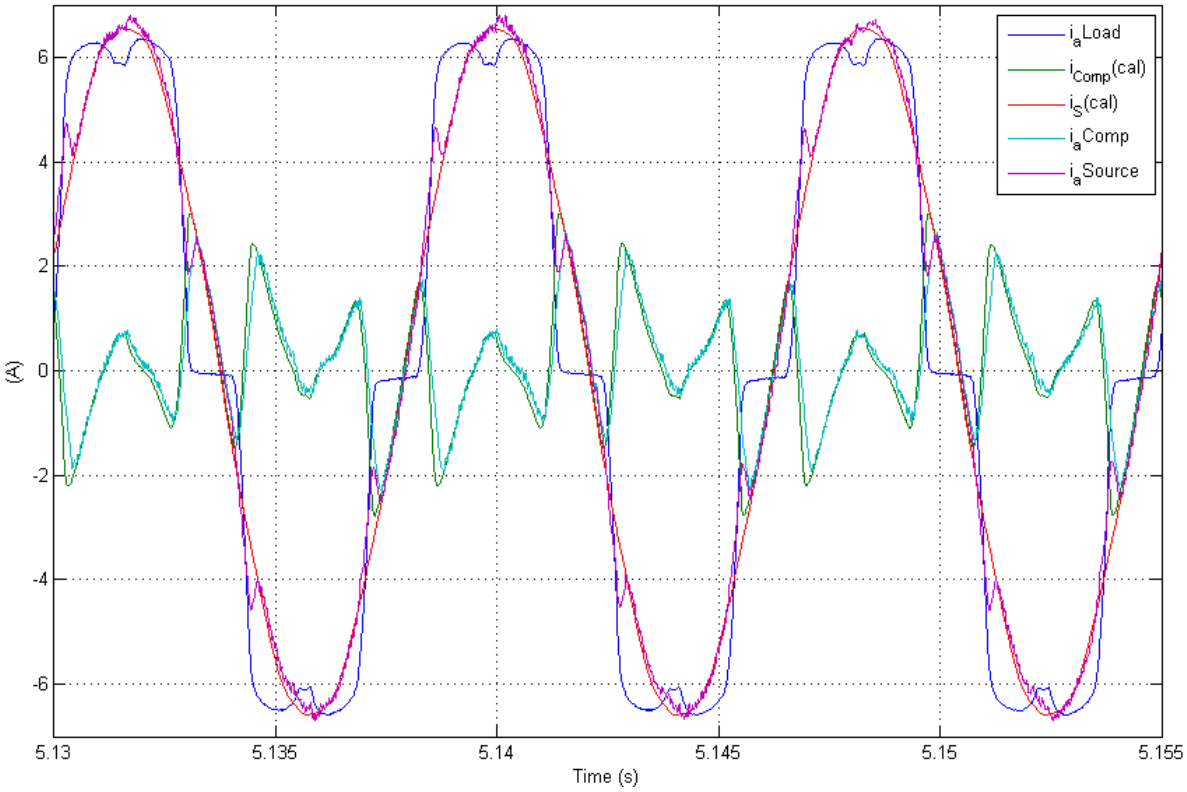

Fig. 4.34 Instantaneous load, source, compensating and calculated currents for the case five

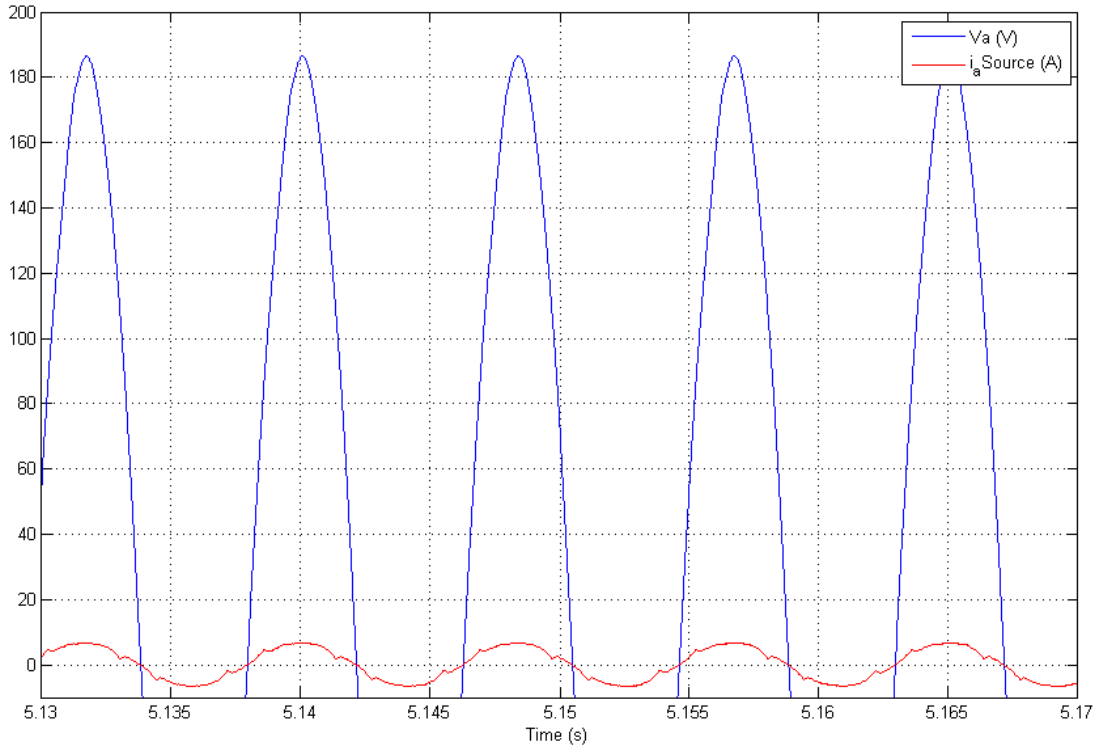

Fig. 4.35 The first phase "a" source voltage and current for the case five

In the preceding figures the voltage of the inverter was adjusted by a three phase auto-transformer.

The frequency spectrum of this result is presented in the figure 4.36. The figure shows a discrete Fourier transformer (DFT) of the load distorted current and the source current after compensation.

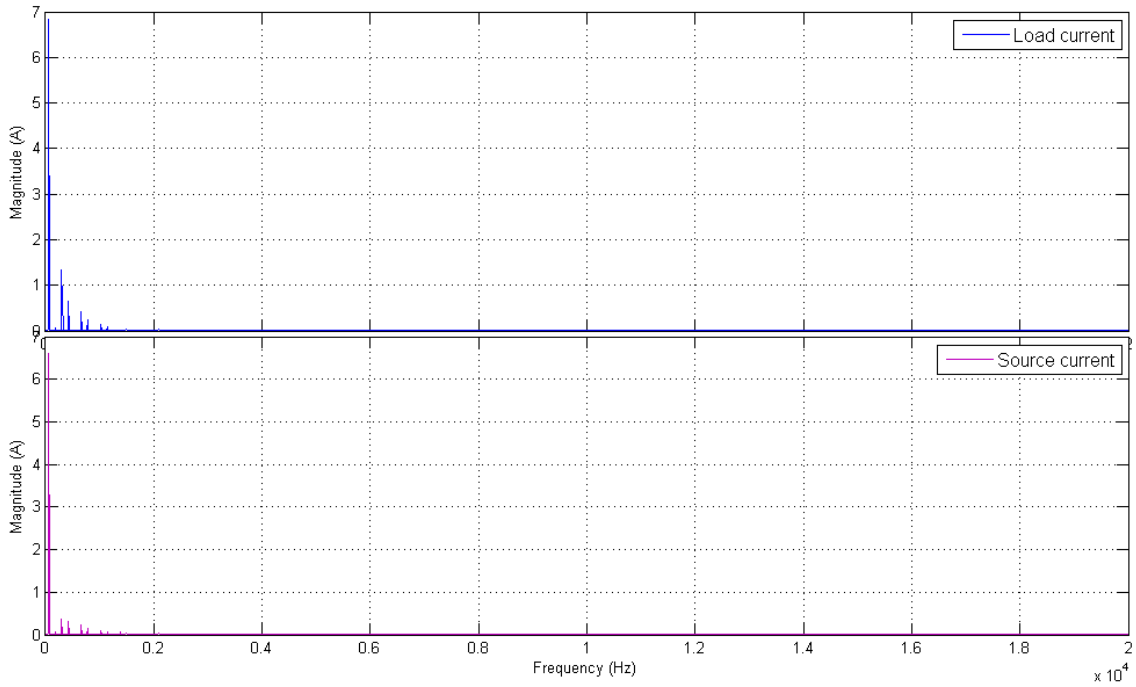

Fig. 4.36 The frequency spectrum before and after harmonic compensation

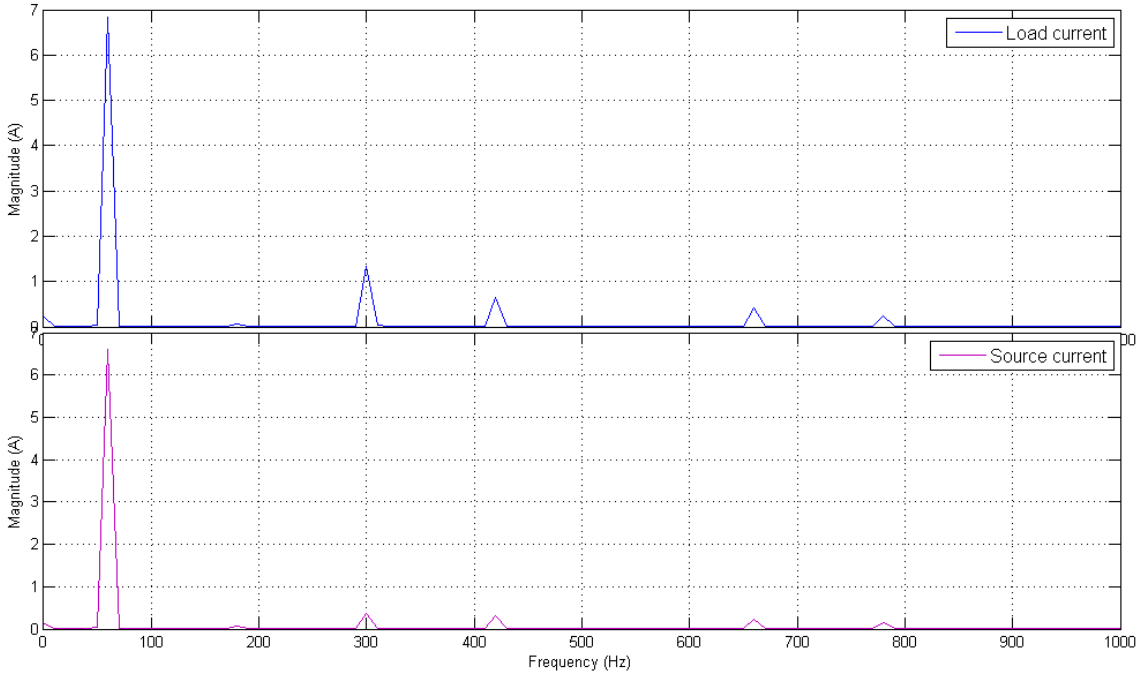

Fig. 4.37 The fundamental, fifth, seventh, eleventh and thirteenth harmonic orders

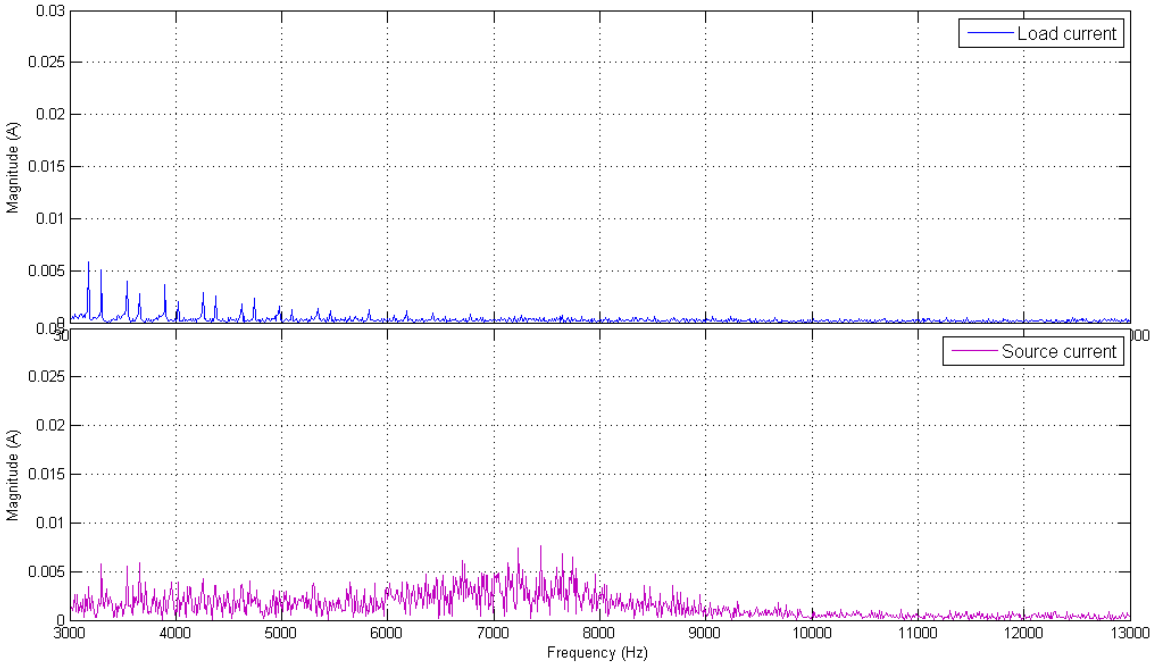

Fig. 4.38 High order harmonics spectrum

As it is possible to observe from the figure 4.36 the amplitude of harmonics has distinctly decreased after the compensation. The figure 4.37 shows the low order harmonics including the fundamental. A comparison of their amplitude is shown in the table 4.1.

Table 4.1 Magnitude of each harmonic before and after compensation

	Load	**Source**
Fundamental (I_1)	6.97 A	6.53 A
5 th (I_5)	1.36 A	0.32 A
7 th (I_7)	0.67 A	0.19 A
9 th (I_9)	0.42	0.098

The remaining low order harmonic could be totally compensated by a fine adjustment of the filter.

The figure 4.38 shows that most of the harmonics are present around the switching frequency of the inverter. As explained previously these high order harmonics could be eliminated by a small passive filter at the output terminals of the inverter.

4.4.3 Compensation during load changes

The experimental tests were followed by the dynamic tests on the active filter. By rapidly changing the load, the response of the active filter was examined. These tests were crucial to demonstrate the instantaneous compensation obtained with the controller. If the results demonstrate an acceptable response, the active filter has accomplished its work.

The following figure shows the result to a sudden reduction of the load current.

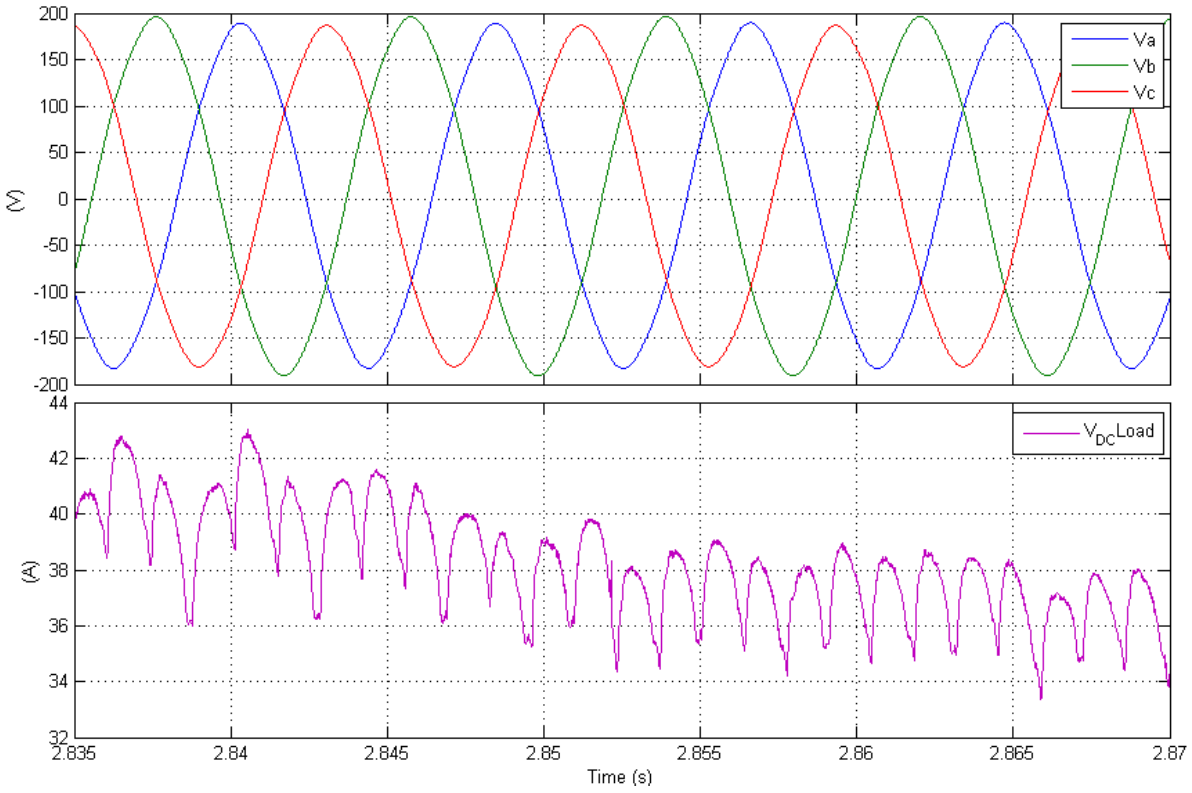

Fig. 4.39 The three phase source voltages, the dc voltage of the non-linear load during transient current tests

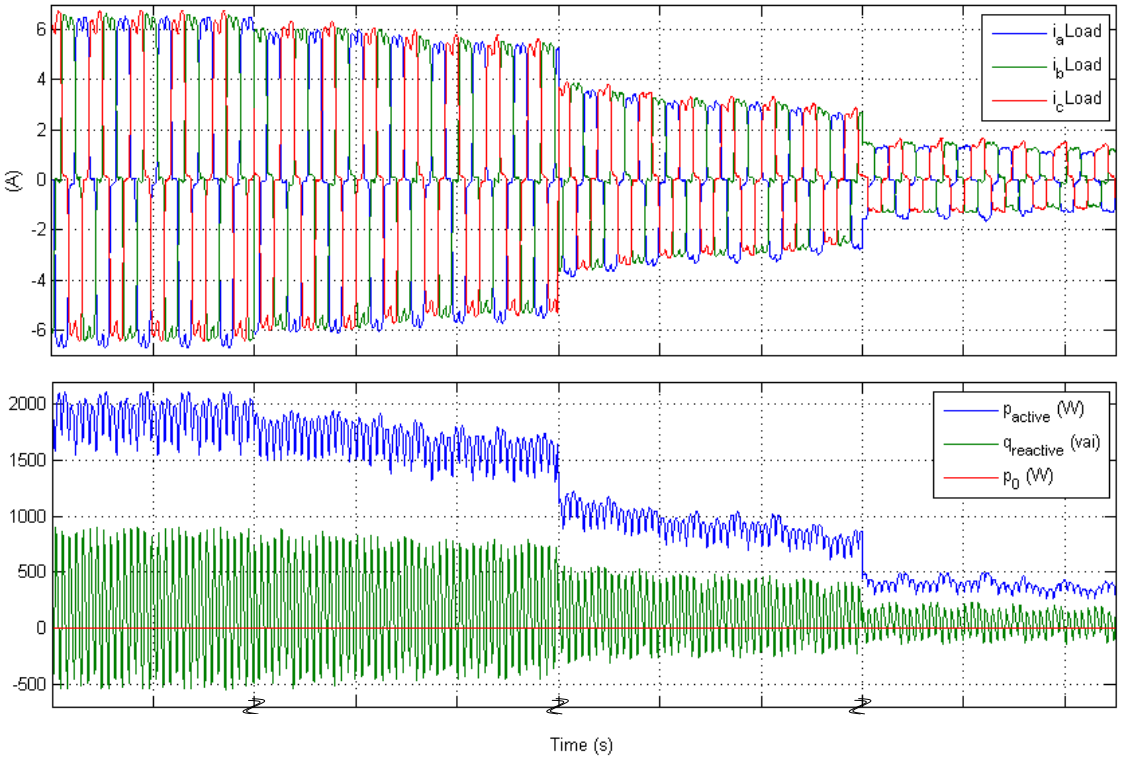

Fig. 4.40 The three phase load currents, the instantaneous active, reactive and zero-sequence powers of the non-linear load for the decreasing load

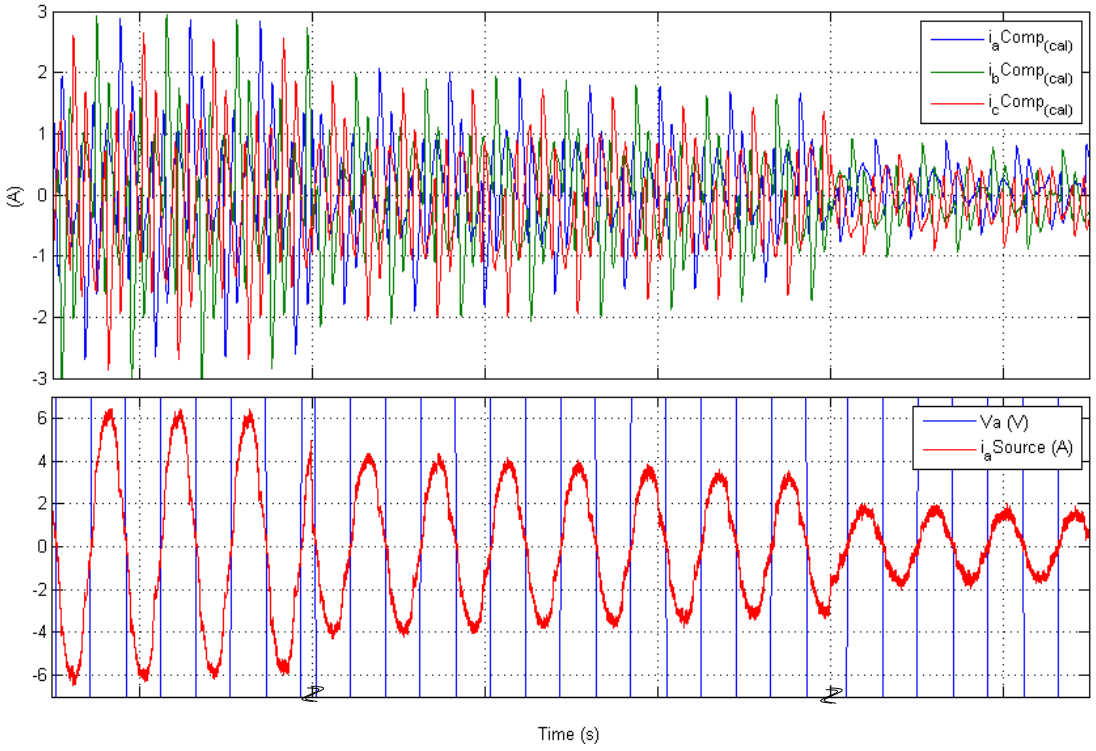

Fig. 4.41 The calculated compensation currents, the phase "a" source voltage and current for the decreasing load

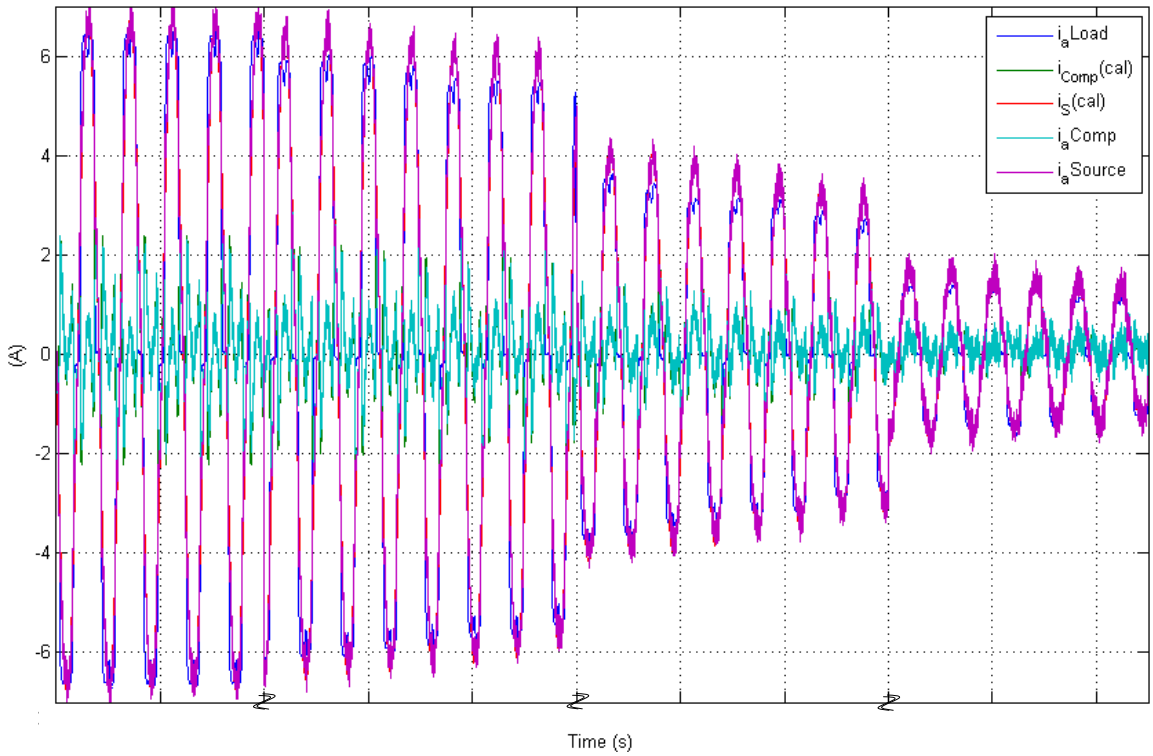

Fig. 4.42 Instantaneous load, source, compensating and calculated currents during the change in the load current for the decreasing load

The figures show an excellent response of the controller. The figures show an instantaneous compensation of harmonics, the active filter reduce the compensating current instantly while the load current is decreasing. These results could not be obtained with a passive filter. This experimental implementation test shows the ability of the new technology for harmonic compensation and correcting the power factor.

Another test consists in increasing the load current (load power). The following frames show the compensation during the increase of the load current. The load current was changed by increasing the dc voltage of rectifiers with the autotransformer in front of the load.

The following figures confirm the hypothesis and the good behavior of the active filter during the increase in the load. These kinds of results could also be obtained upon load is turn on or off in a real application.

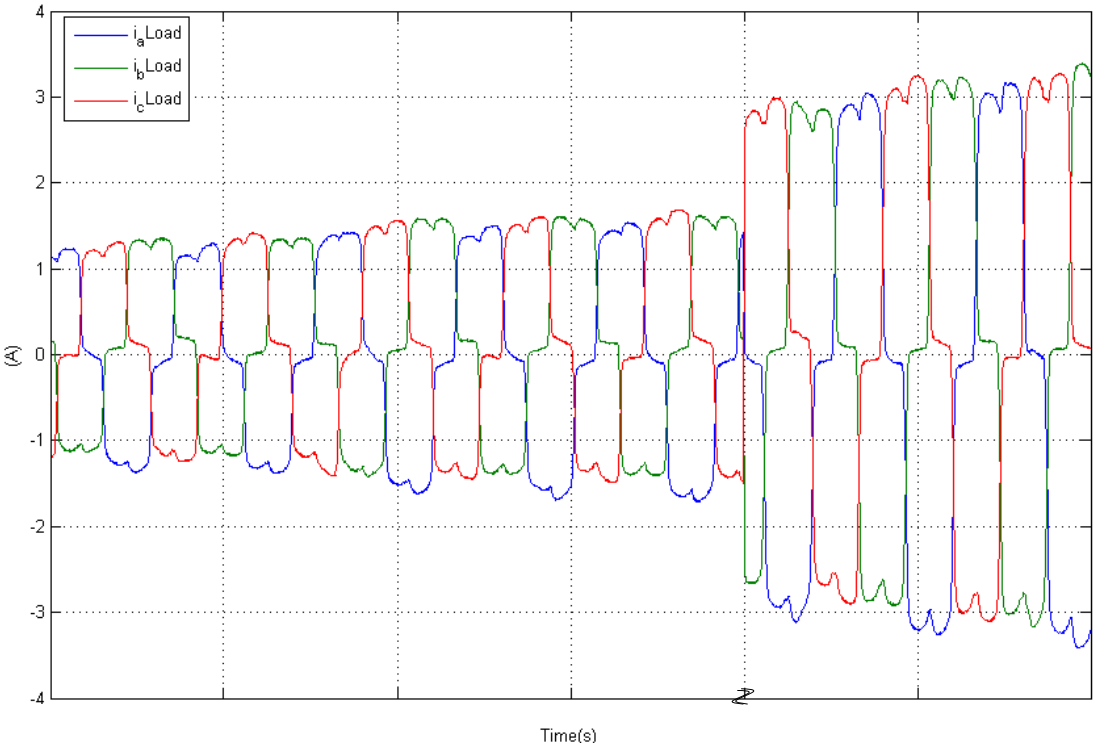

Fig. 4.43 The three phase load currents

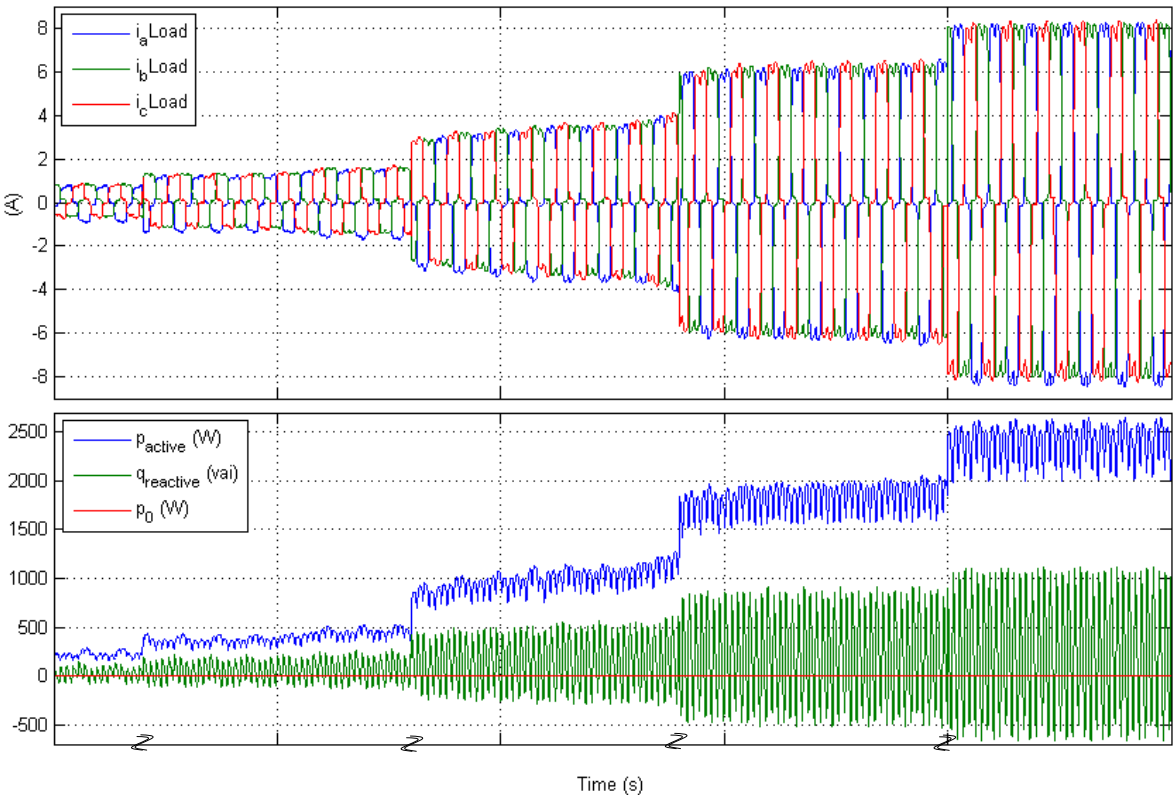

Fig. 4.44 The three phase load currents, the instantaneous active, reactive and zero-sequence powers of the non-linear load for the increasing load

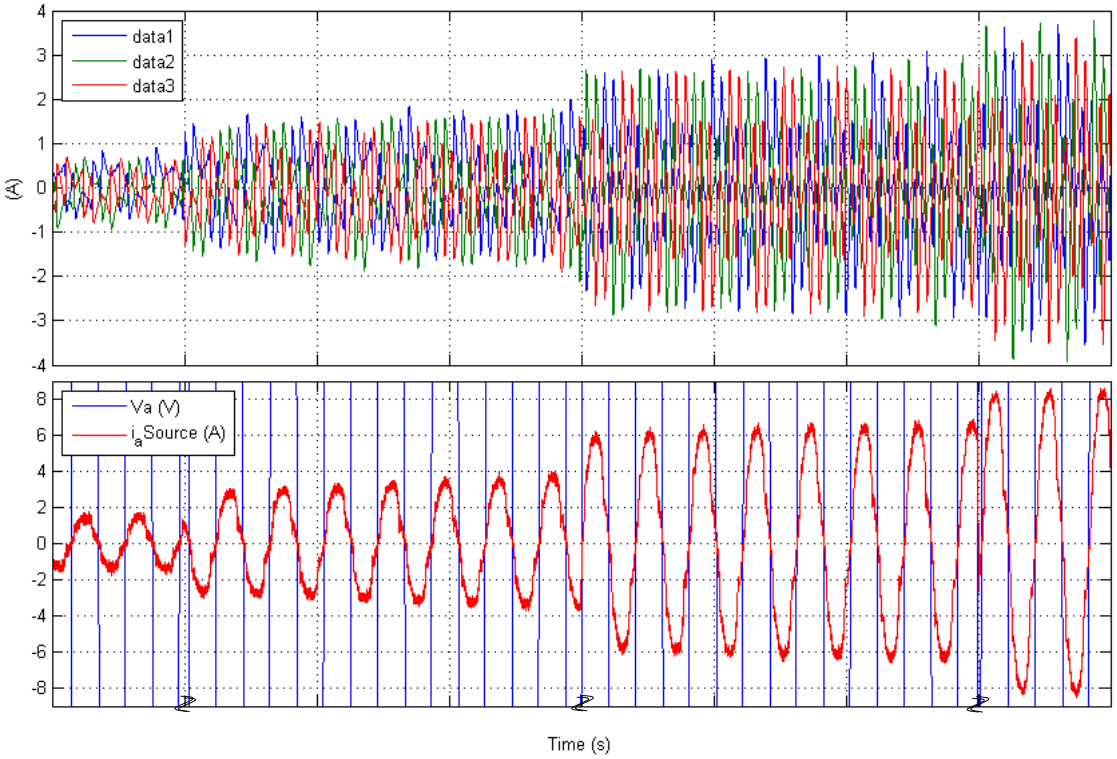

Fig. 4.45 The calculated compensation currents, the phase "a" source voltage and current for the increasing load

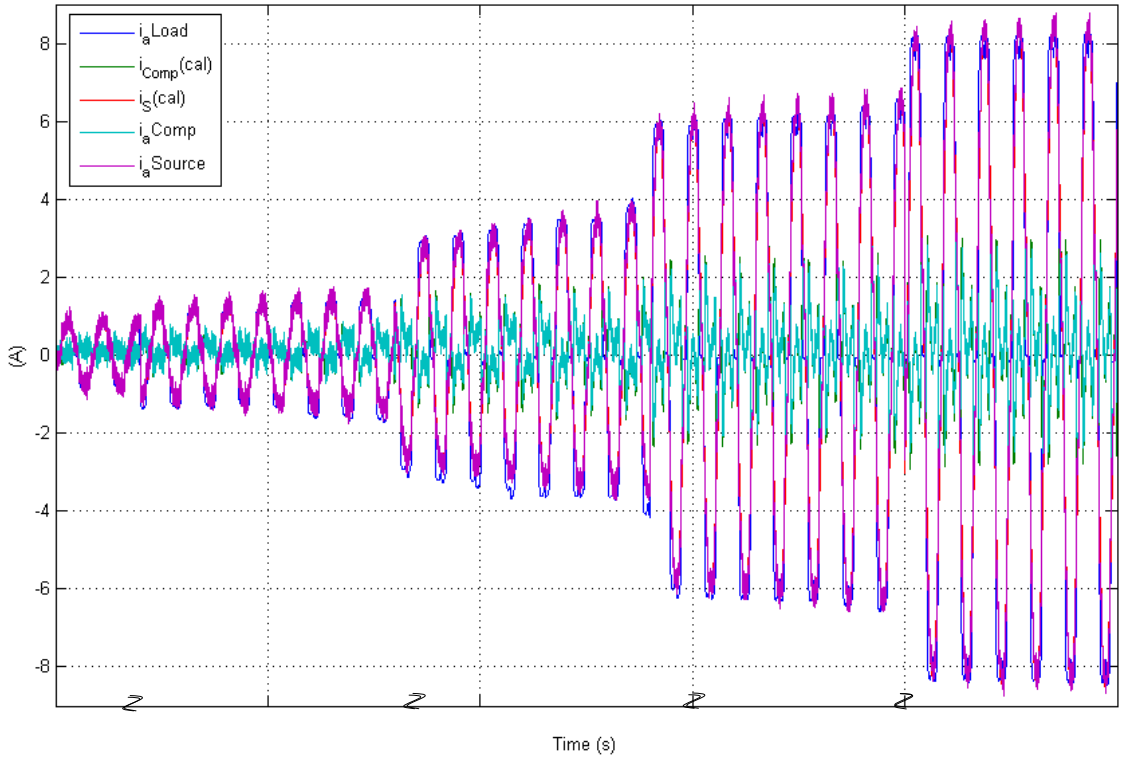

Fig. 4.46 Instantaneous load, source, compensating and calculated currents during the increase of the load current for the increasing load

4.5 Summary

In this chapter, the instruments for the real-time test, the realization and the real-time results were presented. This chapter concentrates on the tests and the methodology used to control the active filters and the real-time realization of such a controller.

In the first part the equipment used within these tests were studied in detail. The real-time simulator, the inverter and the non-linear load were indispensable to realize these tests. The simulator (Mx-Station) and its related equipment (the probes and the PC unit) were explained and the configurations of the instruments were presented. Some physical instruments are necessary to realize a real-time hardware in the loop (HIL). For that purpose, the non-linear load consists of two rectifiers and a resistive load and some other various equipments were used. Since the real-time simulator is not able to produce high voltages and power current, an inverter was used to produce the compensation current.

The Block sets and their configurations are studied. According to the description of the project, it was followed by the modeling of the active filter and the real-time implementation. The real-time simulator acts as the controller of an active filter generating command signals for the inverter to produce the desired compensating currents for a three-phase three-wire power system.

Results obtained for different tests are presented in the third part of this chapter. The results confirm that the project was realized successfully. By such results it is possible to conclude that each part of the project was done correctly; the control theory is appropriate, the model was an appropriate model based on the theory and the real-time simulator is working properly. Of course, the other real parts like the inverter and the non-linear load are adjusted and functioned correctly for these tests.

The objectives defined in the project were based on a simple PWM inverter, but some obtained results were encouraging the author to go further to develop a hysteresis PWM module. The hysteresis modulation eliminates the disadvantages of the simple PWM. Even with the simple PWM block the current produced by the inverter had exactly the same shape as the compensating current. A weak point in this case was that the use of a passive filter to reduce the amplitude of harmonics around the switching frequency was indispensable. The other weak point is the absence of a current control during the normal and faulty operation by this method. The

two problems disappeared by changing the PWM block with the Hysteresis PWM block set. The implementation of the hysteresis PWM block has prolonged the project by the necessity of a short theoretical study, simulation, modeling, and finally implementing the block into the controller. Of course, many configurations should have been set up to put the controller in function.

The use of the hysteresis PWM illustrates the abilities of such filters. By means of the different real-time tests, the powerfulness of such active filters based on the instantaneous theories was illustrated. And finally, with the tests during the changes in the load power, the dynamic response of the active filter was studied.

CHAPITRE 5 CONCLUSION AND FUTURE WORKS

5.1 Conclusion

Production and distribution of electricity were developed considering that the voltage and current waveforms were perfectly sinusoidal. With the progress of electronics in just a few years, issues of harmonic pollution power quality had become one of the most important problems. Communication interferences, losses as heating, solid-state device malfunctions are some typical undesired effects of harmonic distortions.

After a deep study, four methods were found in the literature able to eliminate completely or partially the distortion problem in the power systems; in-line reactor or choke which is a simple solution, passive filter which is a relatively inexpensive method, zigzag transformer which is applied for commercial facilities to control zero-sequence harmonic components, and finally active filters which are relatively new types of devices for eliminating harmonics. These kinds of filters are based on power electronic devices making them more reliable and flexible than others.

In this master dissertation an active filter was modeled and simulated for real-time control to compensate current harmonics in a typical laboratory electric system. The objective of this project was to review the theorems and definitions of electric power concepts under non-sinusoidal conditions and compare different control algorithms found in the literature. In this manner, we have recalled the Akagi's theory of instantaneous power (p-q theory) which is one of the best approaches till nowadays. This master dissertation has focused on simulation and real-time control of an active filter to compensate current harmonics in a typical electric system. A control model appropriate for the active filter based on literature review was proposed. Then the control model was simulated using the Simulink toolbox of MATLAB.

Finally, the model was implemented in the laboratory on a RT-Lab real-time simulator with a three-phase rectifier as the non-linear load. Experimental results were compared with simulation results. Moreover, the provided real-time structure makes it feasible to develop and compare different control designs and their transient state responses.

Experimental results illustrate the innovative work done in this project. The modeled active filter was able to compensate harmonics in the power system and improve the efficiency of power

system without any active power consumption. Compensation of non-active power substantially improves the power factor and reduces the total harmonic distortion index (THD) as well as the total losses. This means an evolution in the power system domain, since the system would have the ability to transfer more active power with the same capacity. The contributions of this project were: the realization of a real-time system in the laboratory and the real-time implementation of the active filter controller on a three-phase power system to compensate the harmonics of a non-linear load.

As a general conclusion of this project, the real-time results obtained demonstrate that by using the instantaneous theories, it is possible to compensate harmonics and correcting the conventional power factor for the three-phase systems with or without the neutral wire. These results demonstrate that the real-time simulator is able to realize any kind of controllers and controlling a physical laboratory system.

Future Works:

- Survey on real-time behavior of an active filter implemented on an Opal-RT simulator connected to the hypersim, a digital power system simulator. This research proposes a real-time test of the active filter with different control approaches through a real-time digital power system which has almost similar characteristics as a real system without having any risk to make any partial or global detriment in the system.
- Elaboration and real-time test of a new method for the control of active filters for multiphase systems based on the generalized power theory.
- Real-time implementation of an active filter based on fast Fourier transformations (FFT) or other frequency domain theories by making a comparison with instantaneous compensation algorithms.

BIBLIOGRAPHY

[1] H. Akagi, Y. Kanazawa, and A. Nabae, "Instantaneous reactive power compensators comprising switching devices without energy storage components," *IEEE Transactions on Industry Applications,* vol. IA-20, pp. 625-630, May-Jun 1984.

[2] H. Akagi, S. Ogasawara, and H. Kim, "Theory of instantaneous power in the three-phase four-wire systems: a comprehensive approach," *Conference Record - IAS Annual Meeting (IEEE Industry Applications Society),* vol. 1, pp. 431-439, 1999.

[3] H. Akagi, E. H. Watanabe, and M. Aredes, *Instantaneous power theory and applications to power conditioning* vol. 1. Psicataway, NJ: Wiley- Interscience, 2007.

[4] M. E. Balci and M. H. Hocaoglu, "Comparison of power definitions for reactive power compensation in nonsinusoidal conditions," in *11th International Conference on Harmonics and Quality of Power*, Lake Placid, NY, 2004, pp. 519-24.

[5] A. Barona, F. Ferrandis, J. Olarte, and J. L. Iribarren, "New power quality solutions especially designed for industrial applications," in *2007 9th International Conference on Electrical Power Quality and Utilisation, EPQU*, Barcelona, Spain, 2007.

[6] Collaboration, *IEEE Trial-Use Standard Definitions for the Measurement of Electric Power Quantities Under Sinusoidal, Nonsinusoidal, Balanced, or Unbalanced Conditions*, 2000.

[7] L. Cristaldi, A. Ferrero, and G. Superti-Furga, "Current decomposition in asymmetrical, unbalanced three-phase systems under nonsinusoidal conditions," *IEEE Transactions on Instrumentation and Measurement,* vol. 43, pp. 63-68, Feb 1994.

[8] L. S. Czarnecki, "Considerations on the reactive power in nonsinusoidal situations," *IEEE Transactions on Instrumentation and Measurement,* vol. IM-34, pp. 399-404, 1985.

[9] L. S. Czarnecki, "Orthogonal decomposition of the currents in a 3-phase nonlinear asymmetrical circuit with a nonsinusoidal voltage source," *IEEE Transactions on Instrumentation and Measurement,* vol. 37, pp. 30-34, Mar 1988.

[10] L. S. Czarnecki, "Reactive and unbalanced currents compensation in three-phase asymmetrical circuits under nonsinusoidal conditions," *IEEE Transactions on Instrumentation and Measurement,* vol. 38, pp. 754-759, Jun 1989.

[11] L. S. Czarnecki, "A time-domain approach to reactive current minimization in nonsinusoidal situations," *IEEE Transactions on Instrumentation and Measurement,* vol. 39, pp. 698-703, Oct 1990.

[12] L. S. Czarnecki, "Distortion power in systems with nonsinusoidal voltage," *IEE Proceedings, Part B: Electric Power Applications,* vol. 139, pp. 276-280, May 1992.

[13] X. Dai, G. Liu, and R. Gretsch, "Generalized theory of instantaneous reactive quantity for multiphase power system," *IEEE Transactions on Power Delivery,* vol. 19, pp. 965-972, July 2004 2004.

[14] M. Depenbrock, V. Staudt, and H. Wrede, "A concise assessment of original and modified instantaneous power theory applied to four-wire systems," in *Proceedings of Power Conversion Conference - Osaka PCC 2002*, Osaka, Japan, 2002, pp. 60-7 vol.1.

[15] M. Depenbrock, V. Staudt, and H. Wrede, "A Theoretical Investigation of Original and Modified Instantaneous Power Theory Applied to Four-Wire Systems," *IEEE Transactions on Industry Applications,* vol. 39, pp. 1160-1168, July/August 2003 2003.

[16] R. C. Dugan, M. F. McGranaghan, and S. Santoso, *Electrical power systems quality*, 2nd ed. vol. 1. New York: McGraw-Hill, 2002.

[17] A. E. Emanuel, "Summary of IEEE standard 1459: Definitions for the measurement of electric power quantities under sinusoidal, nonsinusoidal, balanced, or unbalanced conditions," *IEEE Transactions on Industry Applications,* vol. 40, pp. 869-876, May/June 2004 2004.

[18] A. E. Emanuel, "Summary of IEEE standard 1459: Definitions for the measurement of electric power quantities under sinusoidal, nonsinusoidal, balanced, or unbalanced conditions," *IEEE Transactions on Industry Applications,* vol. 40, pp. 869-876, 2004.

[19] P. Filipski, "A new approach to reactive current and reactive power measurement in nonsinusoidal systems," *IEEE Transactions on Instrumentation and Measurement,* vol. IM-29, pp. 423-6, 1980.

[20] P. Filipski, "The measurement of distortion current and distortion power," *IEEE Transactions on Instrumentation and Measurement,* vol. IM-33, pp. 36-40, 1984.

[21] T. Furuhashi, S. Okuma, and Y. Uchikawa, "Study on the theory of instantaneous reactive power," *IEEE Transactions on Industrial Electronics,* vol. 37, pp. 86-90, Feb 1990.

[22] G. D. Marques, "Comparison of active power filter control methods in unbalanced and non-sinusoidal conditions," in *Proceedings of the 1998 24th Annual Conference of the IEEE Industrial Electronics Society, IECON. Part 1 (of 4)*, Aachen, Ger, 1998, pp. 444-449.

[23] G. D. Marques, "Detection of reference currents for active filters using the Darrieus definition of reactive power," in *2000 IEEE International Symposium on Industrial Electronics (ISIE'2000)*, Puebla, 2000, pp. 73-77.

[24] A. Nava-Segura and J. Arellano-Padilla, "Transient performance of an active filter under harmonic power variations," in *2000 IEEE International Symposium on Industrial Electronics (ISIE'2000)*, Puebla, 2000, pp. 102-106.

[25] C. Patrascu, D. Popescu, and A. Iacob, "Electrical power quality improvement using a DSP controlled active power filter," in *9th International Conference - Electrical Power Quality and Utilisation*, Barcelona, Spain, 2007, pp. 472-5.

[26] F. Z. Peng and J.-S. Lai, "Generalized instantaneous reactive power theory for three-phase power systems," *IEEE Transactions on Instrumentation and Measurement,* vol. 45, pp. 293-297, Feb 1996.

[27] F. Z. Peng, G. W. Ott, and D. J. Adams, "Harmonic and reactive power compensation based on the generalized instantaneous reactive power theory for 3-phase 4-wire

systems," in *Proceedings of the 1997 28th Annual IEEE Power Electronics Specialists Conference. Part 2 (of 2)*, St.Louis, CA, 1997, pp. 1089-1095.

[28] F. Z. Peng, G. W. Ott, Jr., and D. J. Adams, "Harmonic and reactive power compensation based on the generalized instantaneous reactive power theory for three-phase four-wire systems," *IEEE Transactions on Power Electronics,* vol. 13, pp. 1174-1180, Nov 1998.

[29] S. L. Round, H.; Duke, R.; Gardiner, A., "The transient and steady state performance of a shunt active filter using measured site data," in *8th International Conference on Harmonics And Quality of Power*. vol. 1, 1998, pp. 395-400.

[30] M. Saitou and T. Shimizu, "Generalized theory of instantaneous active and reactive powers in single-phase circuits based on Hilbert transform," in *IEEE 33rd Annual Power Electronics Specialists Conference (PESC)*, Cairns, Australia, 2002, pp. 1419-1424.

[31] B. Singh, K. Al-Haddad, and A. Chandra, "Review of active filters for power quality improvement," *IEEE Transactions on Industrial Electronics,* vol. 46, pp. 960-971, 1999.

[32] J. S. Subjak Jr and J. S. McQuilkin, "Harmonics -- Causes, effects, measurements, and analysis: An update," *IEEE Transactions on Industry Applications,* vol. 26, pp. 1034-1042, 1990.

[33] J. L. Willems, "Reflections on apparent power and power factor in nonsinusoidal and polyphase situations," *IEEE Transactions on Power Delivery,* vol. 19, pp. 835-840, April 2004.

[34] J. L. Willems, "A new interpretation of the Akagi-Nabae power components for nonsinusoidal three-phase situations," *IEEE Transactions on Instrumentation and Measurement,* vol. 41, pp. 523-527, Aug 1992.

[35] J. L. Willems, J. A. Ghijselen, and A. E. Emanuel, "The apparent power concept and the IEEE standard 1459-2000," *IEEE Transactions on Power Delivery,* vol. 20, pp. 876-884, 2005.

[36] B. Wu, *High-power converters and ac drives*, 1 ed. vol. 1. Piscstaway, NJ: Wiley-interscience, 2006.

[37] R. Yacamini, "Power system harmonics Part 3 problems caused by distorted supplies," *Power Engineering Journal,* vol. 9, pp. 233-238, 1995.

[38] A. F. Zakeri, K. Kanzi, and M. T. Bina, "A new approach to compensation of instantaneous inactive power," in *IEEE International Electric Machines and Drives Conference, IEMDC 2007*, Antalya, Turkey, 2007, pp. 624-629.

APPENDIX I – Comparison for three phase- three wires system

```
%%**** Alireza Javadi**** Symbolic Calculations
%Willems and Akagi( p-q Theory)differences.
%Calculation of "ip" by the two methods for 3 phases-3 wires:
clear all;clc
syms va vb vc
syms ia ib ic
syms vx vy vo
syms ix iy io
V=[va; vb; vc];
I=[ia; ib; ic];
%Clark transformation matrix for three phases:
C=(sqrt(2)/sqrt(3))*[1 -1/2 -1/2;0 sqrt(3)/2 -sqrt(3)/2;1/sqrt(2) 1/sqrt(2)
1/sqrt(2)];
%Conditions of a three phase three wires:
V(3)=-va-vb;
I(3)=-ia-ib;
% instantaneous active power:
P=dot(V',I)
% Willems:
ipw=(P/dot(V',V))*V
iqw=I-ipw;
% Akagi p-q theory (according to the Formulas in the Thesis):
Vxyo=C*V;
Ixyo=C*I;
Vxy=[Vxyo(1);Vxyo(2)];
Ixy=[Ixyo(1);Ixyo(2)];
Pxy=Vxy(1)*Ixy(1)+Vxy(2)*Ixy(2)
%%% Reactive power for Akagi
qxy=Vxy(2)*Ixy(1)-Vxy(1)*Ixy(2)
% Current division into active and reactive parts:
ipxy=(1/dot(Vxy',Vxy))*[Vxy(1) Vxy(2);Vxy(2) -Vxy(1)]*[Pxy;0];
iqxy=(1/dot(Vxy',Vxy))*[Vxy(1) Vxy(2);Vxy(2) -Vxy(1)]*[0;qxy];
ixy=ipxy+iqxy;
simplify(ixy)
%Comparision:
%comparision of Active current:
ipxy(3)=0;
r=(C^-1)*ipxy;
r=simplify(r)
t=ipw-r;
t=simplify(t)
%comparision of reactive current:
iqxy(3)=0;
k=(C^-1)*iqxy;
s=iqw-k;
iqw=simplify(iqw)
s=simplify(s)
%END
```

APPENDIX II – Comparison for three phase- four wires system

```
%%**** Alireza Javadi**** Symbolic Calculations
%Willems and Akagi( p-q Theory)differences.
%Calculation of "ip" by the two methods for 3 phases-4 wires:
clear all;clc
syms va vb vc
syms ia ib ic
syms vx vy vo
syms ix iy io
V=[va; vb; vc];
I=[ia; ib; ic];
%Clark transformation matrix for three phases:
C=(sqrt(2)/sqrt(3))*[1/sqrt(2) 1/sqrt(2) 1/sqrt(2);1 -1/2 -1/2;0 sqrt(3)/2 -
sqrt(3)/2];
% instantaneous active power:
P=dot(V',I)
% Willems:
ipw=(P/dot(V',V))*V
% Akagi p-q theory (according to the Formulas in the Thesis):
Voxy=C*V;
Ioxy=C*I;
%Voxy=[vo;vx;vy];
%Ioxy=[io;ix;iy];
M=[Voxy(1) 0 0
   0 Voxy(2) Voxy(3)
   0 Voxy(3) -Voxy(2)];
Z=M*Ioxy;
% The active power current is supposed to be the sum of the zero-sequence
% and active part:
ipoxy=(M^-1)*[Z(1);Z(2);0]; %(i0+ip)
iqoxy=(M^-1)*[0;0;Z(3)];
iS=C^-1*(ipoxy);
K=iS-ipw;
K=simplify(K)
%The comparision show that the Willems and Akagi's active power are not
%equal and so the reactive power would not be equal.
%%*********************************************************************
% In case of vo=0 and io=/=0 we have:
V=[va; vb; -va-vb];
Voxy=C*V;
P=dot(V',I);
% Willems:
ipw=(P/dot(V',V))*V;
% Akagi:
M=[0 0 0
   0 Voxy(2) Voxy(3)
   0 Voxy(3) -Voxy(2)];
Z=M*Ioxy;
V2=dot(Voxy',Voxy);
ipoxy=(Z(2)/V2)*[0;Voxy(2);Voxy(3)];
ip=C^-1*ipoxy;
h=ipw-ip;
h=simplify(h)
% the active current are equal.
j=I-ipw;
```

```
iqoxy=(Z(3)/V2)*[0;Voxy(3);-Voxy(2)]
iq=C^-1*iqoxy;
f=j-iq;
f=simplify(f)
% the reactive power of Akagi should be added with i0/sqrt(3)to be equal to
% Willems reactive power.
%END
```

APPENDIX III – Comparison of Generalized theory and Willems

```
%%**** Alireza Javadi**** Symbolic Calculations
%Willems and Generalized Instantaneous theory.
%Calculation of "ip" for a multi-phase system:
clear all;clc
syms va vb vc
syms ia ib ic
syms vx vy vo
syms ix iy io
V=[va; vb; vc];
I=[ia; ib; ic];
%Clark transformation matrix for three phases:
C=(sqrt(2/3))*[1/sqrt(2) 1/sqrt(2) 1/sqrt(2);1 -1/2 -1/2;0 sqrt(3)/2 -
sqrt(3)/2];
Voxy=C*V;
Ioxy=C*I;
%Voxy=[vo;vx;vy];
%Ioxy=[io;ix;iy];
%%Willems:
P=dot(V',I)
q=cross(V,I)
ipw=(P/dot(V',V))*V;
iqw=I-ipw;
% Generalized Theory
Poxy=dot(Voxy',Ioxy)
qoxy=cross(Voxy,Ioxy)
M=[Voxy(1)  Voxy(2) Voxy(3);0   -Voxy(3)    Voxy(2);Voxy(3) 0   -Voxy(1);-
Voxy(2)   Voxy(1) 0];
T=M*Ioxy;
%The comparision show that the Willems and the Generalized are equal
ActiveC=P-T(1);%natige barabare 0 ast.
%hamon tor ke dideh mishavad n yaani maqoose taabee qoxy ba qabc barabar
%ast:
r=[T(2);T(3);T(4)]
% r==qoxy
n=(C^-1)*r;
ReactiveC=q-n;
% mitavan jarayane compensation ro be vasileye
%H darvaghe maacouse M ast vali : (1/(va^2+vb^2+vc^2))*H*M==I "matric vahed"
H=[Voxy(1)  0   Voxy(3) -Voxy(2);Voxy(2)    -Voxy(3)    0   Voxy(1);Voxy(3)
Voxy(2) -Voxy(1)    0];
%hamintor ke mosha hede mishavad baraye etminan hassele zir barabare I
%migardad:
Iakagi_abc=(1/dot(Voxy',Voxy))*H*T;%==[ia; ib; ic]
iCoxy=(1/dot(Voxy',Voxy))*H*[0;r];
iCabc=C^-1*iCoxy;
g=iqw-iCabc
%END
```

APPENDIX IV – Published Papers

Alireza Javadi, Guy Olivier, Frederic Sirois, Radu Cojocaru, "Active filter Dynamic study using Opal-RT Simulator", in *Real Time Conference, real-time 2009*, Montreal, Canada, Aug-Sep 2009. (http://www.realtime2009.com/?q=content/conference-program)